University of Naples Federico II

Department of Agricultural Sciences

Ph.D. in Food Sciences

XXXVIII Cycle

The Role of LuxR/LuxI-Quorum Sensing based System in *P. gessardii* in the Regulation of Proteolytic Activity: Insights into QS Inhibition as a Strategy for Control of Spoilage Activity

Ph.D dissertation by

Mohammed Salman

Tutor: Professor Gianluigi Mauriello

Coordinator: Prof. Amalia Barone

Academic years: 2022-2025

Acknowledgment

Today I close an exciting chapter of my life with submission of my PhD thesis. Despite this journey was full of challenges, I hereby extend my gratitude to many people who either were part of this journey or supporting. In this preface, first and foremost all of my gratitude goes for my family. I would always remember the precious and constant support of my family; without them I would never complete this journey and get to this stage.

I would also to thank my supervisor Prof. Gianluigi Mauriello who was always supporting my research work, PhD journey and independent learning.

I would like to thank my collaborators, in particular, Prof. Vittorio Venturi from International Centre of Genetic Engineering and Biotechnology (ICGEB) and his research group members Iris Bertani and Cristina Bez. Their support reflected on my PhD experiments to end up with scientific and high-quality outcomes. In addition, I extend also my thank to Dr Roberto Abbamondi, Professor Giusepnna Tommonaro and Dr Adele Cutignano from Consiglio Nazionale delle Ricerche (Pozzuoli) and Dr Anabela Borges and Professor Sérgio F. Sousa from the university of Porto, Portugal. They all were involved and supporting in the conduct of some my PhD experiments.

Last but not least, I end my acknowledgment part with a special thanks to my Londoner friend Jamal Akbar, who was always helping behind the scenes at any time.

Summary

Quorum sensing (QS) is a bacterial signaling mechanism regulating the expression of genes associated with spoilage and virulence. In dairy products, psychrotrophic *Pseudomonas* spp. can proliferate during cold storage and produce thermostable proteases that compromise milk quality and processing. This study aimed to characterize the acyl-homoserine lactone (AHL)-mediated QS system in *Pseudomonas gessardii* isolated from raw milk and to investigate the potential of bioactive polyphenols and postbiotics, to mitigate proteolytic spoilage activity by QS inhibition. Raw milk samples were screened for highly proteolytic bacteria, which were identified by MALDI-TOF mass spectrometry and 16S rRNA sequencing. The AHL profile of the isolates was characterized using biosensor strains, thin layer chromatography-overlay assay, and LC-MS analysis. Whole-genome sequencing provided insights into the presence of LuxRI-type QS systems. The AHL-degrading enzyme lactonase was heterologously expressed in the strains to investigate the contribution of AHL signals to spoilage phenotype and proteolytic activity in comparison with wild-type strains. Fifty polyphenols were virtually screened by molecular docking analysis for their ability to interact with the 3D model of LuxR protein, which was built from the amino acid sequences of *P. gessardii* obtained from whole genome sequencing. The compounds that scored higher the reference ligand of the LuxR (C4-HSL) were tested for their inhibitory effect on proteolytic activity at 4 °C and 25 °C in skim milk. Six highly proteolytic isolates were identified as *P. gessardii*. They were found to produce short chain AHL, mainly C4-HSL. Whole genomic sequencing revealed for the first time presence of diverse LuxI and LuxR solo genes in *P. gessardii*. Conjugated *P. gessardii* strains with the expression of the AHL-degrading enzyme lactonase confirmed the regulatory role of AHLs in proteolytic activity. In addition, construction of mutant in the AHL-synthase genes reported that *rhlI*-like gene is involved

in the regulation of proteolytic activity. Cinnamaldehyde and salicylic acid were found to compete with C4-HSL to bind with the LuxR. These 2 compounds showed significant inhibition of proteolytic activity without antibacterial effects. Furthermore, postbiotic compounds from *Lactobacillus acidophillus* LA-5 were also shown to exert anti-proteolytic activity without antimicrobial effect. Docking analysis supporting their function as quorum sensing inhibitors by bind with the LuxR receptors. This work provides new insights into QS-regulated spoilage mechanisms in dairy-associated *Pseudomonas* and demonstrates the potential of polyphenols and postbiotics to stabilize raw milk by restricting proteolytic activity. These results highlight a sustainable strategy to preserve food quality and nutritional value.

Contents

List of tables

List of figures

1 Quorum Sensing Mechanism and its Inhibition: The Role in Food and Gut Health

1.1 Abstract

Background. Quorum sensing (QS) is a cell-to-cell communication mechanism that occurs between inter- and intra-bacterial species and is regulated by signaling molecules called autoinducers (AIs). It has been suggested that probiotics can exert a QS inhibitory effect through their metabolites. **Purpose**. To provide an overview of (1) the anti-QS activity of probiotics and its mechanism against foodborne pathogenic and spoilage bacteria; (2) the potential role of the QS of probiotics in gut health; and (3) the impact of microencapsulation on QS. **Results**. *Lactobacillus* species have been extensively studied for their anti-QS activity and have been found to effectively disrupt QS in vitro. However, their effectiveness in a food matrix is yet to be determined as they interfere with the AI receptor or its synthesis. QS plays an important role in both the biofilm formation of probiotics and pathogenic bacteria. Moreover, in vitro and animal studies have shown that QS molecules can modulate cytokine responses and gut dysbiosis and maintain intestinal barrier function. In this scenario, microencapsulation was found to enhance AI activity. However, its impact on the anti-QS activity of probiotics and its underlying mechanism remains unclear. **Conclusions**: Probiotics are potential candidates to block QS activity in foodborne pathogenic and food spoilage bacteria. Microencapsulation increases QS efficacy. However, more research is still needed for the identification of the QS inhibitory metabolites from probiotics and for the elucidation of the anti-QS mechanism of probiotics (microcapsules and free cells) in food and the human gut.

1.2 Introduction

Quorum sensing (QS) is the mechanism that bacterial cells use for inter- and intraspecies communication after the cell density reaches a specific threshold. This communication is signaled through molecules produced by the cells and named autoinducer (AI) molecules. When these molecules are accumulated at a specific threshold concentration, they bind to a detector protein that initiates the QS transduction pathway. This ultimately leads to the genes responsible for pathogenicity, spoilage, and biofilm formation being expressed (Garg et al., 2014). There are three common QS systems, which are employed by bacteria to regulate gene expression. The first is the LuxRI-type QS system that is used by most Gram-negative bacteria. This QS system is mediated through acyl homoserine lactone (AHL) molecules, which are synthesized by the *luxI* gene as AIs. These then bind to the LuxR-type protein encoded by the *luxR* gene to form an AHL–LuxR complex, which activates the target gene expression (Deep et al., 2011). The second is a two-component QS signaling system that is used by most Gram-positive species. This QS system is peptide-mediated and termed an accessory gene regulator (*agr*) or *agr*-like QS system. The AI peptide (AIP) is produced by *agrD* and processed by *agrB* for transportation into the *agrCA* pathway (two-component signaling cascade), in which a membrane-bound histidine kinase is synthesized by *agrC* to detect AIP. This initiates a series of phosphorylation that ultimately leads to the transcriptional regulator kinase (synthesized by *agrA*) being phosphorylated, which triggers the expression of the target genes (Bourret et al., 2021). A third major QS system is the AI-2/LuxS homolog that is shown both in Gram-negative and Gram-positive bacteria. AI-2 is synthesized by *luxS*, which then binds to the AI-2 receptor according to the type of bacteria (Bai and Rai, 2011). A fourth type of autoinducer is AI-3, which was discovered in *Escherichia coli* as a regulator of virulence factors. This type of AI is produced through a series of reactions induced by threonine

dehydrogenase and aminoacyl-tRNA synthetases (Bourret et al., 2021). Microbiome–microbiome crosstalk in the food and gut through QS plays a role in food quality and gut health, which is important for the food industry and medical therapy (Falà et al., 2022; Bai et al., 2021). QS is involved in microbial pathogenesis and biofilm formation in food products, which is deemed a concern for public health and food safety. For example, milk can be contaminated by pathogenic Gram-positive bacteria such as *Listeria monocytogenes* that use peptides (i.e., AIP) as QS signaling molecules to trigger gene expression for biofilm formation (Machado et al., 2020). Biofilm formation and microbial enzymatic activity (e.g., pectinolytic, proteolytic, and lipolytic) are factors inducing food spoilage, which can be regulated by QS. As a matter of fact, *Pseudomonas* and *Enterobacteriaceae* can spoil milk by the proteolytic activity, whose expression is regulated by the LuxRI-type QS system (Machado et al., 2020; Martins et al., 2018). Spoilage in meat and vegetables is also caused by Gram-negatives, where homoserine lactone (HSL) acts as a signaling molecule to QS (Machado et al., 2020). Several studies have shown the positive effect of probiotics on food safety and quality through anti-QS activity (Davares et al., 2020; Rizzello et al; 2014; Song et al., 2019). In addition, the regulation of intestinal homeostasis and inflammation is also controlled by the QS of gut microbiota. It is worth noting that pathogenic bacteria can boost their survival in the gut by forming biofilms, which are regulated by QS (Deng et al., 2020). Hence, QS acts as a mediator between gut microbiota and intestinal health (Deng et al., 2020). Interestingly, QS inhibition could be one of the mechanisms by which probiotics modulate the gut microbiome and alleviate the harmful health effects of pathogenic bacteria. With QS playing a dual role in both food quality and gut health, disrupting QS could improve food quality and promote gut health. This could potentially be achieved by using probiotics as QS inhibitors (QSIs). Furthermore, the use of probiotics as QSIs may also be considered an alternative therapy to combat antimicrobial

bacterial resistance (Zhao et al., 2020). Many QSIs from different sources were investigated against foodborne pathogenic and food spoilage bacteria. Plant sources of phytochemicals and bioactive compounds, bee products, and bacteria were found effective in disrupting the QS pathway and biofilm formation by spoilage and pathogenic Gram-negative and Gram-positive microorganisms (Machado et al., 2020; Rizzello et al., 2014; Qais et al., 2020). As well described in the literature, the QS inhibition could be classified in one of the following mechanisms: (1) repressing the gene encoding the AI synthase; (2) inactivation of AI signals through quorum quenching (QQ) enzymes, (e.g., hydrolysis of the lactone bond in AHL); and (3) interfering with signal receptors in QS networks (Zhao et al., 2020). There is a growing body of research on the role and mechanism of QS in regulating bacterial biofilm formation and pathogenesis. The food industry is increasingly interested in the use of probiotics for food functionalization and bio-preservation. Therefore, this chapter has a dual purpose. Firstly, it aims to provide an up-to-date overview of the anti-QS activity of probiotics against foodborne pathogens and spoilage bacteria. Secondly, it aims to offer insights into future perspectives for the potential use of probiotics in food products to enhance food quality and gut health by inhibiting QS.

1.3 Mechanism of QS inhibition

In the last decade, there has been growing attention to unveil the mechanism that probiotics use to alter QS activity in foodborne pathogenic and spoilage bacteria. Probiotics, in particular lactic acid bacteria (LAB), are the most studied microorganisms as a promising source of QSIs. The interference with the LuxRI-type, Agr-like, and AI-2/LuxS-type QS systems would result in the repression of virulence genes responsible for pathogenicity, food spoilage, and biofilm formation. In the two sections below, the mechanism of QS disruption in foodborne pathogenic and spoilage bacteria is discussed in detail.

1.3.1 Probiotics as QSIs in foodborne pathogenic bacteria

It is well reported that LAB have a bactericidal effect through the secretion of organic acids, hydrogen peroxide, and bacteriocins, which affect the growth or the survival of pathogenic bacteria (Gao et al., 2019). Interestingly, the detrimental effects of foodborne pathogenic bacteria can be reversed by disrupting the QS mechanism, without their growth/survival necessarily being impacted (Machado et al., 2020). Numerous probiotics are demonstrated as QSIs through interference with the QS signaling pathway of the target bacteria (Rizzello et al., 2014). LAB are the most studied QSI bacteria against a range of common pathogenic bacteria, which rely on QS for biofilm formation and the expression of virulence factors (Rizzello et al., 2014). In **Table 1**, potential probiotic LAB and non-LAB are described as QSIs. Generally, the interference of QSI with one of the QS pathway components would lead to the downregulation of QS-related genes and the inactivation of QS.

Table 1. Probiotics involved in the inhibition of QS mechanisms of foodborne pathogenic bacteria.

Microorganism	QSI	Target	Type of Study	Mechanism	Reference
Lb. reuteri LR 21	Reuterin	*C. perfringens* 13124	In vitro	Repression of toxins-producing genes (*cpa* and *pfo*) and *agrB* and *luxS.*	(Xu et al., 2022)
Lb. acidophilus GP1B	CE/CFS	*C. difficile (ribotype 027)*	In vitro	Inhibition of AI-2 production and downregulation of *luxS* and *tcdA*, *tcdB*, and *txeR* (virulence genes). Growth inhibition of *C. difficile* in the colon.	(Yun et al., 2014)
Lb. fermentum Lim2	Inactivated CE	*C. difficile* 027	In vitro	Anti AI-2 activity due to repression of *lux* gene. Expression of virulence genes also reduced. QSIs are not measured.	(Yong et al., 2019)
Lb. reuteri RC-14	CFS	*Staph. aureus* MN8	In vitro	Cyclo-dipeptides inhibited the expression of *agr* and *tst* genes as well as disrupting *saeRS* system.	(Li et al., 2011)
B. subtilis	Fengycin	*Staph. aureus*	Cross sectional analysis	Fengycin competes with AIP for binding to *agrC*.	Piewngam et al., 2018
Lb. helveticus	Biosurfactant	*Staph. aureus*	In vitro	Inhibition of biofilm formation by interfering with AI-2 signaling and biofilm-related genes expression (*dltB, sarA, agrA, and icdA*).	Jiang et al., 2019
			In vivo	Prevention of hemolytic activity through biofilm formation inhibition.	
Lb. plantarum KCTC10887BP	LPA	*Staph. aureus*	In vitro	Biofilm formation was inhibited. LPA induced AI-2 release in *Staph.* a*ureus*, which repressed biofilm-related genes.	Ahn et al., 2018
Lb. acidophillus 30SC	N/A	*E. coli* O157:H7 43894	In vivo	Inhibition of AI-2 synthesis and modulation of microbial gut community.	Kim et al., 2018

Lb: *Lactobacillus*; *C.*: *Clostridium*; *Staph.*: *Staphylococcus*; *L.*: *Listeria*; *B.*: *Bacillus*; *P.*: *Pseudomonas*; *Ent.*: *Enterococcus*; *Str.*: *Streptococcus*; Pd.: Pediococcus; *V.*: *Vibrio*; *W.*: *Weissella*; CE: cell extract; CFS: cell-free supernatant; LPA: lipoteichoic acid; N/A: not available; EPS: exopolysaccharides; SaeRS: two-component signaling system; DKP: diketopiperazine; AI: autoinducer; QQ: quorum quenching; PQS: Pseudomonas quinolone signal; BIC: biofilm inhibitory compound; QSI: QS inhibitor.

Table 1 continued

Microorganism	QSI	Target	Type of Study	Mechanism	Reference
Lb. rhamnosus GG	N/A	*E. coli*	In vitro	Repression of *lsrK* and *luxS* genes (disruption in AI-2/*luxS*-type QS network).	Deng et al., 2020
Lb. acidophilus A4	EPS	*E. coli* O157:H7	In vitro	Repression levels of curli genes (*crl*, *csgA*, and *csgB*) and chemotaxis (*cheY*) related to biofilm formation.	Kim et al., 2009
Bifidobacterium longum ATCC15707	CE	*E. coli* O157:H7	In vitro	Inhibition of AI-2 activity and virulence gene expression (*nifU*, *dsbA*, and *flgI*).	Kim et al., 2012
Lb. acidophilus A4	N/A	*E. coli* (EHEC)	In vitro	Downregulation of biofilm-related genes (*crl*, *csgA*, and *csgB*) and chemotaxis (*cheY*).	Kim et al., 2008
Lb. brevis 3M004	N/A	*P. aeruginosa* PA002 biofilm formation	In vitro	Degradation of AIs and repression of biofilm formation, pyocyanin, and polysaccharide synthesis-related genes (*lasA*, *lasB,* and *phzAB*).	Liang et al., 2018
Lb. casei CRL 431 *Lb. acidophilus* CRL 730	DKPs	*P. aeruginosa*	In vitro	DKPs compete with AI for binding QS receptors.	Díaz et al., 2020
Lb. rhamnosus GG	CFS	*P. aeruginosa*	In vitro	Inhibition of AHL synthesis.	Devi et al., 2022
Lb. casei PTCC 1608	Lyophilized postbiotics	*P. aeruginosa*	In vitro	Repression of QS genes controlling biofilm formation and virulence (*rhlI*, *rhlR*, and *pelF*), potentially due to organic acid content.	Azami et al., 2022
B. subtilis BR4	Stigmatellin Y	*P. aeruginosa* *(ATCC 27853)*	In vitro	Stigmatellin Y competes with PQS signal for binding with p*qsR* gene, and thus, p*qsR-PQS* QS pathway is disrupted.	Boopathi et al., 2017
B. paralicheniformis ZP1	Lactonase	*P. aeruginosa*	In vitro	Inhibition of biofilm formation due to AHL hydrolysis by lactonase.	Djokic et al., 2022

Table 1 continued

Microorganism	QSI	Target	Type of Study	Mechanism	Reference
Lb. plantarum KU200656	CFS	*Staph. aureus* *L.monocytogenes* *E. coli, S. typhimurium*	In vitro	Biofilm-related genes are downregulated by anti-biofilm activity. (Exact QSI mechanism is not measured).	Lee et al., 2021
Lb. kefiri 8321 and 83113 *Lb. plantarum* 83114	CFS	*S.* enteritidis 115	In vitro	Biofilm formation inhibition. (QSI mechanism not investigated).	Merino et al., 2019
B. subtilis KATMIRA1933 *B. amyloliquefaciens* B-1895	CE/CFS	*S.* (*thompson*, e*nteritidis* phage type 4)	In vitro	Biofilm inhibition due to the subtilosin effect. AI/*luxS* QS pathway is necessary for biofilm formation.	Tazehabadi et al., 2021
W. viridescens WM33 *W. confuse* WM36 (LAB)	CFS	*S. typhi* and *S. t*yphimurium	In vitro	Inhibition of AI-2 activity and biofilm formation.	Pelyuntha et al., 2019
Lb. reuteri PFS4 *Ent. faecium* PFS13 and PFS14.	CFS	*S. typhimurium* and *S.enteritidis*	In vitro	Inhibition of biofilm formation. (Mechanism not investigated).	Siddique et al., 2021
B. subtilis ZK3814	Fengycin and surfactin	*Ent. Faecalis* OG1RF	In vitro	Inhibition of fsr system, which regulates expression of proteolytic activity related-genes (*gelE*/*sprE*).	Piewngam et al., 2021
Pd. Pentosaceus	Crude biosurfactant	*B. subtilis and Staph. aureus* *P. aeruginosa*, *Staph. aureus*, and *E. coli*	In vitro	Anti-QS and anti-biofilm activity.	Adnan et al., 2021
Lb. curvatus BSF206 and Pd. Pentosaceus AC1-2	CFS	*Str. mutans*	In vitro	Biofilm formation inhibition by downregulation of related genes (*tfA*, *gtfB*, *ftf*, and *brpA*). (*Exact mechanism not known*).	Luan et al., 2022
Lb. casei MCJΔ1 (expressed with AHL-lactonase *AiiK* gene)	Lactonase	*Aeromonas hydrophila*	In vitro	Enzymatic QQ activity of lactonase.	Dong et al., 2020

Various strains of *Lb. acidophilus* exhibited anti-QS activity towards *C. difficile*, *Staph. aureus*, and *E. coli* (Yun et al., 2014; Kim et al., 2018; Kim et al., 2008) through the inhibition of AI-2 production or downregulation of biofilm-related genes without an influence on AI-2 synthesis. However, the anti-QS compounds in these studies are not well identified. Other similar studies found that the biofilm-related genes in *E. coli* and *P. aeruginosa* were under-expressed by the activity of EPS and DKP produced by the strains of *Lb. acidophilus* A4 and *CRL* 730, respectively (Kim et al., 2009, Díaz et al., 2020). The anti-biofilm and anti-QS activity of probiotics against Salmonella was also observed, but the QSIs were not identified (Lee et al., 2021; Merino et al., 2019; Tazehabadi et al., 2021; Pelyuntha et al., 2019; Siddique et al., 2021). In these studies, EPS might be produced by the *Lactobacillus* species as the QSI. This was suggested according to the study of Xu et al. (2020), which found that the biofilm formation of S. Typhimurium was repressed by the action of EPS synthesized by *Lb. coryniformis* NA-3. Even though not investigated, EPS from the *Lactobacillus* species could play a role in the interference with the QS in *Salmonella* through the downregulation of the genes encoding the QS regulator proteins [Lee et al., 2021; Merino et al., 2019; Pelyuntha et al., 2019; Xu et al., 2020). Unfortunately, the mechanisms behind the QS inhibition against *E. coli* and *Salmonella* were not well identified. Hypothetically, the QSIs antagonize the QS regulator proteins, which modulate the expression of virulence genes. This was proposed according to the outcomes in other studies that used molecular docking and bioinformatic methods. The chemically produced QSIs interact with the amino acid sequence of the cognate regulator proteins (LsrR and SdiA), which, in part, mediates QS in *Salmonella* and *E. coli* (Xue et al., 2009; Escobar-Muciño et al., 2022). The binding of phosphorylated AI-2 (AI-2-P) with its cognate protein LsrR leads to the inactivation of LsrR, which regulates transcription of the *lsr* operon that controls the cell uptake of AI-2 and pathogenicity (Zuo et al., 2019). Therefore, QSIs

antagonize the LsrR protein by blocking AI-2-P binding, making active LsrR that leads to the repression of the *lsr* operon. Another potential QSI mechanism is the binding of the QSI with SdiA amino acids. This interaction will prevent AHL by binding the *sdiA* receptor, which works as a transcriptional regulator for QS-related virulence genes (Zuo et al., 2019). *Staph. aureus* is one of the common causative factors for foodborne pathogenesis and infectious mortality globally. It is expected that there is a 10 to 30% mortality rate of SAB (*Staph. aureus* bacteremia) cases, and this is exacerbated by the ability of *Staph. aureus* to develop resistance to antibiotics (Van Hal et al., 2012). In comparison with QS in other bacterial species, *Staph. aureus* encompasses 13 QS pathways, each one associated with a different virulence mechanism (Bleul et al 2022). The blocking of QS in *Staph. aureus* could be a surrogate of antibiotic treatment to control virulence expression and infection treatment. Several studies found that probiotics or their metabolites have a QS inhibitory effect against *Staph. aureus*. As a matter of fact, cyclo-dipeptides produced by *Lb. reuteri* showed repression activity on *Staph. aureus* pathogenicity elements, such as the Agr system, *tst* gene, and SaeRS QS system (Li et al., 2011). A cross-sectional study revealed an agr-inhibitory effect via *B. subtilis*-produced lipopeptide (fengycin) (Piewngam et al., 2018). In this study, 200 nasal swapes and fecal samples were collected from a Thai population living in different areas and were analyzed for *Staph. aureus* and *B. subtilis* colonization. There was a positive relationship between the presence of *B. subtilis* and the absence of *Staph. aureus*. Furthermore, *agr* activity declined when the *B. subtilis* culture filtrate was incubated with the *Staph. aureus* reporter strain, and the synthesis of virulence factors (phenol-soluble modulins, α-toxin, and Panton–Valentine leucocidin) was also suppressed (Piewngam et al., 2018). Accordingly, the two-component signaling (fsr) in *E. faecalis* was disrupted by the inhibitory effect of *B. subtilis* ZK3814-secreted lipopeptides (surfactin and fengycin). The result was that the expression of

proteolytic activity-related genes (*gelE*/*sprE*) was quenched. Other anti-QS unraveled compounds are the biosurfactants synthesized by *Lb. helveticus* and *P. pentosaceus*, which were shown to reduce biofilm formation by *B. subtilis, P. aeruginosa, Staph. aureus,* and *E. coli* (Jiang et al., 2019; Adnan et al., 2021). While the anti-QS activity of the biosurfactant from *P. pentosaceus* was not investigated in-depth (Adnan et al., 2021). Jiang et al. (2019) found that the biosurfactant from *Lb. helveticus* reduced the expression of *dltB* in *Staph. aureus*, which is a regulatory gene in the two-component signaling system GraRS. This system controls the resistance to cationic antimicrobial peptides (CAMB), a defense system employed by the host against microbial infection. The response regulator genes *agrA* and *sarA* that are involved in the regulation of biofilm formation were also repressed. Interestingly, the *in vivo* experiment showed that the anti-biofilm activity also reduced the hemolytic activity of *Staph. aureus*. Peculiarly, the AI-2 release was associated with the inhibition of biofilm formation as found by Ahn et al. (2021). LPA produced by *Lb. plantarum* KCTC10887BP reduced the expression of biofilm formation by the induction of AI-2 release. This was confirmed in another study (Melian et al., 2019), which reported an upregulation of biofilm formation in *Staph. aureus* RN6390B with mutation in the *luxS* gene. AI-2 release results in the transcription of the *icaR* gene, which works as a repressor for the *ica* operon, and consequently, the expression of the *icaA* gene that is involved in biofilm formation is deactivated.

Having established the anti-biofilm activity of probiotics, the tooth decay causing bacterium *Str. mutans* relies on biofilm formation for adhesion. Several studies show that the anti-QS activity of probiotics is related to the repression of biofilm-related genes and the inhibition of EPS production, which is an important matrix of biofilm formed by *Str. mutans*. Biosurfactants and a novel compound (iminosugar) were identified as QSIs produced by *Lb. rhamnosus* and *Lb. paragasseri*,

respectively (Dong et al., 2021; Hossain et al., 2021; Melian et al., 2019; Sudan et al., 2022; Shangguan et al., 2021). *Lb. plantarum*-secreted LPA exerted anti-biofilm activity against *Str. mutans, E. faecalis,* and *Str. gordonii* (Lee et al., 2021). This anti-biofilm activity could be due to the same inductive effect of LPA on AI-2 release that was observed by Yu et al. (2012), albeit the QSI mechanism is not described. *P. aeruginosa* is a pathogenic bacterium that causes infections in humans, especially in immunocompromised populations. The treatment of infections with *P. aeruginosa* is cumbersome due to its resilience to various stress conditions and antibiotic administration and its ability to produce diverse types of EPS matrixes for biofilm formation and cell adhesion (Ma et al., 2012; Wilson et al., 2022). There are three QS systems (*las, rhl, and pqs*) in *P. aeruginosa*, which are activated for the expression of biofilm formation and virulence factors. *lasI, rhlI*, and *pqsABCDH* are synthase genes of the autoinducers N-(3-oxododecanoyl)-HSL, N-butyryl-HSL (C4-HSL), and 2-heptyl-3-hydroxy-4-quinolone (PQS), respectively (Venturi, 2006). Extensive research has been conducted to investigate the QSI by probiotics and their metabolites in vitro. QS was blocked through the degradation of QS signal molecules (AHL) by various species of *B. paralicheniformis*. Lactonase and acylase were found to degrade the lactone and acyl rings in the QS signal AHL, respectively (Djokic et al., 2022). *Lb. brevis* showed anti-QS enzymatic activity by unknown AHL-degrading enzymes (Liang et al., 2022). It is noteworthy that as lactonase and acylase only degrade AHLs, these enzymes are only efficient in Gram-negative bacteria, which involve AHL-based QS pathways. Another route of QS inhibition against *P. aeruginosa* is the antagonization of the receptor proteins. Stigmatellin Y from *B. subtilis* BR4 interfered with the PQS QS systems by binding with the PqsR protein in competition with the PQS signal molecule and disruption of AHL-signal transduction (Boopathi et al., 2017). Lyophilized postbiotics from *Lb. casei* disrupted the *rhl* QS system and downregulated the genes for

autoinducer synthase and its cognate regulatory protein, potentially, due to the action of organic acids (Azami et al., 2022). When the CFS of *Lb. rhamnosus* GG was incubated with *P. aeruginosa* PAO1, there was a decrease in AHL activity and levels (Devi et al., 2022). In this study, the authors state that the CFS has inhibited AHL production, potentially by reducing the expression of the AHL-producing gene (*lasI*), albeit this was not evaluated. Perhaps, *Lb. rhamnosus* GG reduced the AHL activity through the newly revealed enzyme (acyl-hydrolase); however, this still needs further investigation (Manasian et al., 2020). Bacteriocins are antimicrobial peptides that are usually secreted from lactic acid bacteria that kill or inhibit the growth of the target pathogenic or spoilage microorganisms. They have lately been linked with the QS mechanism. In Rizzello et al. (2014), QS in *Lb. plantarum* C2 was involved in the production of plantaricin. Reuterin and lactocin released from *Lb. reuteri* LR 21 and *Lb. curvatus* CRL1579, respectively, acted as QSIs [17,49]. Reuterin reduced the expression of the *luxS* and *agrB* genes in *C. perfringens* 13124, which subsequently prevented toxin production by repressing the toxin-producing genes (*cpa* and *pfo*). The QSI mechanism of lactocin is not yet demonstrated. However, in Hossain et al. (2021), the expression of the biofilm-regulatory genes of *L. monocytogenes* (*flaA, fbp, agrA, prfA*, and *hlyA*) was inhibited as an effect of the postbiotics from *Lb. curvatus* B.67 and Lb. plantarum M.2. Very recently, *Lb. curvatus* B67 was reported to produce quercetin that shows anti-biofilm activity against *Listeria monocytogenes* (Toushik et al., 2023). Reasonably, a QS inhibition activity of quercetin could be hypothesized. Apart from the QSI mechanism discussed above, it is suggested the QS pathway for biofilm formation could be disrupted by the inhibition of proton motive forces (PMFs) and efflux pumps. PMFs were associated with the release of AIs from cells, and the inactivation of PMFs would lead to the intracellular accumulation of autoinducers and thus, the downregulation of QS-regulatory genes (Pearson et al., 199). This was also confirmed when QS

peptide export was blocked due to the disruption of PMFs in *Str. pneumoniae* (Domenech et al., 2020). In addition, in Sutyak et al. (2011), the inhibitory effect of subtilosin on PMF in Gordonia vaginalis was reported. Therefore, the anti-biofilm activity of *B. subtilis* KATMIRA1933 against *L. monocytogenes* could be potentially attributed to the inhibitory effect of subtilisin on PMFs (Tazehabadi et al., 2021). In summary, probiotics could exhibit QS inhibitory effects by producing and secreting QSIs. These are reported as lipopeptides (such as fengycin and surfactin), lipoproteins (biosurfactants), organic compounds, cyclic peptides, lipoteichoic acid, exopolysaccharides, bacteriocins (such as reuterin and lactocin), and AHL-lytic enzymes. However, in some studies, there was a gap in the identification of QSI compounds or the elaboration of the QS inhibition mechanism when anti-QS activity was shown. Despite the anti-QS effect of the CFS of probiotics/postbiotics against foodborne pathogens, it is not known whether the same anti-QS activity can be observed if probiotics are investigated as cell cultures. Furthermore, the extensive research on QSI has been conducted in in vitro experiments. In fact, the outcomes of these studies do not necessarily replicate the context in real foods. The chemical composition of food (proteins, lipids, and carbohydrates) might affect the viability and functional properties of probiotics (Ranadheera et al., 2010).

1.3.2 Potential Role of Probiotics in QS Inhibition in Food Spoilage Bacteria

Food spoilage is a consequence of physical changes, such as texture change due to drying, chemical reactions, such as oxidation, and microbial activity. Microbial-induced food spoilage can reduce the shelf-life of food by altering its sensory qualities, such as texture, flavor, and taste, due to enzymatic activity (proteolytic, lipolytic, and pectinolytic) and biofilm formation (Amit et al., 2017). QS molecules have been detected in different types of food products, including meat, milk, and vegetables, and their presence has been suggested to be involved in microbial food spoilage

(Machado et al., 2020). The growth of psychrotrophic Gram-negative bacteria, usually isolated from raw milk (e.g., *Pseudomonas* and *Serratia*), is associated with biofilm formation and the production of extracellular enzymes that are mediated by the LuxI/AHL-type QS system (Yuan et al., 2018). This has also been confirmed in a transcriptome analysis study that evaluated the effect of exogenous AHLs on the virulence activity of *P. azotoformans* and *Serratia liquefaciens* in milk. It was observed that the addition of AHLs upregulated the genes responsible for growth, metabolism, and enzymatic activity (protease, lipase, and glycosidase) (Yang et al., 2021). Fresh meat contains a complex of several bacterial genera (*Enterobacteriaceae, Yersinia, and Pseudomonas*) that induce spoilage. In these species, the expression of biofilm formation and virulence factors of spoilage are stimulated by the LuxI/AHL-type QS signaling pathways. Proteolytic activity and AHLs with different carbon chain lengths were found in chilled meat products, and this was associated with the growth of Enterobacteriaceae and Pseudomonas. Moreover, the luxS/AI-2-type QS system is known to be implicated by *Leuconostoc citreum*, a lactic acid bacterium that causes meat spoilage in biofilm formation (Martins et al., 2018; Pothakos et al., 2015; Yuan et al., 2018; Yang et al., 2021; Ng et al., 2018). Post-harvest contamination of vegetables with pectinolytic and proteolytic bacteria could impact the quality of the product and reduce the shelf-life. *Pectobacterium carotovorum* is one of the common plant pathogenic bacteria that causes soft-rot disease in a wide range of vegetables (potato, onion, tomato, and radish) through enzymatic activity, which is a concern for the agriculture industry and farmers due to the economic loss (Opara et al., 2016). The production of pectinolytic and proteolytic enzymes is regulated by QS. It was found that LuxS-mutant *Pectobacterium carotovorum* reduced the expression of pectate lyase and cellulase in addition to protease enzymes, which demonstrates the role of the LuxS/AI-2- type QS system in enzymatic activity expression (Põllumaa et al., 2012).

Similarly, in LuxS-mutant *Erwinia carotovora*, there was a four- and three-times decrease in the production of pectate lyase and polygalacturonase compared with the wild-type strain, after 6 and 8 h of growth, respectively (Laasik et al., 2018). In the same species, another study showed the role of the *luxI*/AHL-type QS system in the rot–spoilage of bean sprouts by proteolytic and pectinolytic activity. However, when the bean sprouts were inoculated with the *luxI*-mutant strain, the spoilage took longer to occur compared with sprouts contaminated with the wild-type strain (Rasch et al., 2005). *Shewanella baltica* is the primary bacterium that causes fish to deteriorate. It also employs the LuxS/AI-2-type QS system to activate genes related to spoilage and biofilm formation through DKPs as signaling molecules for QS induction (Fu et al., 2018). Overall, QS plays a crucial role in microbial food spoilage. Therefore, disrupting QS signaling in spoilage bacteria could extend the shelf life of fish products by preventing the expression of virulence factors and biofilm formation. A wide range of QSIs, including plant-derived compounds (such as phenol acids), chemicals such as furanone, and QS signal-degrading enzymes, have been demonstrated (Machado et al., 2020). This section explores the potential role of probiotics as a source of QSIs. Notably, QS inhibition against microbial spoilage is a recent focus of research. As shown in **Table 2**, only five studies have investigated potential probiotics as a source of QSIs. The anti-QS activity of *Bacillus* strains was identified through the QQ activity of lactonase and the antagonistic effect of DKPs on QS receptors. Li et al. (2022a) showed that QS promoted the growth of *Lb. plantarum* ss-128, but they did not investigate its anti-QS activity against spoilage bacteria. Research on the anti-QS activity of lactic acid bacteria against food spoilage bacteria is still lacking.

Table 2. Probiotic strains investigated as a source of QSIs against foodborne spoilage bacteria

Microorganism	QSI	Target	Type of Study	Mechanism	Reference
B. sp. AI96	Lactonase	*Aeromonas veronii* LP-11	In vitro	Spoilage inhibition due to QS disruption by lactonase.	Gui et al., 2017
B. amyloliquefaciens SBF1	Culture extract	*P. aeruginosa* PAO1	In vitro	Biofilm inhibition due to anti-QS activity.	Husain et al., 2016
Lysinibacillus sp. Gs50	Lactonase	*Pectobacterium carotovorum*	Food matrix	Vegetables soft rot reduced due to QQ of AHLs.	Garge et al., 2016
B. cereus RC1	DKPs	*Lelliottia amnigena*	Food matrix (vegetables)	Soft rot decreased due to anti-QS activity. DKPs compete for binding QS receptors with the AI.	Kachhadia et al., 2022

Spoilage bacteria can cause changes in food quality due to both enzymatic activity and the release of chemical compounds, including volatile organic compounds (VOCs), volatile fatty acids, ethyl esters, aldehydes, and sulfur compounds, which can result in sensory defects such as off-odor, off-flavor, and discoloration (Pothakos et al., 2015). It is unclear, however, whether QS directly influences the expression of these virulence factors.

The interaction between probiotics and spoilage bacteria in food microbiomes has the potential to play a key role in prolonging food shelf-life by modulating the expression of spoilage factors. However, the effect of such an interaction on QS in spoilage bacteria is still not well-researched. If probiotics are found to have an anti-QS effect against spoilage bacteria, this could be a significant step towards replacing chemical preservatives with bio-preservatives and enhancing the efficacy of other preservatives.

1.4 QS, biofilm formation, and gut health

Table 3. Association of QS molecules with gut health.

QS Molecule	Source	Type of Study	Health Outcomes	Reference
3-oxo-C12:2-HSL	Synthetic	In vitro	Anti-inflammatory effect.	Coquant et al., 2022
3-oxo-C12:2 HSL	Human gut microbiota	Cross sectional (analysis of fecal samples of patients with IBDs)	Positive correlation with normobiosis (increased levels of Firmicutes). Anti-inflammatory and positive in vitro effect on gut epithelial cell function.	Landman et al., 2018
AI-2	Mutant *E. coli* engineered to overproduce AI-2	Animal study	Increased ratio of *Firmicutes* to *Bacteroidetes* in antibiotic-treated mice group.	Thompson et al., 2015
AI-2	*Lb. rhamnosus* GG (LGG)	Animal study	Protective effect of Δ*luxS* LGG on intestinal cells is significantly lower than effect of wild-type LGG.	Deng et al., 2022
AI-2	Exogenous AI-2 added to milk	Animal study	Dysbiosis was reversed, and inflammation was ameliorated.	Ji et al., 2020
DPD (precursor of AI-2)	Exogenous (synthetic)	In vitro (co culture of WCE of *Prevotella. intermedia*, *Prevotella*)	DPD modulated the pro-inflammatory effect of estradiol + and inhibited biofilm formation.	Fteita et al., 2018
AI-2	*Fusobacterium nucleatum*	Cross-sectional (analysis of fecal saliva, and serum samples from patients with CRC and healthy people)	AI-2 levels are higher in CRC samples compared with control samples.	Li et al., 2019
AI-2	Non-pathogenic *E. coli* BL21 and W3110	In vitro (co-culture with HCT-cells)	Increased expression of pro-inflammatory cytokine IL-8 but downregulated after 24 h.	Zargar et al., 2015

IBDs: inflammatory bowel diseases; HMK: human gingival keratinocytes; HCT: human colon cancer; CRC: colorectal cancer; WCE: whole cell extract; DPD: dihydroxy-2,3-pentanedione

The induction or inhibition of QS signaling is associated with the expression or repression of biofilm-related genes, respectively. In fact, biofilm is necessary for pathogenic bacteria to maintain their growth and infect the host environment (Vestby et al., 2020). The protective effect of probiotics against pathogenic bacteria in the gut could be attributed to their anti-QS and anti-biofilm activity, as shown in **Table 1**. Additionally, the QS system is involved in the regulation of

biofilm formation by probiotics in the host gut (Davares et al., 2010). This forms a biological barrier and maintains intestinal immunity against pathogenic bacteria that cause infection (Davares et al., 2010). The importance of the AI-2/*luxS*-type QS system in biofilm formation and stress resistance of the probiotics (*Lactobacillus* and *Bifidobacterium*) was observed. The promotion of AI-2 synthesis by the overexpression of *luxS* in *Lb. paraplantarum* L-ZS increased resistance to heat- and bile-salt stress compared with the wild-type strain (Liu et al., 2018). Moreover, the biofilm formation of *Lb. paraplantarum* L-ZS and *Bifidobacterium longum* NCC2705 was augmented (Liu et al., 2018, Sun et al., 2014).

An emerging field of research highlights the ability of QS molecules to modulate the inflammatory response. One type of AHL QS molecule, 3-oxo-C12:2-HSL, was described as anti-inflammatory through the activation of bitter taste receptors and the inactivation of cell signaling cascades (JAK-STAT signaling pathway, NF-κB signaling, and TNF signaling pathway) that upregulate the inflammatory response (Coquant et al., 2022; Coquant et al., 2020). Additionally, the presence of 3oxo-C12:2-HSL in the gut was negatively correlated with inflammatory bowel disease (IBD) incidence, indicating the role of this type of AHL as an anti-inflammatory (Landman et al., 2018). Another type of QS molecule, AI-2, was recently found to be able to modulate the inflammatory response and gut microbiota composition in vivo (Deng et al.,2022; Ji et al., 2021). In a study by Thompson et al. (2015), a group of mice was induced into dysbiosis by antibiotic administration and then supplemented with genetically engineered *E. coli* overproducing AI-2. After treatment, the antibiotic effect was reversed, and the abundance of *Firmicutes* was significantly promoted compared to *Bacteroidetes*. The authors of this study propose that AI-2 improved the signaling response among the *Firmicutes*, a recurrent producer of AI-2. In another study (Deng et al.,2022), a group of early weaning stress-induced piglets was treated with either the wild type (WT) or *luxS*

mutant (Δ*luxS*) of *Lb. rhamnosus* GG. The ability of Δ*luxS* to preserve the gut barrier function was significantly lower than the WT. As previously discussed, this is due to the role of AI-2 in biofilm formation, which the Δ*luxS* strain lacks to colonize and adhere in the intestine cells. This postulates the role the AI-2/*luxS*-type QS system has in gut health. Recently, an animal study showed that AI-2 supplementation of mouse pups with necrotizing enterocolitis reduced the expression of pro-inflammatory cytokines and increased the anti-inflammatory cytokine (IL-10) production. Furthermore, AI-2 rebalanced the composition of gut flora. In the mice group treated with AI-2, *Lactobacillus* was increased, while *Helicobacter* and *Clostridum_sensu_stricto_1* were reduced compared with the not-AI-2treated group [90]. In another study, the butyl-DPD analog (the precursor for AI-2) was able to alleviate the inflammatory response of human gingival keratinocyte cells when incubated with two *Prevotella* species. The interleukins' (IL-6 and IL-8) expression was reduced (Fteita et al., 2018). Nevertheless, a cross-sectional study in patients with colorectal cancer (CRC) demonstrated the association of AI-2 secreted from gut microbiota with CRC occurrence (Li et al., 2019). In addition, AI-2 from non-pathogenic *E. coli* mediated the transcription of the cytokine response pathway, which as a result, induced inflammatory interleukin IL-8 through the upregulation of the transcription factor NF-κB pathway that regulates cytokine production (Zargar et al., 2015).

There are chemically synthesized QSIs that can be considered anti-virulence agents for infection treatment. Nevertheless, it is proposed that some species such as *E. coli* and *Salmonella* can develop resistance to these QSIs, which is partially due to the opportunity for bacteria to shift from the QS system to another strategy for virulence expression. In the review study by Escobar-Muciño et al. (2022), the ability of bacteria to develop QSI resistance via enhancing the affinity of QS-receptor proteins to QSIs is discussed. In addition, there are critics that were reported to point out

the limitations of QSI use as a therapeutic strategy against infectious pathogens (Krzyzek et al., 2019). As discussed above, AI-2 signaling is required for biofilm formation for both probiotics and pathogenic bacteria. The interruption of AI-2 signaling using unselective chemical inhibitors, such as furanone, would also act on probiotic gut microbiota, which would then reduce their resistance to pathogenic microorganisms (Krzyzek et al 2019). Furthermore, in Δ*agr*-mutant *Staph. aureus*, biofilm formation and higher survivability were observed, and in Δ*lasR*-mutant *P. aeruginosa*, higher production of pyocyanin (virulence factor) and pro-inflammatory responses have also been reported. These observations might restrict the efficacy of chemical QSIs (Desai et al., 2005). Finally, foodborne pathogenic bacteria could develop resistance to QSIs as shown by studies that revealed the ability of *P. aeruginosa* to develop resistance to antibiotics (carbapenems and azithromycin) that show anti-QS activity (Krzyzek et al 2019).

The potentiality to develop resistance to QSI-based therapy is prompting the opening of a new line of investigation to unravel the mechanism of probiotics for use as a substitutive chemical QSI-based therapy against infectious diseases to overcome the microbial QSI resistance.

It can be deduced that QS is an interplay in host–gut microbiome interaction. The health benefit mechanism of probiotics is either by reducing the expression of QS biofilm related genes of pathogenic bacteria or by direct impact of QS molecules on intestinal cells. However, the results are still contradictory. In Li et al. (2019), AI-2 was suggested to be involved in the progression of CRC and can be used as a marker, whereas as described by the abovementioned studies (Li et al., 2019; Zargar et al., 2015; Vestby et al., 2020; Liu et al., 2018), there is a positive role of AI-2 in the alleviation of pro-inflammatory responses. Furthermore, the AI-2 used in some of the above studies was chemically synthesized and supplemented exogenously in in vivo studies. It will be

intriguing to investigate the effect of the AI-2 secretions from probiotics on gut dysbiosis, inflammatory response, and intestine barrier health in in vivo and human studies. In addition, research on the mechanism of probiotic health benefits in the gut via QS is still lacking.

1.5 Microencapsulation and QS

Probiotic microencapsulation is used to increase stress resistance and cell viability after exposure to the outside environment, such as during passage in the gastrointestinal tract, processing, and storage (Desai et al., 2005; Shori et al., 2017). Microencapsulation of probiotics also boosts the health benefits of probiotics. An animal study found that microcapsules of *Lb. plantarum* LIP-1 reversed dysbiosis, increased colonization, and reduced lipid concentration in hyperlipidemic rats compared with free cells of LIP-1 (Song et al., 2017). In addition, microencapsulation of *Lb. plantarum* LN66 increased the survival rate under different packaging conditions and simulated a gastrointestinal environment compared with free cells (Zhang et al., 2022). It is possible that the microencapsulation mode of action on bacterial behavior is partially regulated by QS. During the incubation of microcapsulated cells, bacteria are grown in aggregates with shorter in-between cell distances than in free cells. This conduces to better AI activity and cell-to-cell communication, that is, the QS efficacy is not the same when bacterial cells are free or encapsulated. This was found in the study by Gao et al. (2016a) when *V. harveyi* cells were incorporated into microcapsules, and the QS capacity was evaluated in comparison with free cells. The results showed that the luxS gene expression was significantly higher in microencapsulated cells than in free cells, despite the cell density being lower in microcapsules after 12 h of incubation. In contrast, another study found that the viable Lb. plantarum AB-1 cells were significantly higher in microcapsules compared with free cells after 48 h of growth culturing, but the same outcome of enhanced QS was observed (Yang et al., 2019). This might be due to different types of bacteria or the experimental design. Moreover,

the size of cell aggregates plays a part in the impact of microencapsulation on QS mediated by the spatiality effect. Large cell aggregates demonstrated more effective QS than small cell aggregates (Gao et al., 2016b). Prominently, bacterial QS can be also regulated by manipulation of the microenvironment inside the microcapsules (diameter, core state, and alginate concentration). Alginate concentration and microcapsule diameter are positively correlated with AI activity and, thus, stronger QS capacity. Furthermore, when the core state of a microcapsule is solid, the size of the cell aggregate is larger than in a liquid core state. As mentioned previously, the QS is more enhanced in large cell aggregates than in small cell aggregates. The underlying mechanism of these microenvironment parameter effects is that the mass transfer of AIs inside the microcapsule is reduced in response to the increase in diameters and alginate concentration and the solidified core state. This makes the AIs restricted inside the microcapsules, which is, in turn, how the interaction of the AIs with cells is facilitated (Li et al., 2022). Considering the impact of microencapsulation on QS efficacy, it would be worth investigating whether the anti-QS and anti-biofilm effect of probiotics can be improved by microencapsulation. Until now, there is only one study that investigated the anti-biofilm activity of *Lb. rhamnosus* GG microcapsules in co-culture with *E. coli* (Deng et al., 2020). The results indicated that *E. coli* QS-related genes encoding biofilm formation (*lsrK* and *luxS*) were significantly downregulated as a result of the anti-QS activity of the microencapsulated cells of *Lb. rhamnosus* GG. Interestingly, microcapsules have not only been able to cause a remarkable decline in biofilm formation but also to erase mature biofilm. In a study conducted by Song et al. (2021), the anti-biofilm properties of microencapsulated *Lb. rhamnosus* GG were confirmed through a proteomic quantitative analysis of a co-culture of *E. coli* and the microcapsules. The microcapsules disrupted the metabolic pathway of *E. coli*, resulting in a reduction of biofilm formation and led to decreased expression of genes related to biofilm

formation and stress resistance (*dnaK* and *bamE*), although it is unclear whether this was due to QS inhibition. However, the efficacy of the anti-QS activity of the microcapsules was not compared to that of free cells, and it is important to determine to what extent the microcapsules enhance anti-QS activity. Furthermore, the QQ compounds were not identified in these studies.

1.6 Concluding remarks and future perspectives

QS serves a crucial and integral function in regulation of expression of virulence factors and in response to stress and environmental conditions. This makes QS a recent focus of research to maintain food safety and quality. Probiotics can act as QSIs by interfering with the QS activity of the target bacteria through the secretion of metabolites. The microencapsulation of probiotics is a promising strategy to enhance the anti-QS activity of probiotics. However, most of the studies in the literature are *in vitro,* with little focus on replicating the outcomes in the food matrix. Probiotics, through anti-QS activity, could play a potential role in gut health through the modulation of pro-inflammatory responses and gut microbiota. Taken together, the future research hotspot could be focused on the investigation of the following: 1) Characterization of QS system in foodborne spoilage bacteria not yet investigated for the presence of QS system, in particular spoilage *Pseudomonas* spp. 2) Identification of anti-QS compounds, and their mechanism against foodborne spoilage bacteria, particularly *Pseudomonas* spp, in food matrix; 3) The impact of microencapsulation on the anti-QS activity of probiotics and its mechanism in the food matrix; and 4) the potential role of probiotic QS in the modulation of inflammatory responses and gut microbiota in human studies. In this PhD project, the first two objectives will be researched in details to identify spoilage *Pseudomonas* species for the purpose of characterization of QS systems and control of spoilage activity by QS inhibition.

1.7 References

Garg, N.; Manchanda, G.; Kumar, A. Bacterial quorum sensing: Circuits and applications. *Antonie Leeuwenhoek* **2014**, *105*, 289–305.

Deep, A.; Chaudhary, U.; Gupta, V. Quorum sensing and bacterial pathogenicity: From molecules to disease. *J. Lab. Physicians* **2011**, *3*, 4–11.

Bourret, R.B. *Two-Component Signal Transduction*; Hoch, J.A., Silhavy, T., Eds.; ASM Press: Washington, WA, USA, 1995; Volume 2. 4. Wu, L.; Luo, Y. Bacterial quorum-sensing systems and their role in intestinal bacteria-host crosstalk. *Front. Microbiol.* **2021**, *12*, 611413.

Bai, A.J.; Rai, V.R. Bacterial quorum sensing and food industry. *Compr. Rev. Food Sci. Food Saf.* **2011**, *10*, 183–193. [] 6. Falà, A.K.; Álvarez-Ordóñez, A.; Filloux, A.; Gahan, C.; Cotter, P.D. Quorum sensing in human gut and food microbiomes: Significance and potential for therapeutic targeting. *Front. Microbiol.* **2022**, 13.

Bai, X.; Nakatsu, C.H.; Bhunia, A.K. Bacterial biofilms and their implications in pathogenesis and food safety. *Foods* **2021**, *10*, 2117.

Machado, I.; Silva, L.R.; Giaouris, E.D.; Melo, L.F.; Simões, M. Quorum sensing in food spoilage and natural-based strategies for its inhibition. *Food Res. Int.* **2020**, *127*, 108754.

Martins, M.L.; Pinto, U.M.; Riedel, K.; Vanetti, M.C.D. Quorum sensing and spoilage potential of psychrotrophic *Enterobacteriaceae* isolated from milk. *BioMed Res. Int.* **2018**, *2018*, 2723157.

Davares, A.K.L.; Arsene, M.M.J.; Viktorovna, P.I.; Vyacheslavovna, Y.N.; Vladimirovna, Z.A.; Aleksandrovna, V.E.; Nikolayevich,

S.A.; Nadezhda, S.; Anatolievna, G.O.; Nikolaevna, S.I.; et al. Quorum-Sensing Inhibitors from Probiotics as a Strategy to Combat Bacterial Cell-to-Cell Communication Involved in Food Spoilage and Food Safety. *Fermentation* **2022**, *8*, 711.

Rizzello, C.G.; Filannino, P.; Di Cagno, R.; Calasso, M.; Gobbetti, M. Quorum-sensing regulation of constitutive plantaricin by Lactobacillus plantarum strains under a model system for vegetables and fruits. *Appl. Environ. Microbiol.* **2014**, *80*, 777–787.

Song, H.; Zhang, J.; Qu, J.; Liu, J.; Yin, P.; Zhang, G.; Shang, D. Lactobacillus rhamnosus GG microcapsules inhibit Escherichia coli biofilm formation in coculture. *Biotechnol. Lett.* **2019**, *41*, 1007–1014.

Deng, Z.; Luo, X.M.; Liu, J.; Wang, H. Quorum sensing, biofilm, and intestinal mucosal barrier: Involvement the role of probiotic. *Front. Cell. Infect. Microbiol.* **2020**, *10*, 538077.

Zhao, X.; Yu, Z.; Ding, T. Quorum-sensing regulation of antimicrobial resistance in bacteria. *Microorganisms* **2020**, *8*, 425.

Qais, F.A.; Ahmad, I. Anti-quorum sensing and biofilm inhibitory effect of some medicinal plants against Gram-negative bacterial pathogens: In Vitro and in silico investigations. *Heliyon* **2022**, *8*, e11113.

Gao, Z.; Daliri, E.B.M.; Wang, J.U.N.; Liu, D.; Chen, S.; Ye, X.; Ding, T. Inhibitory effect of lactic acid bacteria on foodborne pathogens: A review. *J. Food Prot.* **2019**, *82*, 441–453.

Xu, Y.; Wang, Y.; Ding, X.; Wang, J.; Zhan, X. Inhibitory effects of reuterin on biofilm formation, quorum sensing and virulence genes of Clostridium perfringens. *LWT* **2022**, *162*, 113421.

Yun, B.; Oh, S.; Griffiths, M.W. Lactobacillus acidophilus modulates the virulence of Clostridium difficile. *J. Dairy Sci.* **2014**, *97*, 4745–4758.

Yong, C.; Lim, J.; Kim, B.K.; Park, D.J.; Oh, S. Suppressive effect of Lactobacillus fermentum Lim2 on Clostridioides difficile 027 toxin production. *Lett. Appl. Microbiol.* **2019**, *68*, 386–3933.

Li, J.; Wang, W.; Xu, S.X.; Magarvey, N.A.; McCormick, J.K. Lactobacillus reuteri-produced cyclic dipeptides quench agr-mediated expression of toxic shock syndrome toxin-1 in staphylococci. *Proc. Natl. Acad. Sci. USA* **2011**, *108*, 3360–3365.

Piewngam, P.; Zheng, Y.; Nguyen, T.H.; Dickey, S.W.; Joo, H.-S.; Villaruz, A.E.; Glose, K.A.; Fisher, E.L.; Hunt, R.L.; Li, B.; et al. Pathogen elimination by probiotic Bacillus via signalling interference. *Nature* **2018**, *562*, 532–537.

Jiang, X.; Yan, X.; Gu, S.; Yang, Y.; Zhao, L.; He, X.; Chen, H.; Ge, J.; Liu, D. Biosurfactants of Lactobacillus helveticus for biodiversity inhibit the biofilm formation of Staphylococcus aureus and cell invasion. *Future Microbiol.* **2019**, *14*, 1133–1146.

Ahn, K.B.; Baik, J.E.; Yun, C.H.; Han, S.H. Lipoteichoic acid inhibits Staphylococcus aureus biofilm formation. *Front. Microbiol.* **2018**, *9*, 327.

Kim, J.; Kim, J.; Kim, Y.; Oh, S.; Song, M.; Choe, J.H.; Whang, K.-Y.; Kim, K.H.; Oh, S. Influences of quorum-quenching probiotic bacteria on the gut microbial community and immune function in weaning pigs. *Anim. Sci. J.* **2018**, *89*, 412–422.

Kim, Y.; Kim, S.H. Released exopolysaccharide (r-EPS) produced from probiotic bacteria reduce biofilm formation of enterohemorrhagic Escherichia coli O157: H7. *Biochem. Biophys. Res. Commun.* **2009**, *379*, 324–329.

Kim, Y.; Lee, J.W.; Kang, S.G.; Oh, S.; Griffiths, M.W. Bifidobacterium spp. influences the production of autoinducer-2 and biofilm formation by Escherichia coli O157: H7. *Anaerobe* **2012**, *18*, 539–545.

Kim, Y.; Oh, S.; Park, S.; Seo, J.B.; Kim, S.H. Lactobacillus acidophilus reduces expression of enterohemorrhagic Escherichia coli O157: H7 virulence factors by inhibiting autoinducer-2-like activity. *Food Control.* **2008**, *19*, 1042–1050.

Liang, Y.; Pan, Y.; Li, Q.; Wu, B.; Hu, M. RNA-seq-based transcriptomic analysis of AHL-induced biofilm and pyocyanin inhibition in Pseudomonas aeruginosa by Lactobacillus brevis. *Int. Microbiol.* **2022**, *25*, 447–456.

Díaz, M.A.; González, S.N.; Alberto, M.R.; Arena, M.E. Human probiotic bacteria attenuate Pseudomonas aeruginosa biofilm and virulence by quorum-sensing inhibition. *Biofouling* **2020**, *36*, 597–609.

Devi, S.; Chhibber, S.; Harjai, K. Optimization of cultural conditions for enhancement of anti-quorum sensing potential in the probiotic strain Lactobacillus rhamnosus GG against Pseudomonas aeruginosa. *3 Biotech* **2022**, *12*, 133.

Azami, S.; Arefian, E.; Kashef, N. Postbiotics of Lactobacillus casei target virulence and biofilm formation of Pseudomonas aeruginosa by modulating quorum sensing. *Arch. Microbiol.* **2022**, *204*, 157.

Boopathi, S.; Vashisth, R.; Manoharan, P.; Kandasamy, R.; Sivakumar, N. Stigmatellin Y–An anti-biofilm compound from Bacillus subtilis BR4 possibly interferes in PQS–PqsR mediated quorum sensing system in Pseudomonas aeruginosa. *Bioorg. Med. Chem. Lett.* **2017**, *27*, 2113–2118.

Djokic, L.; Stankovic, N.; Galic, I.; Moric, I.; Radakovic, N.; Šegan, S.; Pavic, A.; Senerovic, L. Novel Quorum Quenching YtnP Lactonase from Bacillus paralicheniformis Reduces Pseudomonas aeruginosa Virulence and Increases Antibiotic Efficacy In Vivo. *Front. Microbiol.* **2022**, *13*, 1812.

Algburi, A.; Zehm, S.; Netrebov, V.; Bren, A.B.; Chistyakov, V.; Chikindas, M.L. Subtilosin prevents biofilm formation by inhibiting bacterial quorum sensing. *Probiotics Antimicrob. Proteins* **2017**, *9*, 81–90.

Lee, J.E.; Lee, N.K.; Paik, H.D. Antimicrobial and anti-biofilm effects of probiotic Lactobacillus plantarum KU200656 isolated from kimchi. *Food Sci. Biotechnol.* **2021**, *30*, 97–106.

Merino, L.; Trejo, F.M.; De Antoni, G.; Golowczyc, M.A. Lactobacillus strains inhibit biofilm formation of Salmonella sp. isolates from poultry. *Food Res. Int.* **2019**, *123*, 258–265.

Tazehabadi, M.H.; Algburi, A.; Popov, I.V.; Ermakov, A.M.; Chistyakov, V.A.; Prazdnova, E.V.; Weeks, R.; Chikindas, M.L. Probiotic bacilli inhibit Salmonella biofilm formation without killing planktonic cells. *Front. Microbiol.* **2021**, *12*, 615328.

Pelyuntha, W.; Chaiyasut, C.; Kantachote, D.; Sirilun, S. Cell-free supernatants from cultures of lactic acid bacteria isolated from fermented grape as biocontrol against Salmonella Typhi and

Salmonella Typhimurium virulence via autoinducer-2 and biofilm interference. *PeerJ* **2019**, *7*, e7555.

Siddique, A.; Azim, S.; Ali, A.; Adnan, F.; Arif, M.; Imran, M.; Ganda, E.; Rahman, A. Lactobacillus reuteri and Enterococcus faecium from Poultry Gut Reduce Mucin Adhesion and Biofilm Formation of Cephalosporin and Fluoroquinolone-Resistant Salmonella enterica. *Animals* **2021**, *11*, 3435.

Xu, X.; Peng, Q.; Zhang, Y.; Tian, D.; Zhang, P.; Huang, Y.; Ma, L.; Qiao, Y.; Shi, B. A novel exopolysaccharide produced by Lactobacillus coryniformis NA-3 exhibits antioxidant and biofilm-inhibiting properties In Vitro. *Food Nutr. Res.* **2020**, *64*.

Piewngam, P.; Chiou, J.; Ling, J.; Liu, R.; Pupa, P.; Zheng, Y.; Otto, M. Enterococcal bacteremia in mice is prevented by oral administration of probiotic Bacillus spores. *Sci. Transl. Med.* **2021**, *13*, eabf4692.

Adnan, M.; Siddiqui, A.J.; Hamadou, W.S.; Ashraf, S.A.; Hassan, M.I.; Snoussi, M.; Badraoui, R.; Jamal, A.; Bardakci, F.; Awadelkareem, A.; et al. Functional and structural characterization of pediococcus pentosaceus-derived biosurfactant and its biomedical potential against bacterial adhesion, quorum sensing, and biofilm formation. *Antibiotics* **2021**, *10*, 1371.

Luan, C.; Jiang, N.; Zhou, X.; Zhang, C.; Zhao, Y.; Li, Z.; Li, C. Antibacterial and anti-biofilm activities of probiotic Lactobacillus curvatus BSF206 and Pediococcus pentosaceus AC1-2 against Streptococcus mutans. *Microb. Pathog.* **2022**, *164*, 105446.

Tahmourespour, A.; Kasra-Kermanshahi, R.; Salehi, R. Lactobacillus rhamnosus biosurfactant inhibits biofilm formation and gene expression of caries-inducing Streptococcus mutans. *Dent. Res. J.* **2019**, *16*, 87.

Zhang, G.; Lu, M.; Liu, R.; Tian, Y.; Vu, V.H.; Li, Y.; Liu, B.; Kushmaro, A.; Li, Y.; Sun, Q. Inhibition of Streptococcus mutans biofilm formation and virulence by Lactobacillus plantarum K41 isolated from traditional Sichuan pickles. *Front. Microbiol.* **2020**, *11*, 774.

Dong, W.; Cai, Y.; Xu, Z.; Fu, B.; Chen, Q.; Cui, Y.; Ruan, Z.; Liang, Y.; Peng, N.; Zhao, S. Heterologous expression of AHL lactonase AiiK by Lactobacillus casei MCJΔ1 with great quorum quenching ability against Aeromonas hydrophila AH-1 and AH-4. *Microb. Cell Factories* **2020**, *19*, 191.

Hossain, M.I.; Mizan, M.F.R.; Roy, P.K.; Nahar, S.; Toushik, S.H.; Ashrafudoulla, M.; Ha, S.D. Listeria monocytogenes biofilm inhibition on food contact surfaces by application of postbiotics from Lactobacillus curvatus B. 67 and Lactobacillus plantarum M.2. *Food Res. Int.* **2021**, *148*, 110595.

Melian, C.; Segli, F.; Gonzalez, R.; Vignolo, G.; Castellano, P. Lactocin AL705 as quorum sensing inhibitor to control Listeria monocytogenes biofilm formation. *J. Appl. Microbiol.* **2019**, *127*, 911–920.

Sudan, S.; Li, J. Dispersal of pathogen-associated multispecies biofilm by novel probiotic Bacillus subtilis in a contact-dependent manner. *J. Appl. Microbiol.* **2022**, *133*, 2501–2515.

Shangguan, W.; Xie, T.; Zhang, R.; Lu, C.; Han, X.; Zhong, Q. Anti-biofilm potential of kefir-derived Lactobacillus paracasei L10 against Vibrio parahaemolyticus. *Lett. Appl. Microbiol.* **2021**, *73*, 750–758.

Lee, D.; Im, J.; Park, D.H.; Jeong, S.; Park, M.; Yoon, S.; Park, J.; Han, S.H. Lactobacillus plantarum Lipoteichoic Acids Possess Strain-Specific Regulatory Effects on the Biofilm Formation of Dental Pathogenic Bacteria. *Front. Microbiol.* **2021**, *12*, 758161.

Jeong, D.; Kim, D.H.; Song, K.Y.; Seo, K.H. Antimicrobial and anti-biofilm activities of Lactobacillus kefiranofaciens DD2 against oral pathogens. *J. Oral Microbiol.* **2018**, *10*, 1472985.

Xue, T.; Zhao, L.; Sun, H.; Zhou, X.; Sun, B. LsrR-binding site recognition and regulatory characteristics in Escherichia coli AI-2 quorum sensing. *Cell Res.* **2009**, *19*, 1258–1268.

Escobar-Muciño, E.; Arenas-Hernández, M.M.; Luna-Guevara, M.L. Mechanisms of Inhibition of Quorum Sensing as an Alternative for the Control of E. coli and Salmonella. *Microorganisms* **2022**, *10*, 884.

Zuo, J.; Yin, H.; Hu, J.; Miao, J.; Chen, Z.; Qi, K.; Wang, Z.; Gong, J.; Phouthapane, V.; Jiang, W.; et al. Lsr operon is associated with AI-2 transfer and pathogenicity in avian pathogenic Escherichia coli. *Veter. Res.* **2019**, *50*, 109.

Van Hal, S.J.; Jensen, S.O.; Vaska, V.L.; Espedido, B.A.; Paterson, D.L.; Gosbell, I.B. Predictors of mortality in Staphylococcus aureus bacteremia. *Clin. Microbiol. Rev.* **2012**, *25*, 362–386.

Bleul, L.; Francois, P.; Wolz, C. Two-component systems of S. aureus: Signaling and sensing mechanisms. *Genes* **2022**, *13*, 34.

Yu, D.; Zhao, L.; Xue, T.; Sun, B. Staphylococcus aureus autoinducer-2 quorum sensing decreases biofilm formation in an icaR-dependent manner. *BMC Microbiol.* **2012**, *12*, 288.

Ma, L.; Wang, J.; Wang, S.; Anderson, E.M.; Lam, J.S.; Parsek, M.R.; Wozniak, D.J. Synthesis of multiple Pseudomonas aeruginosa biofilm matrix exopolysaccharides is post-transcriptionally regulated. *Environ. Microbiol.* **2012**, *14*, 1995–2005.

Wilson, M.G.; Pandey, S. *Pseudomonas Aeruginosa*; StatPearls: Treasure Island, FL, USA, 2022.

Venturi, V. Regulation of quorum sensing in *Pseudomonas*. *FEMS Microbiol. Rev.* **2006**, *30*, 274–291.

Manasian, P.; Bustos, A.S.; Pålsson, B.; Håkansson, A.; Peñarrieta, J.M.; Nilsson, L.; Linares-Pastén, J.A. First evidence of Acyl-Hydrolase/Lipase activity from human probiotic bacteria: Lactobacillus rhamnosus GG and Bifidobacterium longum NCC 2705. *Front. Microbiol.* **2020**, *11*, 1534.

Toushik, S.H.; Kim, K.; Park, S.-H.; Park, J.-H.; Ashrafudoulla; Ulrich, M.S.I.; Mizan, F.R.; Hossain, I.; Shim, W.-B.; Kang, I.; et al. Prophylactic efficacy of Lactobacillus curvatus B67-derived postbiotic and quercetin, separately and combined, against Listeria monocytogenes and Salmonella enterica ser. Typhimurium on processed meat sausage. *Meat Sci.* **2023**, *197*, 109065.

Pearson, J.P.; Van Delden, C.; Iglewski, B.H. Active efflux and diffusion are involved in transport of Pseudomonas aeruginosa cell-to-cell signals. *J. Bacteriol.* **1999**, *181*, 1203–1210.

Domenech, A.; Brochado, A.R.; Sender, V.; Hentrich, K.; Henriques-Normark, B.; Typas, A.; Veening, J.W. Proton motive force disruptors block bacterial competence and horizontal gene transfer. *Cell Host Microbe* **2020**, *27*, 544–555.e3.

Sutyak Noll, K.; Sinko, P.J.; Chikindas, M.L. Elucidation of the molecular mechanisms of action of the natural antimicrobial peptide subtilosin against the bacterial vaginosis-associated pathogen Gardnerella vaginalis. *Probiotics Antimicrob. Proteins* **2011**, *3*, 41–47.

Ranadheera, R.D.C.S.; Baines, S.K.; Adams, M.C. Importance of food in probiotic efficacy. *Food Res. Int.* **2010**, *43*, 1–7.

Amit, S.K.; Uddin, M.; Rahman, R.; Islam, S.M.; Khan, M.S. A review on mechanisms and commercial aspects of food preservation and processing. *Agric. Food Secur.* **2017**, *6*, 51.

Yuan, L.; Sadiq, F.A.; Burmølle, M.; Liu, T.; He, G. Insights into bacterial milk spoilage with particular emphasis on the roles of heat-stable enzymes, biofilms, and quorum sensing. *J. Food Prot.* **2018**, *81*, 1651–1660.

Yuan, L.; Wang, N.; Sadiq, F.A.; He, G. RNA sequencing reveals the involvement of quorum sensing in dairy spoilage caused by psychrotrophic bacteria. *LWT* **2020**, *127*, 109384.

Pothakos, V.; Devlieghere, F.; Villani, F.; Björkroth, J.; Ercolini, D. Lactic acid bacteria and their controversial role in fresh meat spoilage. *Meat Sci.* **2015**, *109*, 66–74.

Yuan, L.; Sadiq, F.A.; Liu, T.J.; Li, Y.; Gu, J.S.; Yang, H.Y.; He, G.Q. Spoilage potential of psychrotrophic bacteria isolated from raw milk and the thermo-stability of their enzymes. *J. Zhejiang Univ. B* **2018**, *19*, 630–642.

Yang, Q.; Wang, Y.; An, Q.; Sa, R.; Zhang, D.; Xu, R. Research on the role of LuxS/AI-2 quorum sensing in biofilm of *Leuconostoc citreum* 37 based on complete genome sequencing. *3 Biotech* **2021**, *11*, 189.

Ng, Y.K.; Grasso, M.; Wright, V.; Garcia, V.; Williams, P.; Atkinson, S. The quorum sensing system of *Yersinia enterocolitica* 8081 regulates swimming motility, host cell attachment, and virulence plasmid maintenance. *Genes* **2018**, *9*, 307.

Opara, E.U.; Asuquo, A.A. An overview of characterization and identification of soft rot bacterium Erwinia in some vegetable crops. *Greener J. Biol. Sci.* **2016**, *6*, 46–55.

Põllumaa, L.; Alamäe, T.; Mäe, A. Quorum sensing and expression of virulence in pectobacteria. *Sensors* **2012**, *12*, 3327–3349.

Laasik, E.; Andresen, L.; Mäe, A. Type II quorum sensing regulates virulence in Erwinia carotovora ssp. carotovora. *FEMS Microbiol. Lett.* **2006**, *258*, 227–234.

Rasch, M.; Andersen, J.B.; Nielsen, K.F.; Flodgaard, L.R.; Christensen, H.; Givskov, M.; Gram, L. Involvement of bacterial quorum-sensing signals in spoilage of bean sprouts. *Appl. Environ. Microbiol.* **2005**, *71*, 3321–3330.

Fu, L.; Wang, C.; Liu, N.; Ma, A.; Wang, Y. Quorum sensing system-regulated genes affect the spoilage potential of Shewanella baltica. *Food Res. Int.* **2018**, *107*, 1–9.

Gui, M.; Wu, R.; Liu, L.; Wang, S.; Zhang, L.; Li, P. Effects of quorum quenching by AHL lactonase on AHLs, protease, motility and proteome patterns in Aeromonas veronii LP-11. *Int. J. Food Microbiol.* **2017**, *252*, 61–68.

Husain, F.M.; Ahmad, I.; Al-Shabib, N.A.; Khan, M.S.; Mohammed, Y.A.; Althubiani, A.S. Quorum sensing and biofilm inhibition by lactonase producing Bacillus amyloliquefaciens SBF1 strain isolated from date palm rhizosphere of Saudi Arabia. *J. Pure Appl. Microbiol.* **2016**, *10*, 1745–1755.

Garge, S.S.; Nerurkar, A.S. Attenuation of quorum sensing regulated virulence of Pectobacterium carotovorum subsp. carotovorum through an AHL lactonase produced by Lysinibacillus sp. Gs50. *PloS ONE* **2016**, *11*, e0167344.

Kachhadia, R.; Kapadia, C.; Singh, S.; Gandhi, K.; Jajda, H.; Alfarraj, S.; Ansari, M.J.; Danish, S.; Datta, R. Quorum sensing inhibitory and quenching activity of Bacillus cereus RC1 extracts on Soft Rot-Causing Bacteria Lelliottia amnigena. *ACS Omega* **2022**, *7*, 25291–25308.

Coquant, G.; Aguanno, D.; Brot, L.; Belloir, C.; Delugeard, J.; Roger, N.; Pham, H.-P.; Briand, L.; Moreau, M.; de Sordi, L.; et al. 3-oxo-C12: 2-HSL, quorum sensing molecule from human

intestinal microbiota, inhibits pro-inflammatory pathways in immune cells via bitter taste receptors. *Sci. Rep.* **2022**, *12*, 9440.

Landman, C.; Grill, J.P.; Mallet, J.M.; Marteau, P.; Humbert, L.; Le Balc'h, E.; Maubert, M.-A.; Perez, K.; Chaara, W.; Brot, L.; et al. IBD Network. Inter-kingdom effect on epithelial cells of the N-Acyl homoserine lactone 3-oxo-C12: 2, a major quorum-sensing molecule from gut microbiota. *PLoS ONE* **2018**, *13*, e0202587.

Thompson, J.A.; Oliveira, R.A.; Djukovic, A.; Ubeda, C.; Xavier, K.B. Manipulation of the quorum sensing signal AI-2 affects the antibiotic-treated gut microbiota. *Cell Rep.* **2015**, *10*, 1861–1871.

Deng, Z.; Dai, J.; Wei, Y.; Ma, Y.; Mao, Y.; Zhang, J.; Hua, W.; Wang, H. Comparison between Lactobacillus rhamnosus GG and LuxS-deficient strain in regulating gut barrier function and inflammation in early-weaned piglets. *Front. Immunol.* **2022**, *13*, 1080789.

Ji, Y.-C.; Sun, Q.; Fu, C.-Y.; She, X.; Liu, X.-C.; He, Y.; Ai, Q.; Li, L.-Q.; Wang, Z.-L. Exogenous Autoinducer-2 Rescues Intestinal Dysbiosis and Intestinal Inflammation in a Neonatal Mouse Necrotizing Enterocolitis Model. *Front. Cell. Infect. Microbiol.* **2021**, *11*, 694395.

Fteita, D.; Könönen, E.; Gürsoy, M.; Ma, X.; Sintim, H.O.; Gürsoy, U.K. Quorum sensing molecules regulate epithelial cytokine response and biofilm-related virulence of three Prevotella species. *Anaerobe* **2018**, *54*, 128–135.

Li, Q.; Peng, W.; Wu, J.; Wang, X.; Ren, Y.; Li, H.; Peng, Y.; Tang, X.; Fu, X. Autoinducer-2 of gut microbiota, a potential novel marker for human colorectal cancer, is associated with the activation of TNFSF9 signaling in macrophages. *Oncoimmunology* **2019**, *8*, e1626192.

Zargar, A.; Quan, D.N.; Carter, K.K.; Guo, M.; Sintim, H.O.; Payne, G.F.; Bentley, W.E. Bacterial secretions of nonpathogenic Escherichia coli elicit inflammatory pathways: A closer investigation of interkingdom signaling. *Mbio* **2015**, *6*, e00025-15.

Vestby, L.K.; Grønseth, T.; Simm, R.; Nesse, L.L. Bacterial biofilm and its role in the pathogenesis of disease. *Antibiotics* **2020**, *9*, 59.

Liu, L.; Wu, R.; Zhang, J.; Li, P. Overexpression of luxS promotes stress resistance and biofilm formation of Lactobacillus paraplantarum L-ZS9 by regulating the expression of multiple genes. *Front. Microbiol.* **2018**, *9*, 2628.

Sun, Z.; He, X.; Brancaccio, V.F.; Yuan, J.; Riedel, C.U. Bifidobacteria exhibit LuxS-dependent autoinducer 2 activity and biofilm formation. *PLoS ONE* **2014**, *9*, e88260.

Coquant, G.; Grill, J.P.; Seksik, P. Impact of N-acyl-homoserine lactones, quorum sensing molecules, on gut immunity. *Front. Immunol.* **2020**, *11*, 1827.

Krzyzek, P. Challenges and limitations of anti-quorum sensing therapies. *Front. Microbiol.* **2019**, *10*, 2473.

Desai, K.G.H.; Jin Park, H. Recent developments in microencapsulation of food ingredients. *Dry. Technol.* **2005**, *23*, 1361–1394.

Shori, A.B. Microencapsulation improved probiotics survival during gastric transit. *HAYATI J. Biosci.* **2017**, *24*, 1–5.

Song, J.J.; Tian, W.J.; Kwok, L.Y.; Wang, Y.L.; Shang, Y.N.; Menghe, B.; Wang, J.G. Effects of microencapsulated Lactobacillus plantarum LIP-1 on the gut microbiota of hyperlipidaemic rats. *Br. J. Nutr.* **2017**, *118*, 481–492.

Zhang, M.; Yin, C.; Qian, J. Microencapsulation of Lactobacillus plantarum LN66 and its survival potential under different packaging conditions. *J. Microencapsul.* **2022**, *39*, 601–608.

Gao, M.; Song, H.; Liu, X.; Yu, W.; Ma, X. Improved quorum sensing capacity by culturing Vibrio harveyi in microcapsules. *J. Biosci. Bioeng.* **2016**, *121*, 406–412.

Yang, X.; Li, J.; Shi, G.; Zeng, M.; Liu, Z. Improving 3-phenyllactic acid production of Lactobacillus plantarum AB-1 by enhancing its quorum-sensing capacity. *J. Food Sci. Technol.* **2019**, *56*, 2605–2610.

Gao, M.; Zheng, H.; Ren, Y.; Lou, R.; Wu, F.; Yu, W.; Liu, X.; Ma, X. A crucial role for spatial distribution in bacterial quorum sensing. *Sci. Rep.* **2016**, *6*, 34695.

Li, C.; Gao, M.; Zheng, G.; Ma, X.; Liu, X.; Yu, W. Enhanced quorum sensing capacity via regulating microenvironment to facilitate stress resistance of probiotic in alginate-based microcapsules. *Int. J. Biol. Macromol.* **2022**, *225*, 605–614.

Song, H.; Lou, N.; Liu, J.; Xiang, H.; Shang, D. Label-free quantitative proteomic analysis of the inhibition effect of Lactobacillus rhamnosus GG on Escherichia coli biofilm formation in co-culture. *Proteome Sci.* **2021**, *19*, 4.

2 Isolation and Characterization of AHL-QS Based System of Highly Proteolytic *Pseudomonas* Species

2.1 Introduction

Microbial spoilage is a primary limiting factor of shelf-life of dairy products. Psychrotrophic bacteria, in particular *Pseudomonas* spp, are the main responsible of spoilage in dairy foods (Rauh et al., 2022). This microorganisms' effect on shelf-life is a direct consequence of their ability to produce thermostable proteases, which remain active even at low temperatures during cold storage (Meng et al., 2017). An example is represented by the production of a thermostable protease encoded by *aprX* gene in the *P. fluoroscens* group isolated from dairy products (Andreani et al., 2016). Raw milk is a main harbor of *Pseudomonas* spp, and this makes it a concern for the dairy industry that refrigerates raw milk until thermal processing (Capodifoglio et al., 2016). As a general role, the production of spoilage virulence factors such as proteases, lipases, and biofilm formation is regulated by a mechanism called quorum sensing (QS) (Abbamondi et al. 2022). It is a bacterial mechanism for cell-to-cell communication that takes place within the same or different species when the bacteria grow to high cell density, and it is controlled by molecules called autoinducers (AIs). These molecules bind to their cognate receptor proteins to induce QS-related gene expression. In most Gram-negative bacteria, the LuxI-LuxR-type QS system is involved in the regulation of gene expression. In this system, N-acyl homoserine lactones (AHLs) are synthesized by the *luxI* gene or its homologues. The AHLs then bind to their receptor protein (LuxR-type), encoded by the *luxR* gene, to form the LuxR-AHL complex. QS-related genes are then expressed after this complex bind to the genomic DNA (Garg et al., 2014). The association of QS with food spoilage was demonstrated in several types of foods (fish, meat, milk, and

vegetables), where QS signals such as 3-oxo-C6-HSL, C4-HSL, and C6-HSL were detected following spoilage (Machado et al., 2020, Yuan et al., 2018). The regulation of spoilage activity (protease, lipase, off-flavours and pigments) by AHL-QS system in dairy-borne *Pseudomonas* spp was previously discussed. For example, due to the activity of QS-regulated *aprX-lipA2* operon by *P. azotoformans* and *P. fluorescence*, or by the synthesis of the dark pigment pyomelanin by *P. lactis* strain isolated from mozzarella cheese (Quintierei et al., 2019; Quintieri et al., 2020). Besides the role in food quality, QS is also associated with the regulation of antimicrobial resistance (AMR) in foodborne pathogenic bacteria (Raju et al., 2022). The wide use of antibiotics and food preservatives enhances the emergence of AMR. This was reported in many studies that isolated antibiotic resistant spoilage Pseudomonas species from dairy samples (Quintieri et al., 2019). The application of QS inhibitors reduces the risk of AMR development and would be advantageous for the food industry, albeit the relation of QS with AMR in foodborne-spoilage bacteria is still not explored. QS inhibitors are less likely to promote AMR because this microbial communication mechanism controls virulence factors that are not critical for bacterial survival in the environment. As a result, targeting this pathway applies minimal selective pressure, reducing the chance of resistance emerging (Vendeville et al., 2005).

A few species of spoilage *Pseudomonas* isolated from raw milk are identified with the AHL-type QS system. This study aimed to characterize the AHL-type QS system in *Pseudomonas* isolates with high proteolytic activity sourced from raw milk for the purpose to identify QS inhibitors for controlling milk proteolysis.

2.2 Material and methods

2.2.1 Reference bacterial strains and their experimental roles

The C6-HSL overproducing strain *Chromobacterium subtsugae* ATCC 31532, and its AHL-negative mutant *C. subtsugae* CV026, were purchased from the American Type Culture Collection (ATCC) and National Collection of Type Collection (NCTC), respectively. *C. subtsugae* CV026 was used as biosensor strain for short chain AHL production. The *Agrobacterium tumefaciens* NT1 was kindly provided by Prof. Vittorio Venturi from International Center for Genetic Engineering and Biotechnology (34149 Trieste, Italy). Unless stated, the strains were routinely grown overnight in Luria Bertani (LB; Sigma Aldrich, Milan, Italy) at 25℃.

2.2.2 Chemicals

AHL standards (C4-HSL, C6-HSL, C8-HSL, 3-oxo-C6-HSL, and 3-oxo-C10-HSL), formic acid (FA), acetonitrile (ACN), trifluoroacetic acid (TFA), 5-bromo-4-chloro-3-indolyl-β-D-galactopyranoside (X-gal) were purchased from Sigma-Aldrich (Milan, Italy). 2-Cyano-3-(4-hydroxyphenyl) acrylic acid (HCCA) was purchased from Bruker Daltonics (Germany). AHL standards were dissolved in methanol to prepare the stock solution and stored at -20℃. Similarly, X-gal was dissolved at a concentration of 20 mg/ml in N, N-dimethylformamide.

2.2.3 Isolation of Pseudomonas

Eight samples of raw milk were collected from dairy factories, transported to the laboratory within 4 hours at 4°C, and processed within 24 hours. For isolation of *Pseudomonas*, 1 ml of each sample was 10-fold diluted in quarter strength Ringer solution and spread plated on *Pseudomonas* CFC Selective Agar (Oxoid Ltd., Basingstoke, United Kingdom). The plates were incubated at 25℃ for 48 hours. Five colonies were selected from each plate and purified onto a new Pseudomonas CFC

Selective Agar plate and incubated at 25℃ for 48 hours. Purified isolates were then tested for oxidase, catalase, and Gram as previously described in the study of Zarei et al. (2020).

2.2.4 Screening of proteolytic activity

The potential Pseudomonas isolates were screened for their proteolytic activity by skim milk assay. Briefly, fresh colonies of each putative *Pseudomonas* isolate grown on LB agar were line streaked on skim milk agar (5%, w/v, Oxoid Ltd, Basingstoke, United Kingdom) and incubated at 25℃ and 4℃ for 2-3 days. The presence of a clear halo around the streak line was indicative of proteolysis.

2.2.5 Molecular identification of the putative Pseudomonas *isolates*

2.2.6 *Identification by MALDI-TOF mass spectrometry*

Isolates showing high proteolytic activity at 25℃ and 4℃ were subjected for identification by MALDI-TOF mass spectrometry analysis by using the MALDI Biotyper® (Bruker). Briefly, the *Pseudomonas* isolates were first grown on LB agar for 24 hours at 25℃. Loopful of colonies was directly smeared onto the MALDI target plate and overlaid with 1 µl of 70% formic acid. After air dry, 1 µl of HCCA matrix solution (prepared with standard solvent composed of ACN 50%, water 47.5%, and TFA 2.5% was dropped and the plate left again to dry at room temperature before the analysis. The identification outcome of the MALDI Biotyper® (Bruker) is released as a log (score). A score ≥ 2 indicates a high-confident identification at the species level, and a score between 1.77 and 2 indicates a successful identification at the genus level, according to the manufacturer's instructions.

2.2.7 *16S rRNA gene sequencing*

The same isolates were identified by 16S rRNA gene analysis. Each isolate was grown in LB overnight at 25°C and the DNA was extracted from cell pellets using the bacterial DNA isolation kit (Qiagen, Milan, Italy). The 16S rRNA analysis was conducted as previously described by Senatore et al. (2020). The isolates were identified by searching for the 16S rRNA nucleotide sequence using the BLAST program in the NCBI databases, with a cut-off value of 97%.

2.2.8 Cross feeding assay for AHL detection

CV026 biosensor strain was employed for the detection of short-chain AHLs. CV026 is unable to produce violacein by itself due to the lack of *luxI* gene for AHL synthesis. Instead, it produces violacein in response to an exogenous source of short chain AHLs. A cross-feeding assay was applied to qualitatively assess AHL production in the *Pseudomonas* isolates exhibiting high proteolytic activity as stated before (Ravn et al., 2001). Briefly, fresh colonies of the reporter strain CV026 and the test *Pseudomonas* isolates were streaked in parallel, at minimal distance, on LB agar and incubated for 48 hours at 27°C. ATCC 31532 was set for positive control. The production of violacein by CV026 indicates the test isolate is an AHL-producing strain.

2.3 Identification of AHLs

2.3.1 *AHL extraction*

A volume of 350 ml of *Pseudomonas* culture, grown in LB until the stationary phase, was centrifuged (6483 × *g* for 20 minutes at 4°C) to obtain a cell-free medium (CFM). CFM was extracted thrice with an equal volume of ethyl acetate (EA). The extract was first concentrated at 35°C by using a rotary evaporator (Rotovapor®, BUCHI), then dried under nitrogen gas flow until total desiccation. The CFM extract was stored at -20°C until processing.

2.3.2 *Thin layer chromatography (TLC)-overlay assay*

CFM extracts (2.5 mg) and standards (C4-HSL 400 μM, C6-HSL 100 μM, C8-HSL 400 μM, 3-oxo-C6-HSL 100 μM, 3-oxo-C8-HSL 100 μM, and 3-oxo-C10-HSL 400 μM) were applied to RP-C18 thin-layer chromatography (TLC) plates (20 × 20 cm; VWR International), and developed by using methanol/H_2O 60:40 as mobile phase. After the mobile phase reached the top, the plates were left to dry for 10 minutes at room temperature and overlaid with the biosensor cultures. For the detection of short chain AHLs, 200 ml of LB soft agar (0.6% w/v) supplemented with kanamycin (50 μg/ml) and inoculated with 1% fresh overnight culture of CV026 was poured onto the TLC plate. For medium and long chain AHLs detection, the TLC plate was overlaid with 200 ml of ATGN (Tempé et al. 1977) soft agar supplemented with glucose (0.5% w/v), X-Gal (40 μg/ml), gentamycin (30 μg/ml), and inoculated with 1% fresh overnight culture of NT1. The TLC plates were kept in sterilized containers and incubated at 28℃ for 24-48 hours.

2.3.3 *UPLC-MS analysis of AHL extract*

LC-MS analyses were performed as reported in Abbamondi et al (2016), with a slight modification. Briefly, chromatographic runs were acquired on an Acquity UPLC System (Waters, Milford, MA, USA) coupled to a API 3200 Triple Quadrupole mass spectrometer (Sciex, Foster City, CA, USA) with Turbo VTM interface equipped with a turbo ion spray probe used in positive ion mode, using an Acquity UPLC BEH C_{18} column (100 × 2.1 mm, i.d. 1.7 μm, Waters, Milford, MA, USA). MilliQ water was used as eluent A and ACN as eluent B. A linear gradient profile was programmed from 10% to 100% B in 1.0 min and remained at 100% B for 3.0 min, followed by a re-equilibration step at 10% B of 2 min. Separations were performed at a temperature of 60 °C, using

a flow rate of 0.7 mL min^{-1}. The extracts were resuspended in methanol at a final concentration of 5 mg/ml, and an injection volume of 5 µL was used.

Multiple Reaction Monitoring (MRM) experiment was used to collect data by setting the following source parameters: curtain gas (N_2), 20 psi; ion source gas (GS1), 55 psi; turbo-gas (GS2), 70 psi; desolvation temperature, 550°C; collision activated dissociation gas (CAD), 4 a.u.; and ion spray voltage, 5500 V. The ions monitored in Q1 included the parent AHL molecular ions $[M+H]^+$, while Q3 was set at *m/z* 102 corresponding to the lactone moiety. Analyst software (version 1.6.2; SCIEX) was used for data acquisition and analysis.

2.4 Results and discussion

2.4.1 Molecular identification of highly proteolytic Pseudomonas isolates

A total of 40 isolates potentially belonging to *Pseudomonas* were obtained according to the results of the biochemical characteristics (oxidase and catalase positive, Gram-negative and microscopic rod-shaped cells). Six isolates exhibited high proteolytic activity at 4℃ and 25℃ after 2 and 3 incubation days, respectively. The results of skim milk assay are shown in **Appendix A**: Skim milk assay for *P. gessardii* isolates. The six isolates were then identified at species level.

Both MALDI-TOF MS and 16S rRNA analyses shared the same identification results at the genus level and confirmed that all the proteolytic isolates are *Pseudomonas*. A slight discrepancy in the result at species level was found by comparing the two methods. The 16S rRNA sequencing reported 1 strain as *P. gessardii*, 3 strains with equal identity percentage between *P. gessardii* and *P. synxantha*, and 2 strains with the same identity percentage between *P. gessardii, P. synxantha,* and *P. mucidolens* (**Table 4**). Such inconclusive identification could be potentially due to the high similarity of sequencing between these 3 species, which is one of the limitations of bacterial

identification by 16S rRNA gene sequencing. However, the MALDI-TOF MS analysis confirmed the isolates as *P. gessardii* with high confidence level (log score > 2) and they are classified in the group of *P. fluorescens* (**Table 4**). Additionally, growth curve analysis during 48-hour incubation at 25℃ revealed that all the isolates displayed variant growth patterns (**Appendix B**: Growth curves of *P. gessardii* strains), showing that they are probably different strains of *Pseudomonas*.

Table 4. Results of identification of the *Pseudomonas* isolates at the species level by using 16S rRNA and MALDI-TOF MS analyses.

Isolate	16S rRNA		MALDI-TOF MS	
	Identified species	Identity percentage	Identified species	Log score
BV1	*P. synxantha* *P. gessardii*	99.31	*P. gessardii*	2.21
BV5	*P. synxantha* *P. gessardii* *P. mucidolens*	99.00	*P. gessardii*	2.10
BV6	*P. synxantha* *P. gessardii*	99.91	*P. gessardii*	2.12
CP15	*P. synxantha* *P. gessardii*	98.50	*P. gessardii*	2.19
RWV1	*P. synxantha* *P. gessardii* *P. mucidolens*	98.45	*P. gessardii*	2.19
RWV6	*P. gessardii*	98.59	*P. gessardii*	2.17

As visually observed from the results of skim milk assay, the proteolytic activity was higher at 25℃. However, despite at a lower level, all the strains produced remarkable levels of proteases to induce proteolytic activity at 4℃. Amongst the isolates, *P. gessardii* RWV6 was the most proteolytic active at the latter temperature, while *P. gessardii* CP15 was the least active (**Appendix A**: Skim milk assay for *P. gessardii* isolates). Earlier studies similarly reported *P. gessardii* as one of the most occurring spoilage species isolated from raw milk and capable of inducing proteolytic activity during cold storage conditions (Zarei et al., 2020; Zhang et al., 2020). In the work of Meng et al. (2017), the proteolytic activity of *P. gessardii* isolates was seen after 2-3 days at 4℃. In accordance, *P. gessardii* is a frequent spoilage species in dairy products at a wide range of temperatures. Yet, the regulatory mechanism of the proteolytic activity by AHL-based QS system is not characterized.

2.4.2 Detection of short chain AHL production

CV026 biosensor strain responds well to C4-HSL, C6-HSL, and C8-HSL by production of violacein, but it is insensitive to AHL with acyl chain C10 and longer. Here, it was utilized to qualitatively screen for the presence of AHL-QS based system in the *P. gessardii* isolates. As seen in (**Figure 1**), all the strains were able to induce violacein production in CV026, indicating the production of short chain AHLs by the tested isolates. Seemingly, each tested strain prompted violacein synthesis at different degrees, supporting the point that these isolates are different strains of *Pseudomonas*.

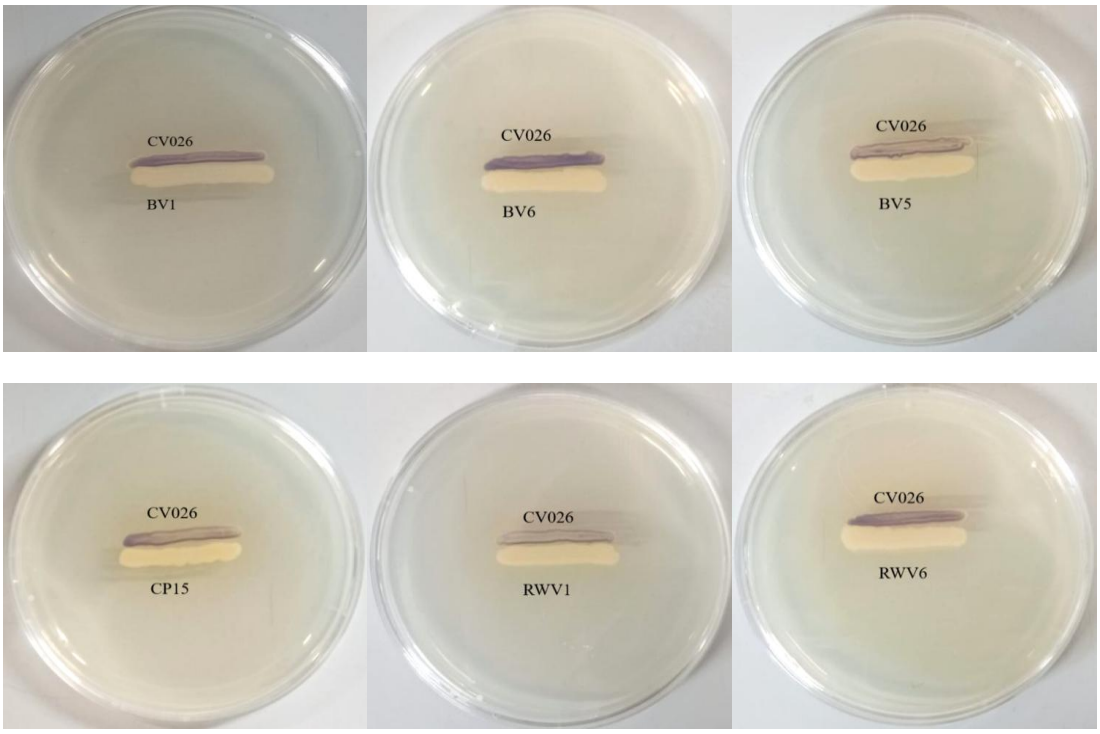

Figure 1. Cross feeding assay with CV026 biosensor for detection of AHL synthesis by the *P. gessardii* strains.

2.4.3 Characterization of AHLs by TLC-overlay assay

The ethyl acetate AHL extracts obtained from the cell-free medium of *Pseudomonas* cultures were loaded onto a C18-reversed phase plate to allow for chromatographic separation of the acylated homoserine lactones. Each type of AHL exhibits characteristic mobility on the TLC-plate, and the response of the biosensor strain is visualized by the formation of colored spots on the plate (violacein purple and blue in the case CV026 and NT1 biosensor strains, respectively). TLC-CV026 assay showed that all the extracts induced production of violacein spots (**A & B**), and their migration pattern were identical to those of C6-HSL and C4-HSL, respectively (**Figure 2**), marking first evidence that all the tested strains produce C4-HSL and C6-HSL. In the TLC-overlay assay with the *A. tumefaciens* NT1 biosensor, we observed the development of light blue spots in some of the extracts, suggesting the possible presence of long-chain and 3-oxo-AHLs (**Figure S6**).

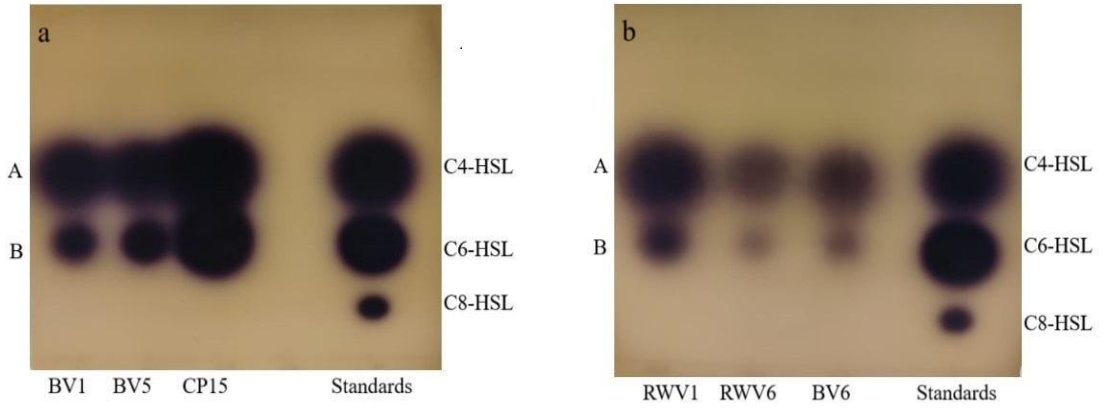

Figure 2. TLC-overlay assay using CV026 (a & b) as biosensor. The letters A and B represent the induction spots produced from C4-HSL and C6-HSL putatively present in the extract, respectively.

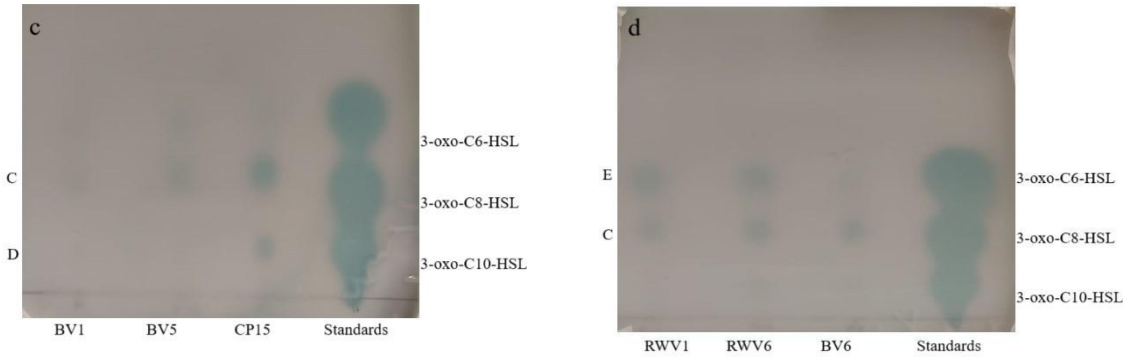

Figure 3. TLC-overlay assay using NT1 (c & d) as biosensor. 3-oxo-C8-HSL, 3-oxo-C10-HSL, and 3-oxo-C6-HSL were used as reference standards. Light blue spots indicating positive responses in the TLC-overlay assay are visible in the figure; their Rf values are marked with the letters C, D, and E, respectively.

To confirm the molecular identification of the AHLs, the extracts were analyzed by UPLC-MS/MS by using the MRM method. The characteristic product ion *m/z* 102, which represents the protonated homoserine lactone obtained by fragmentation of the AHL parental ion ($[M+H]^+$), was selected for the specific identification of AHL derivatives

(Cutignano, 2019; Abbamondi et al., 2016). In all the extracts (**Figure 6A-F**), a peak at a retention time (Rt) of 0.63 minutes was clearly identified as corresponding to C4-HSL (**Figure 6**), consistent with TLC-CV026 overlay results. Conversely, C6-HSL (Rt 0.84, **Figure 6B**) was unambiguously detected only in BV5 and CP15 (**Figure 6B** and **D**). In the other strains, the C6-HSL was either barely detectable or possibly present at concentrations below the detection limit under our experimental conditions (**Figure 6A, C, E-F**). No long-chain or 3-oxo-AHLs were detected by MS in the extracellular medium, hence the light blue spots observed in the TLC-overlay assay with the NT1 biosensor should be attributed to false positive response due to AHL-mimicking compounds. This behavior has been already described in the literature, where biosensors for AHL detection were activated by diketopiperazines, as shown in the study of Tommonaro et al. (2012).

The genes for AHL synthase and its cognate receptor were previously determined in *P. gessardii* and are deposited in the GenBank database of NCBI with accession numbers of BBLQ94_RS12060 and BLQ94_RS12065, respectively. Yet, this is the first report that phenotypically characterizes the AHL-QS based system in *P. gessardii*. Based on our qualitative analysis, C4-HSL was consistently detected in all tested *P. gessardii* isolates, while C6-HSL was clearly identified in BV5 and CP15. No evidence of long-chain AHL production was found in the present study; however, this aspect warrants further investigation under alternative cultivation conditions.

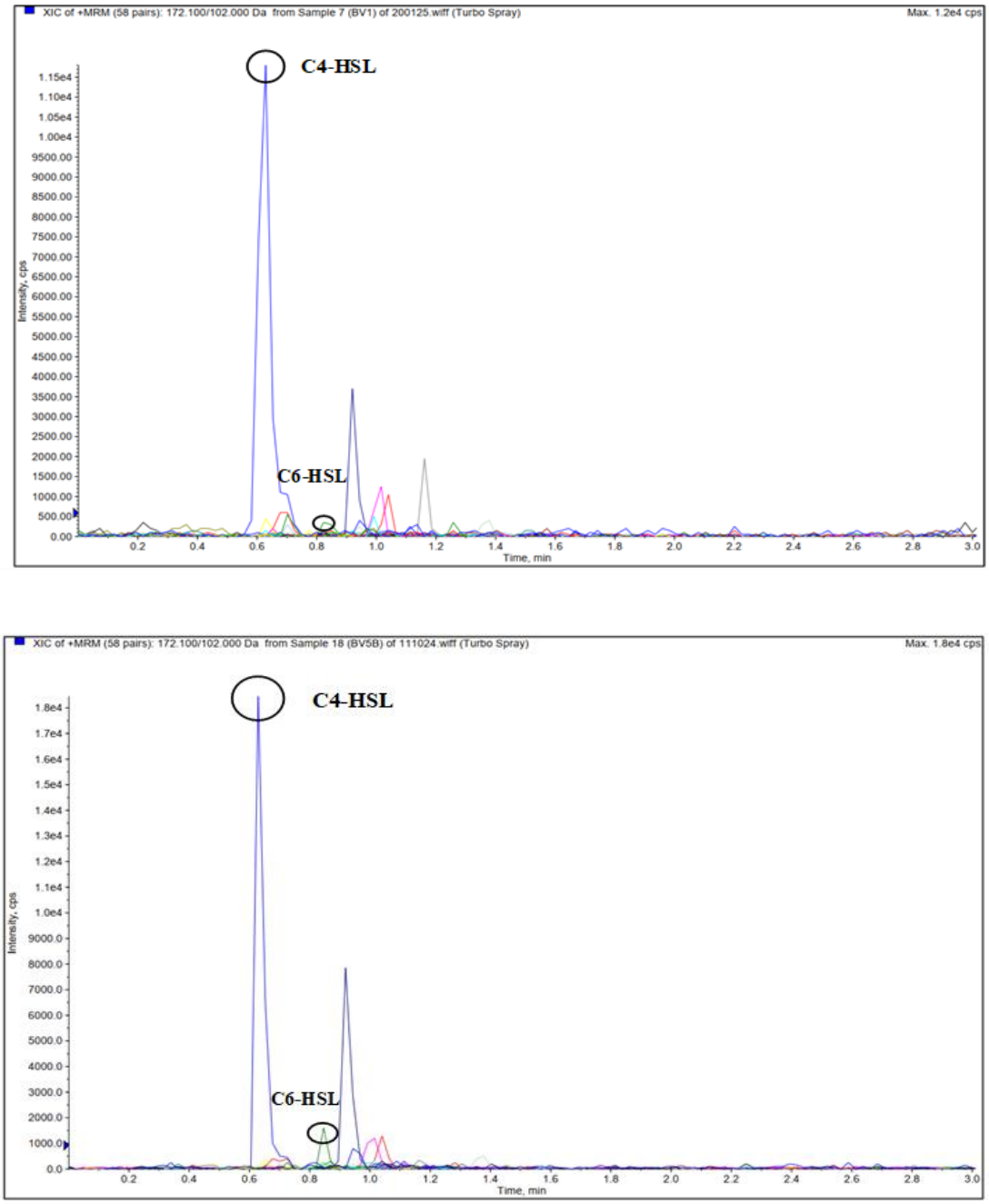

Figure 4A. Product ions chromatograms of the AHL extracts obtained by UPLC-MS/MS analysis. The peaks of ion transitions 172 > 102 m/z at Rt of 0.63 min and 200.20 > 102 m/z at Rt of 0.84 min are attributed to C4-HSL and C6-HSL, respectively. Letters A and B represent the data for *P. gessardi* BV1 and BV5, respectively.

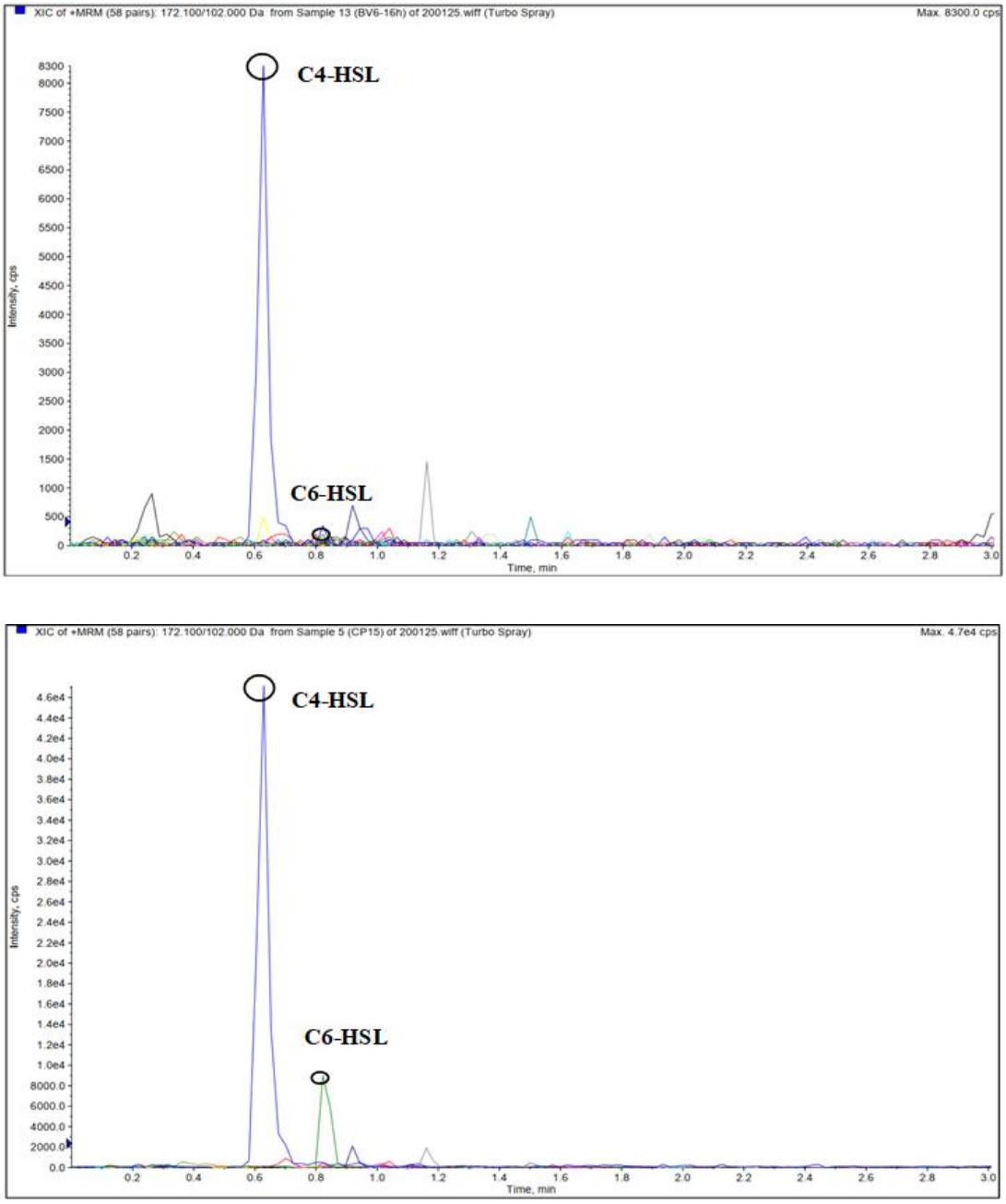

Figure 5B. Product ions chromatograms of the AHL extracts obtained by UPLC-MS/MS analysis. The peaks of ion transitions 172 > 102 m/z at Rt of 0.63 min and 200.20 > 102 m/z at Rt of 0.84 min are attributed to C4-HSL and C6-HSL, respectively. Letters C and D represent the data for *P. gessardi* BV6 and CP15, respectively.

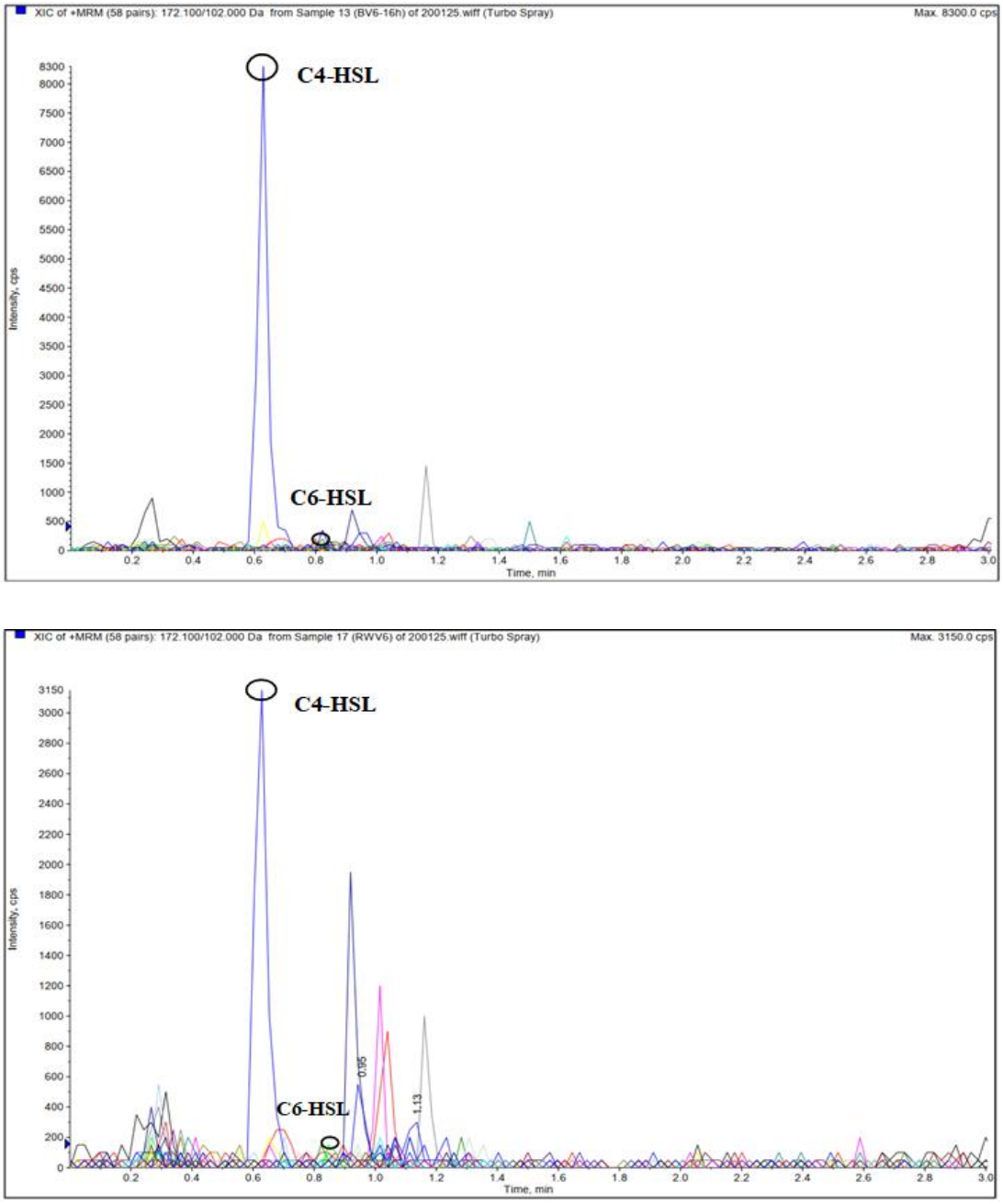

Figure 6C. Product ions chromatograms of the AHL extracts obtained by UPLC-MS/MS analysis. The peaks of ion transitions 172 > 102 m/z at Rt of 0.63 min and 200.20 > 102 m/z at Rt of 0.84 min are attributed to C4-HSL and C6-HSL, respectively. Letters F and H represent the data for *P. gessardi* RWV1 and RWV6, respectively.

The production of different AHLs by *Pseudomonas* spp was previously shown in similar studies. In Lui et al. (2007), C4-HSL and 3-oxo-C8-HSL were produced by *P. flouroscens* 395, which was isolated from Canadian raw milk samples. *P. azotoformans*, an isolate from Chinese raw milk samples, was reported to produce C6-HSL (Yuan et al., 2018). These are the only two reported cases in the literature where the AHL-QS system has been investigated in *Pseudomonas* isolates from raw milk.

2.5 Conclusion

P. gessardii is a main proteolytic activity species at 4℃ and 25℃ found in the raw milk that causes spoilage in dairy products during the storage. CV026 biosensor assays and LC-MS/MS analysis showed production of C4-HSL by all the strains. The regulation of the spoilage activity by LuxR/LuxI-QS system is then potential.

2.6 References

Rauh, V., & Xiao, Y. (2022). The shelf life of heat-treated dairy products. International Dairy Journal, 125, 105235.

Meng, L., Zhang, Y., Liu, H., Zhao, S., Wang, J., & Zheng, N. (2017). Characterization of *Pseudomonas* spp. and associated proteolytic properties in raw milk stored at low temperatures. Frontiers in microbiology, 8, 2158.

Andreani, N. A., Carraro, L., Fasolato, L., Balzan, S., Lucchini, R., Novelli, E., & Cardazzo, B. (2016). Characterisation of the thermostable protease AprX in strains of Pseudomonas fluorescens and impact on the shelf-life of dairy products: Preliminary results. Italian journal of food safety, 5(4).

Capodifoglio, E., Vidal, A. M. C., Lima, J. A. S., Bortoletto, F., D'Abreu, L. F., Gonçalves, A. C. S., ... & Netto, A. S. (2016). Lipolytic and proteolytic activity of *Pseudomonas* spp. isolated during milking and storage of refrigerated raw milk. Journal of Dairy Science, 99(7), 5214-5223.

Abbamondi GR, Tommonaro G (2022). Research Progress and Hopeful Strategies of Application of Quorum Sensing in Food, Agriculture and Nanomedicine. Microorganisms, 10(6), 1192.

Garg, N., Manchanda, G., & Kumar, A. (2014). Bacterial quorum sensing: circuits and applications. Antonie Van Leeuwenhoek, 105, 289-305.

Machado, I., Silva, L. R., Giaouris, E. D., Melo, L. F., & Simões, M. (2020). Quorum sensing in food spoilage and natural-based strategies for its inhibition. Food Research International, 127, 108754.

Yuan, L., Sadiq, F. A., Burmølle, M., Liu, T., & He, G. (2018). Insights into bacterial milk spoilage with particular emphasis on the roles of heat-stable enzymes, biofilms, and quorum sensing. Journal of Food Protection, 81(10), 1651-1660.

Quintieri, L., Caputo, L., De Angelis, M., & Fanelli, F. (2020). Genomic analysis of three cheese-borne *Pseudomonas lactis* with biofilm and spoilage-associated behavior. Microorganisms, 8(8), 1208.

Quintieri, L., Caputo, L., Brasca, M., & Fanelli, F. (2021). Recent Advances in the Mechanisms and Regulation of QS in Dairy Spoilage by Pseudomonas spp. *Foods*, *10*(12), 3088.

Zarei, M., Mohammadpour, H., Gharibi, D., & Borujeni, M. P. (2020). Identification of *Pseudomonas jessenii* and *Pseudomonas gessardii* as the most proteolytic Pseudomonas isolates in Iranian raw milk and their impact on stability of sterilized milk during storage. Journal of Dairy Research, 87(3), 368-374.

Zhang, D., Palmer, J., Teh, K. H., & Flint, S. (2020). Identification and selection of heat-stable protease and lipase-producing psychrotrophic bacteria from fresh and chilled raw milk during up to five days storage. Lwt, 134, 110165.

Tommonaro, G., Abbamondi, G. R., Iodice, C., Tait, K., & De Rosa, S. (2012). Diketopiperazines produced by the halophilic archaeon, Haloterrigena hispanica, activate AHL bioreporters. Microbial ecology, 63, 490-495.

3 Genetic Characterization of AHL-QS system in *P. gessardii* and Regulation of Proteolytic Activity by AHLs

3.1 Introduction

LuxR/I-type is the primary QS system present in spoilage Gram-negative bacteria, including *Pseudomonas* spp., and it is involved in the expression of spoilage virulence factors. In addition to the presence of canonical AHL-QS system, some *Pseudomonas* strains have the same system but incomplete, where the *luxR* gene is not paired with its cognate *luxI*. This type of *luxR* is called *luxR* solo or orphan *luxR*. *P. fluoroscens* is a main type of spoilage species widely investigated in terms of the of AHL-QS system. In the study of Tang et al (2019), *P. fluorescence* PF07 an isolate from fish spoiler, was found to have one canonical *luxR* and one *luxR* solo. In this study, the construction of mutation in *luxI* was associated with a decrease in biofilm formation, exopolysaccharides and protease production, and low stress resistance. However, the role of *luxR* solo in this strain remains unclear. In a similar way, the addition of exogenous C4-HSL to *P. fluoroscens* PF08 culture resulted in repression of biofilm, motility and protease-related genes (Wang et al., 2022). In the same strain, the gene of *luxR* solo was detected in the genome and was annotated as *evgA*, and it is expressed in response to exogenous C14-HSL. The deletion of this gene attenuated the spoilage activity by the strain (proteolytic and lipolytic activity, motility and biofilm formation) when it was inoculated in salmon fillets (Li et al., 2024). Recent research revealed, in an isolate of *P. fluoroscens* from fish meat, carbohydrate and amino acid metabolism and their related genes were downregulated due to the induced mutation in *luxI*, that ultimately lead to reduction in biogenic amines (Ding et al., 2025). In the same study, the QS-related phenotypes (protease, EPS, motility, biofilm formation) were reduced in the mutant-type,

comparing with the wild-type. Another strain of *P. psychrophila* isolated from fish freshwater, its AHL-QS system is related with production of protease enzymes and biofilm formation (Bai and Rai 2014). However, these isolates of *P. fluoroscens* are obtained from aquatic products. Only two species of *P. fluoroscens* and *P. azotoformans* from raw milk, were investigated for their AHL-QS system to be linked with proteolytic and spoilage activity (Liu et al., 2007, Yuan et al., 2020). When the latter strain was added to UHT supplemented with exogenous C6-HSL, there was a dysregulation in the flavor profile and milk particles size.

This chapter aims at the following: 1) whole genomic sequencing of *P. gessardii* strains. 2) identification and characterization of LuxR and LuxI proteins. 3) investigating the association of AHLs with spoilage activity by *P. gessardii*.

3.2 Material and methods

3.2.1 Strains, plasmids and cultural conditions

Bacterial strains and plasmids used in this study are listed in **Table 5**. *Pseudomonas gessardii* strains were cultivated in Luria-Burtani (LB) at 25℃. *Escherichia coli* DH5α (pME6863) was grown in LB containing tetracycline (15 µg/ml) at 37℃ while *E. coli* DH5α (pRK2013), *E. coli* CC118 and *Chromobacterium subtsugae* CV026 were grown in LB added with kanamycin (100 µg/ml) at 28℃ and 32℃, respectively.

Table 5. Bacterial strains and plasmids used in the present study.

Strain or plasmid	Relevant characteristics or sequence	Reference
Strain		
P. gessardii BV1, BV5, BV6, RWV1, RWV6 and CP15	AHL-producing spoilage strains isolated from raw milk	This study
E. coli DH5α	F′endA1 hsdR17 supE44 thi-1 recA1 gyrA relA1 (lacZYA-argF) U169 deoR [80dlac(lacZ)M15recA1]	Sambrook et al., 1989
C. subtsugae CV026	Double mini-Tn5 mutant from *C. subtsugae* ATCC 31532, AHL biosensor	McClean et al., 1997
E. coli CC118	Competent cells as a host for pKNOCK cloning	Lorenzo et al., 2001
Plasmid/Vector		
pRK2013	Tra^+ Mob^+ ColE1 replicon; Km^r	Figurski et al., 1979
pME6863	*aiiA* gene under constitutive *lac* control; Tc^r	Reimmann et al., 2002
pGEM®-T Vector	Cloning PCR products	Robels and Doeris 1995
pKNOCK-km suicide vector	Plasmid used for homologous recombination and DNA insertion into the chromosome	Alexeyev 1999

3.2.2 DNA extraction, whole genome sequencing and annotation

Genomic DNA was extracted from 24-hour *Pseudomonas* cultures by the pronase Sarkosyl lysis method (Better et al., 1983). Whole genomic sequencing was analyzed by SeqCentre services (Pittsburgh, Pennsylvania, USA) using Illumina technique on an Illumina NovaSeq X Plus sequencer in one or more multiplexed shared-flow-cell runs, producing 2x151bp paired-end reads. Unicycler (Version 0.2.0) was used for reads assembly. The genomes were then annotated by JGI-Integrated Microbial Genomes and Microbiomes (JGI-IMG/M: https://img.jgi.doe.gov/) pipeline. The genomic sequences were compared according to the average nucleotide identity (ANI) and number of COGs (cluster of orthologues groups) using the same platform.

3.2.3 Identification and multiple alignment of luxI, luxR and luxR solo homologs

The genomes were mined for *luxI* and *luxR* homologs as described in the protocol below (**Figure 7**). In general, authenticated *luxI* homolog must contain the protein domain of autoinducer synthase (PF00765) while *luxR* homolog must include the protein domain of autoinducer binding (PF03472). Canonical *luxR* was distinguished from the solo homologs by the presence of the paired *luxI* gene. Multiple alignment was performed for the same genes using MAFFT online platform (http://mafft.cbrc.jp/alignment/server/large.html). Phylogenic tree was constructed with neighboring-joining method.

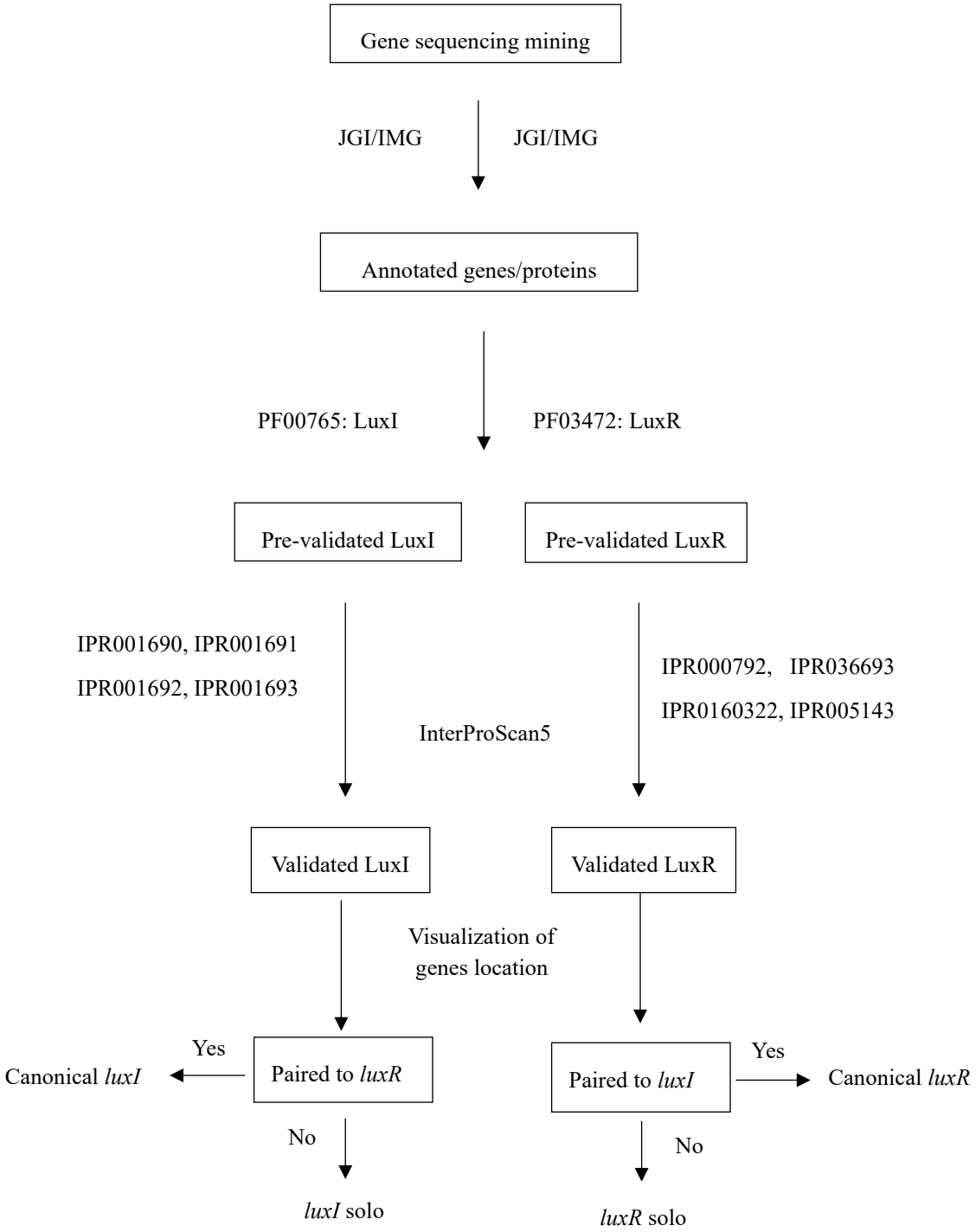

Figure 7. Identification of *luxR* and *luxI* genes in the assembled genomes of *P. gessardii* by JGI/IMG platform.

3.2.4 Evaluation of antibiotic resistance

P. gessardii isolates were assessed for their resistance to ampicillin (100 µg/ml), kanamycin (100 µg/ml), tetracycline (50 µg/ml), gentamycin (50 µg/ml), nitrofurantoin (100 µg/ml) , rifampicin (100 µg/ml) and nalidixic acid (25 µg/ml). Fresh colony of each strain was refreshed on LB agar added with the antibiotics at the mentioned concentration and incubated for 48 hours at 25℃. The growth indicates the resistance to the antibiotic added.

3.2.5 Heterologous expression of lactonase in P. gessardii

To investigate the role of AHL-based QS system in spoilage activity by *P. gessardii*, the AHL-degrading enzyme known as lactonase was heterologously expressed in the strains using triparental conjugation test. Briefly, *E. coli* DH5α (pME 6863) harboring the *aiiA* gene was used in a triparental mating with *P gessardii* as receipt, in which *E. coli* HB101 (pRK 2013) was the helper strain to facilitate the plasmid transformation. *E. coli* DH5α (pME6863) and HB101 (pRK2013) were routinely grown in LB containing tetracycline (15 µg/ml) and kanamycin (100 µg/ml), respectively, at 32℃. Fresh colony from each strain (donor, helper and receipt) was parallelly straked in LB agar and thoroughly mixed before incubation for 24 hours at 30℃. Selection of transconjugant *P. gessardii* strains was performed in LB supplemented with ampicillin (100 µg/ml), nitrofurantoin (100 µg/ml) and tetracycline (10 µg/ml), considering the donor and helpers strains are sensitive to ampicillin and nitrofurantoin. *P. gessardii* strains were naturally resistant to ampicillin (100 µg/ml) and nitrofurantoin (100 µg/ml) and sensitive to tetracycline. However, *P. gessardii* RWV6 was resistant to tetracycline and therefore, it was excluded from triparental conjugation. Successful growth of *P. gessardii* strains indicates that they acquired the plasmid pME683 carrying the *aiiA* and tetracycline resistance gene. T-streak assay with CV026 biosensor

strain was performed to confirm the AHL degradation in the transconjugant strains comparing with the wild type strains.

3.2.6 Effect of lactonase expression on spoilage activity in milk

After that, fresh overnight cultures from wild-type and conjugated strains were inoculated in skim milk (5%) at 1% and incubated for 2 days at 25℃, uninoculated milk sample was set as blank sample. General spoilage activity was visually assessed. The proteolytic activity was estimated by trinitrobenzenesulfonic acid (TNBS) assay as previously conducted in the study of Sakaridis and Lewis (2016). The main principle of this assay is that the reaction of the free α-amino groups with the TNBS reagent (Sigma-Aldrich, Germany) gives a yellow-orange color at basic pH medium. The color intensity is then measured by absorption at 420 nm. Briefly, 1 ml of milk sample was added with 40 µl of trichloroacetic acid (TCA) to precipitate the undigested protein and centrifuged at 6500 rpm for 5 minutes. From the supernatant, 50 µl was then mixed with 0.5 ml borate buffer (pH 8.5) and 1 ml of TNBS reagent (0.05 %, *v/v*). The samples were then incubated for 2 hours at 37℃ and the absorbance was taken at 420 nm, which was used to estimate the proteolytic activity. The OD value was adjusted to the blank value. The assay was independently replicated three times, and the mean and standard deviation were calculated. Independent t-test using Excel software 2016 was used to test the statistical difference between the control and test group.

3.2.7 Construction of luxI gene knockout

P. gessardii BV6 and RWV6 strains pose two types of AHL-producing genes (*lasI* and *rhlI*), to determine which QS system is most involved in the regulation of proteolytic activity, construction of gene knockout was constructed for *lasI* and *rhlI*, separately.

For this purpose, pKNOCK-kanamycin suicide vector was used. It is a plasmid that contains multiple restriction sites and can be easily ligated into the competent cells (E.g. *E. coli* CC118) and transformed into the chromosome in other bacteria by conjugation. For disruption in the gene of interest, the inner part of this gene is first amplified, purified, added with restriction sites and ligated into the pKNOCK-km plasmid. After that, it is transformed to *E. coli* CC118 and conjugated with *P. gessardii* to allow for the homologous recombination to occur. As a result, two copies of the target gene are produced. One copy lacks the 5′ region and the other lacks the 3′ region, which are mediated by pKNOCK plasmid (Alexeyev 1999).

3.2.8 PCR amplification and purification of the internal DNA fragment of luxI

Two DNA fragments of *luxI* were amplified representing the inner parts of *lasI* and *rhlI* in *P. gessardii* BV6. The primers used for this purpose are shown in **Table 6** and used for both strains as the *luxI* genes are conserved between both strains (**Appendix C**: Multiple alignment of *rhlI* and *lasI* genes). In the PCR reaction, 10 mM dNTPs and primers at final concentration of 200 µM and 0.5 µM, respectively, 1X Phusion™ HF buffer, high–fidelity DNA polymerase at final concentration of 0.02 U/µL and 3 µL of DNA template were added. The reaction was made to 50 µL with water. PCR conditions were initial denaturation at 96 °C (5 min); 30 cycles of denaturation at 96 °C (30 s), annealing at 59 °C (30 s), and extension at 72 °C (40 s); final extension at 72 °C for 5 minutes. The samples were stored at 10 ◦C until further processing. The PCR products were analysed by gel electrophoresis. The gel slice containing the amplified fragment was excised and the DNA was purified by DNA gel extraction kit (Norgen Biotek Corp, Canada).

Table 6. Primers used for PCR amplification of inner part of the *luxI* gene. XbaI and XhoI were added to forward (fw) and reverse (rwd) primers, respectively, as restriction sites. These are shown in bold in the primers.

Primers	Sequence (5′-3′) description	Product size (bp)
BV6 – *rhlI* - forward	**gcTCTAGAgc**AGGCCAGGTCTGCGGTTG	226
BV6 – *rhlI* – reverse	**ccgCTCGAGcgg**ACCGCCACCACCCGGTTG	226
BV6 – *lasI* – forward	**gcTCTAGAgc**AGGGTGCTGGCGTTTATTAC	262
BV6 – *lasI* – reverse	**ccgCTCGAGcg**GATCAACATTCGCTCTACC	262

3.2.9 Ligation of the purified DNA fragment into pGEM vector

The pGEM-T or pGEM®-T Easy Vector (Promega) is used for cloning of PCR products. It has T-overhangs, that make it ideally accepts DNA inserts with A-overhangs (as a result of amplification by Taq polymerase). This step is recommended before the DNA fragment ligation into the pKNOCK suicide vector, to ensure that the DNA insert with the restriction enzymes sites (XbaI and XhoI) is clean, correct and no blunt-ends is produced during the PCR reaction. In the ligation reaction the following was added according to the supplier's instruction (New England BioLabs, USA): 5 µl pf 2X rapid ligation buffer; 1 µl of T4 DNA ligase; the purified DNA insert and pGEM®-T or pGEM®-T Easy Vector at molar ratio of 3:1. The mixture was then incubated at 4°C overnight.

3.2.10 Transformation of the DNA insert ligated in the pGEM into E. coli DH5α

The ligated DNA inserts were transformed into the competent cells for multiplication. Fifty µl of *E. coli* DH5α cells were mixed with 2 µl of ligation reaction and heat-shocked in water bath at 42°C for 40-45 seconds followed by 2 minutes incubation in ice bath. After that, 950 µl of LB broth was added and the sample was incubated at 37°C for 1.5 hours, 100 µl of the culture was spread on LB plates supplemented with ampicillin (100 µg/ml) and X-gal (80 µg/ml) and incubated at 37°C overnight. The pGEM vector includes a cloning region that encodes for the production of the X-gal hydrolyzing enzyme β-galactosidase, this will result in growth of blue colonies. If successful insertion of the DNA fragment occurs, the expression of this enzyme will be inactivated and white colonies will grow. For further validation, these colonies were tested for the presence of the DNA insert. Briefly, a swab of cells from each colony was suspended in 50 µl of water and heated at 96°C for 10 minutes. This solution was used as DNA template. The PCR was performed as the same conditions mentioned in 3.2.8 section.

3.2.11 Digestion of the DNA insert from the pGEM

Positive colonies for presence of the DNA insert were grown in liquid LB with ampicillin (100 µg/ml) at 32 °C overnight. The pGEM was extracted from cultures using Miniprep plasmid DN kit (Norgen Biotek Corp, Canada). After extraction, the purified pGEM was digested with XbaI and XhoI restriction enzymes according to the supplier's instruction (New England BioLabs, USA) as follows: 10 µl of purified pGEM was mixed with 2 µl of 10X CutSmart® buffer and 0.5 µl each enzyme. The reaction volume was added up to 20 µl with water and incubated at 37 °C for 2 hours. The digest was analysed by gel electrophoresis to confirm the digestion process and separation of

the DNA insert. The digested fragments were isolated from the gel by DNA gel extraction kit (Norgen Biotek Corp, Canada).

3.2.12 Transformation of DNA fragment into the pKNOCK-km vector

The pKNOCK vector was first linearized with the same restriction enzymes used to digest the DNA fragment (XbaI and XhoI). The Insert was then ligated as described in 0 section, instead 10X ligase buffer was used here. *E. coli* CC118 was used for pKNOCK transformation and the procedure were the same mentioned in 3.2.10 section. The culture mixture was spread on LB plate supplemented with kanamycin (100 µg/ml). Colony PCR was performed to select the positive colonies with successful transformation with the same primers (**Table 6**).

3.2.13 Triparental conjugation and selection of P. gessardii knockout mutants

E. coli CC118 containing the DNA insert as donor strain, *E. coli* HB101 (pRk2013) as helper strain and *P. gessardii* as receipt strains were streaked on LB plates and thoroughly mixed to allow efficient transformation in which the homologous recombination will occur. After incubation at 30 °C for 24 hours, a large quantity of cells was swabbed from the conjugation culture mixture were streaked on LB plates supplemented with nalidixic acid (25 µg/ml), ampicillin (100 µg/ml) and kanamycin (100 µg/ml). *E. coli* strains are sensitive to nalidixic acid and ampicillin. *P. gessardii* strains are naturally resistant and if successful homologous recombination occurs, they will acquire resistance to kanamycin, it was therefore added for counter-selective of candidate mutants.

3.2.14 Validation of pKNOCK mutation in P. gessardii *BV6 and RWV6*

To ensure that the homologous recombination successfully occurred. PCR amplification was conducted with external forward primer (no 2, **Figure 10**) and reverse primer of the *luxI* gene (no 3, **Figure 10**), both in wild type and the candidate mutant, primers used are shown in **Table 7**. Sucuussful recombination would result in positive and negative amplification in the wild-type and candidate mutant, respectively, tested and observed by gel electrophoresis.

Figure 8. Cartoon representation of *luxI* gene in the wild-type strain. No 1 indicates the internal DNA fragment that was amplified and transformed into the pKNOCK vector.

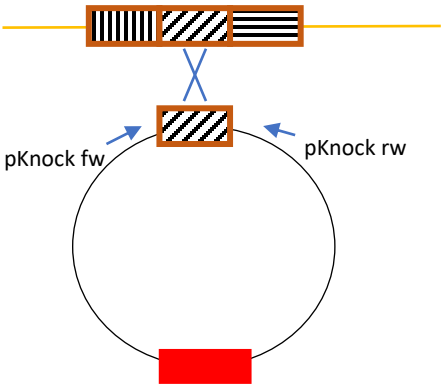

Figure 9. Cartoon representation of homologous recombination between the *luxI* gene and pKNOCK vector ligated with the internal DNA insert of *luxI*.

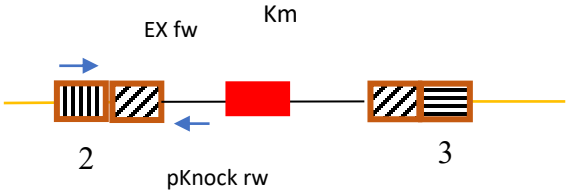

Figure 10. Cartoon representation of the *luxI* after homologous recombination. Two external parts of the *luxI* are now mediated by the pKNOCK vector.

Table 7. Primers used for validation of *luxI*-like genes in the wild-type and candidate mutants.

Primers	Sequence (5′-3′) description	Product size (bp)
BV6 – *rhlI* - forward	TCACCATGAACTGTCTGCAGCC	542
BV6 – *rhlI* – reverse	ACTGCGCCTGTAACGCGAGT	
BV6 – *lasI* – forward	TCGGTCGGCGGGATGAAATAG	584
BV6 – *lasI* - reverse	CTGCAACGTAGCGCCACAAC	

3.2.15 Effect of luxI mutants on proteolytic activity

Both wild-type and mutant versions of *P. gessardii* BV6 and RWV6 were grown overnight in LB at 25℃ and inoculated at 1% in skim milk, then incubated for 2 days at 25℃. The proteolytic activity was evaluated by TNBS assay as previously explained in **section 3.2.6.**

3.3 Results and discussion

3.3.1 Whole genomic features of the isolates putatively identified as P. gessardii

As summarized in **Table 8**, the assembled genomes showed different numbers of base pairs (size), GC content, and number of coding sequences. For further confirmation of species identification, the sequences of the 16S rRNA gene were extracted from the genomes and blasted in the NCBI database for species re-identification and the results are in line with MALDI-TOF MS analysis, confirming that the isolates putatively belong to *P. gessardii*. Multiple genome alignment was applied using Mauve software. Visual observation of the alignment indicated a high genes

similarity but in variant chromosomic positions. At the same time, non-conserved genes were identified and labeled as gene gaps (**Figure 11**). Taken together, this underlines that these strains are distinct.

Table 8. Whole genomic features of assembled genomes of *P. gessardii* strains.

Strain	Size (bp)	% of GC content	No of coding sequences	16S rRNA similarity*
BV1	6,039,762	60.70	5594	99.80%
BV5	6,329,419	60.20	5959	99.80%
BV6	5,9817,62	61.00	5422	99.80%
CP15	5,975,819	60.60	5534	99.80%
RWV1	6,036,365	60.60	5638	99.80%
RWV6	6,292,833	60.70	5594	99.80%

* Similarity to *P. gessardii*

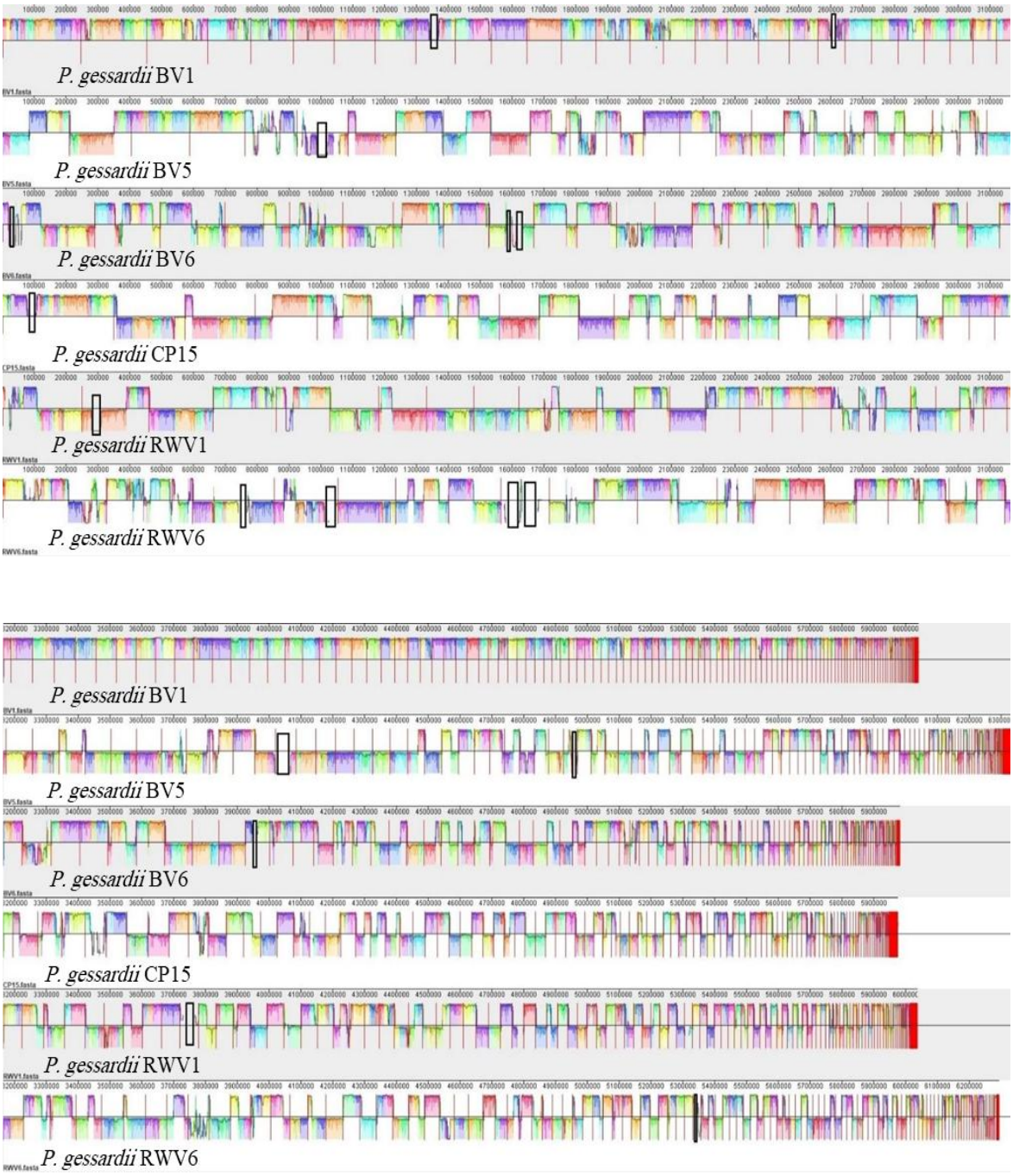

Figure 11. Multiple alignment of the assembled *P. gessardii* strains genomes. Plots with similar color indicates similar genes. Areas marked with rectangles shows the gene gaps.

Principal Coordinate Analysis (PCoA) clustering based on total number of COGs in the whole genome revealed that the strains are classified into 3 groups. Group 1(BV5 and CP15 strains), group 2 (BV1 and RWV1 strains) and group 3 (BV6 and RWV6 strains).

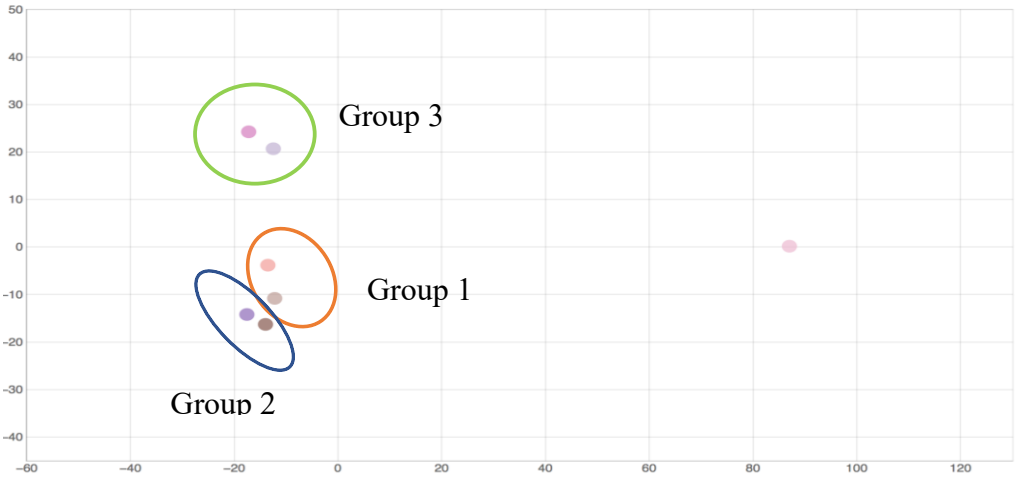

Figure 12. PCoA clustering of *P. gessardii* strains based on total number of COGs.

3.3.2 Identification of luxI gene in P. gessardii isolates

Two types of *luxI* gene were found in the genomes. The first one, which is present in all the genomes is *rhlI*-like gene that is typically found in *P. aeruginosa* (Tashiro et al., 2013). The sequence is composed of 579 nucleotides and. The second one, which is found only in BV6 and RWV6 strains is *lasI* gene that is also typically present in *P. aeruginosa* (Tashiro et al., 2013). The annotated sequence contains 616 nucleotides. PCoA clustering based on the *luxI* variance is shown in **Figure 13**. The clustering here is in accordance with the grouping generated based on the number of COGs in **Figure 12**. Multiple alignment of *luxI* genes is reported **Appendix C**: Multiple alignment of *rhlI* and *lasI* genes.

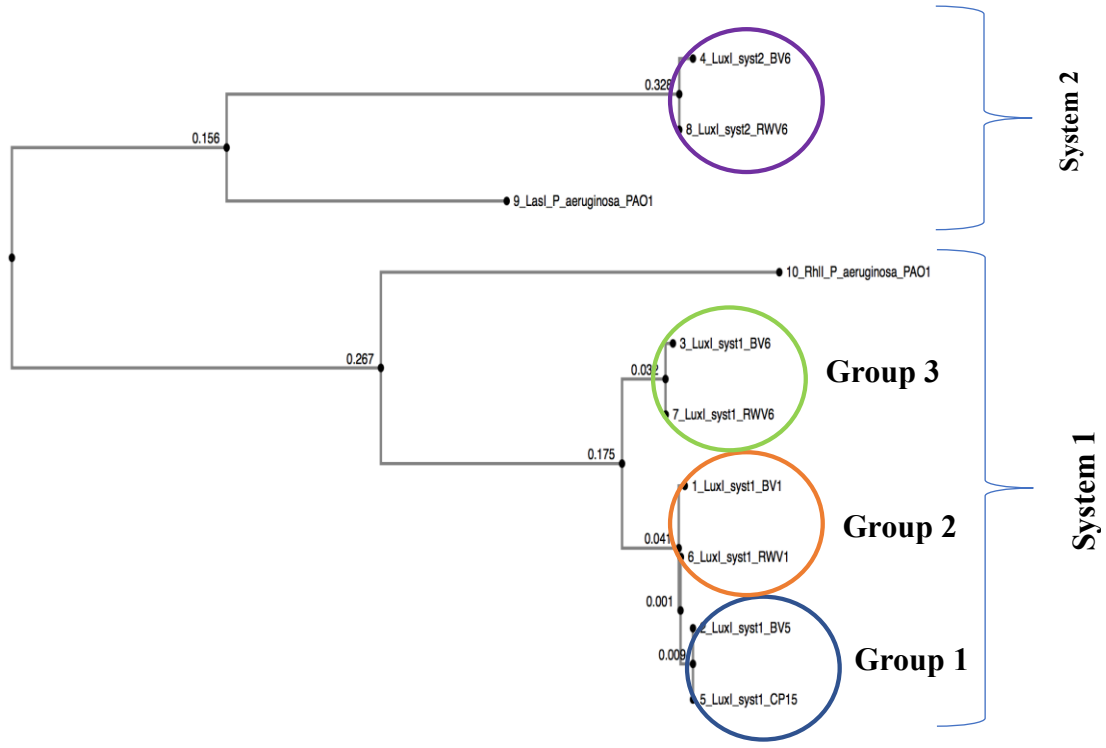

Figure 13. Phylogenetic tree of *P. gessardii* isolates derived from *luxI* sequence nucleotides alignment using Mafft. Phylogentic tree made with NJ method and Jukes-Cantor substitution model.

3.3.3 Identification of luxR gene in P. gessardii isolates

The identified *luxR* gene that is encoding the AHL receptor protein was annotated as the transcriptional regulator *rhlR* gene, which is the *luxR*-like gene present in *P. aeruginosa* as well (Tashiro et al., 2013). All of the annotated LuxR proteins are composed of 726 nucleotides. **Figure 14** shows clustering into 3 groups, RWV1 strain is still however highly similar to group 1 (at 99 %). Group 3 is similar at 92% with group 2 & 3. Multiple alignment indicated that it is highly conserved between these strains of *P. gessardii* **(Appendix D**: Multiple alignment of *rhlR* and *lasR* genes). In all the strains, the *rhlR*-like genes are flanked by the AHL synthase gene (*rhlI*-like gene) and rhamnosyltransferase subunit B (*rhlB*) (**Figure 15**), a necessary gene for the synthesis of

rhamnolipids that also plays a role in the regulation of swarming motility. It is generally known that the transcriptional regulators strongly control the expression of the adjacent genes within the same operon. Taking this into account, the rhamnolipids and swarming motility could be regulated by LuxR/I-QS based system in *P. gessardii*. This was demonstrated in earlier studies in *P. aeruginosa* (Wittgens et al., 2017). However, the transcriptional regulators could still control non-flanking genes expression. A second *luxR* that was also found is *lasR*-like gene in BV6 and RWV6 strains only. It is flanked by *lasI*-like and catechol 2,3-dioxygenase-like lactoylglutathione lyase (**Figure 16**), an enzyme involved in methylglyoxal detoxification.

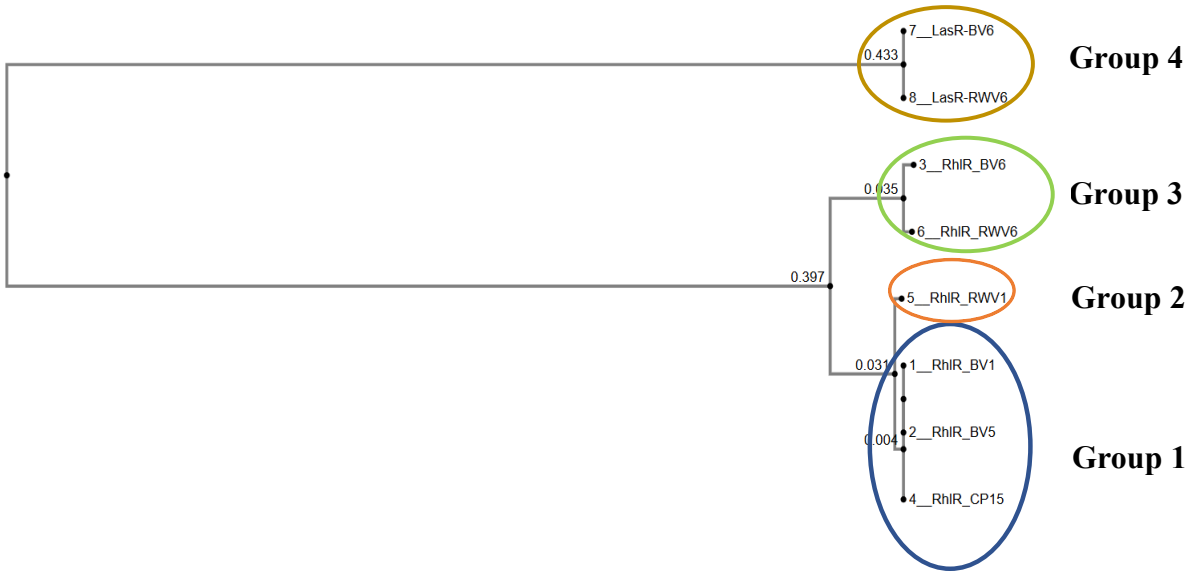

Figure 14. Phylogenetic tree of *P. gessardii* isolates derived from *rhlR*-like and *lasR*-like genes sequence alignment using Mafft. Phylogentic tree made with NJ method and Jukes-Cantor substitution model.

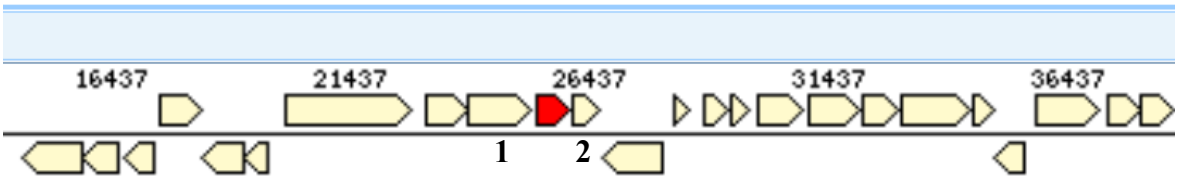

Figure 15. Flanking genes of *rhlR*-like gene in *P. gessardii.* Figure generated by JGI/IMG platform. No 1 and 2 refers to *rhlB* and *rhlI* genes, respectively.

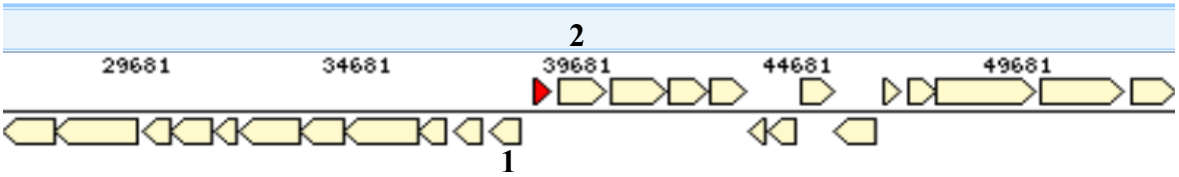

Figure 16. Flanking genes of *lasR*-like gene in *P. gessardii*. Figure generated by JGI/IMG platform. No 1 and 2 refer to catechol 2,3-dioxygenase-like lactoylglutathione lyase and *lasI*-like genes, respectively.

3.3.4 Identification luxR solo in P. gessardii *isolates*

Two types of *luxR* solo were identified (**Figure 17**). The first is annotated as DNA-binding CsgD family transcriptional regulator and found in all the strains. It is completely conserved between RWV1, BV1, BV5 and CP15 and between BV6 and RWV6 strains (**Appendix D** Multiple alignment of *luxR* solo genes). This gene is flanked by 23S rRNA (guanine1835-N2)-methyltransferase and ferredoxin/flavodoxin---NADP+ reductase. This is in line with other studies where the *luxR* solo in *P. fluorescence* was flanked by the same genes, which potentially one of them is involved in redox metabolic pathways. This type of *luxR* solo flanked by these genes is commonly found in *P. putida* (Bez et al., 2021). In another study, the *luxR* solo in *P. putida* KT2440 controlled the expression of swarming motility independently of AHL (Fernández-Piñar et al., 2011). The second *luxR* solo is annotated as quorum-sensing system regulator BjaR1 and only present in CP15 and BV5 strains with similar sequence (**Appendix D** Multiple alignment of *luxR*

solo genes). It is flanked by D-lactate dehydratase/protein deglycase and NAD(P)-dependent dehydrogenase that plays a role in pyruvate metabolism. The gene of D-lactate dehydratase was also found in *P. putida* 16A flanking the *luxR* solo that named as Ppu16R2 (Bez et al., 2021). However, in this study, the *luxR* solo was neither associated with expression of the adjacent loci in the same operon nor responds to exogenous AHLs. Possible explanation to this is that this *luxR* solo independently functions or it is regulated by unknown yet non-AHL endogenous compounds. All together indicates the diversity of QS-regulator genes within the same species.

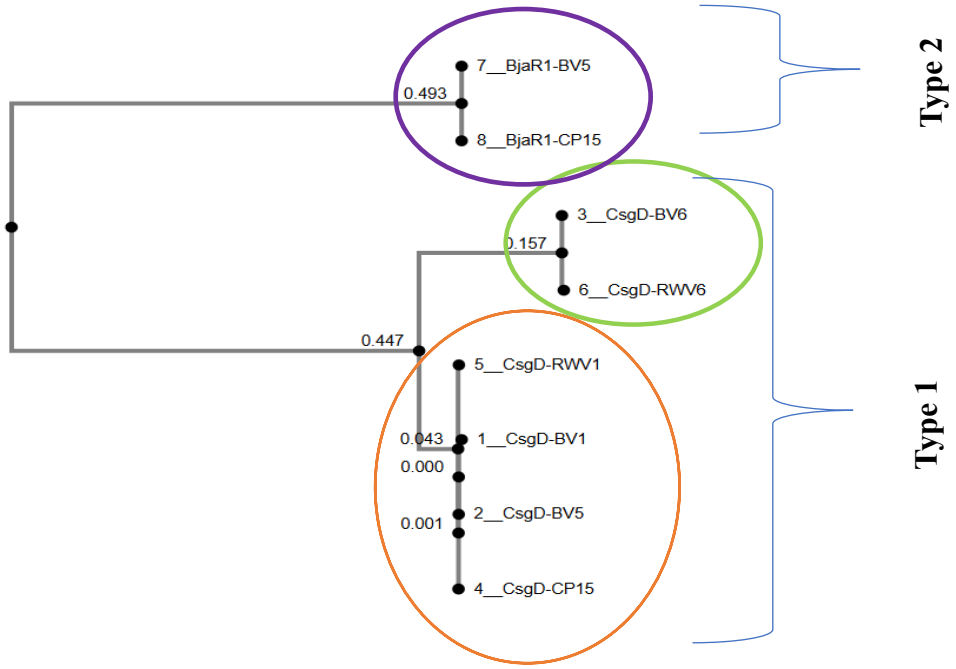

Figure 17. Phylogenetic tree of *P. gessardii* isolates derived from *luxR* solo genes sequence alignment using Mafft. Phylogentic tree made with NJ method and Jukes-Cantor substitution model.

3.3.5 Antibiotic resistance of P. gessardii

As summarized in **Table 9**, all the strains were resistant to nalidixic acid, nitrofurantoin and ampicillin. Only RWV6 strain was resistant to tetracycline. The antibiotic resistance in *Pseudomonas* species sourced from dairy and raw milk products was reported in several studies. For example, a range of raw milk isolates (*P. putida*, *P. fulva*, *P. fragi*, *P. mosselii*, *P. rhodesiae*, *P. libanensis*, *P. teatrolens*, *P. chlororaphis*, *P. fluorescens*) were found resistant to aminoglycosides, carbapenems, penicillin and nitrofurans (Quintieri et al., 2019). This is not surprising due to the fact that the antibiotics use is still widely used in the dairy farms.

Table 9. Antibiotic resistance of *P. gessardii* isolates to Nx: nalidixic acid; Rf: rifampicin; Nt: nitrofurantoin; Gm: gentamycin; Tet: tetracycline; Km: kanamycin; Amp: ampicillin

Antibiotic resistance							
Strain	**Amp**	**Km**	**Tet**	**Gm**	**Nt**	**Rf**	**Nx**
	100 µg/ml	100 µg/ml	50 µg/ml	50 µg/ml	100 µg/ml	100 µg/ml	25 µg/ml
BV1	+	-	-	-	+	-	+
BV5	+	-	-	-	+	-	+
BV6	+	-	-	-	+	-	+
CP15	+	-	-	-	+	-	+
RWV1	+	-	-	-	+	-	+
RWV6	+	-	+	-	+	-	+

3.3.6 Regulation of spoilage activity by AHL-QS based system

Heterologous expression of the AHL-degrading enzyme known as lactonase was used to test the effect of AHL on spoilage activity. The transconjugant strains of *P. gessardii* didn't induce violacein production by CV026 as seen in the T-streak CV026 assay (**Figure 18**), comparing with the wild type strains, indicating that lactonase was successfully conjugated and expressed.

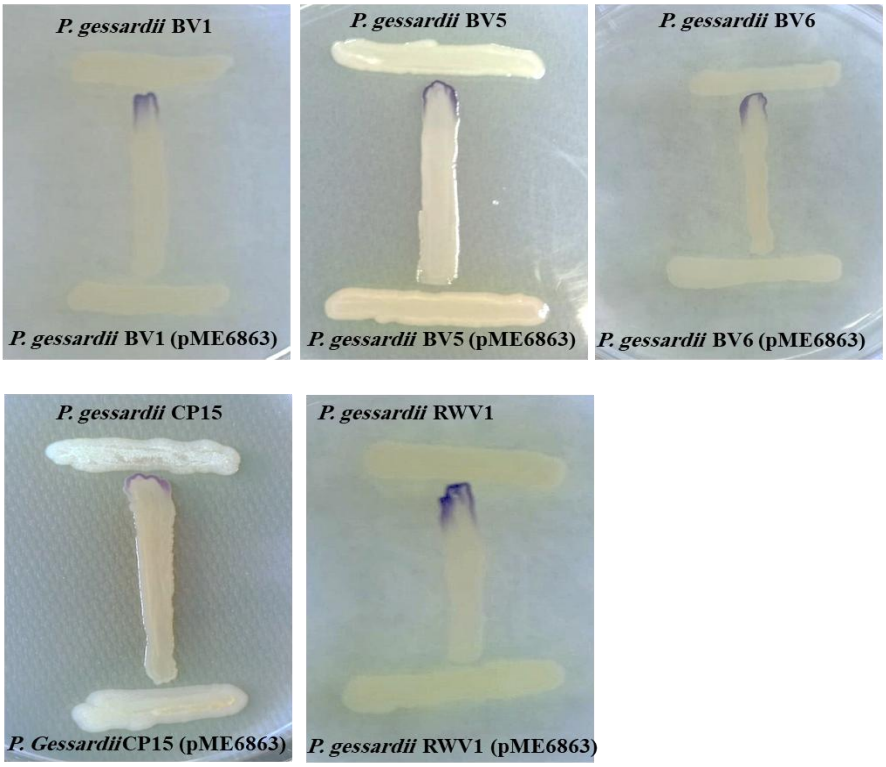

Figure 18. Cross feeding assay with CV026 biosensor for detection of AHL production by transconjugant strains with pME683 carrying the lactonase synthase gene and wild-type strains.

In addition, the general spoilage activity in milk was generally reduced when it was inoculated with conjugated *P. gessardii* strains comparing with wile-type strains (**Figure 19**).

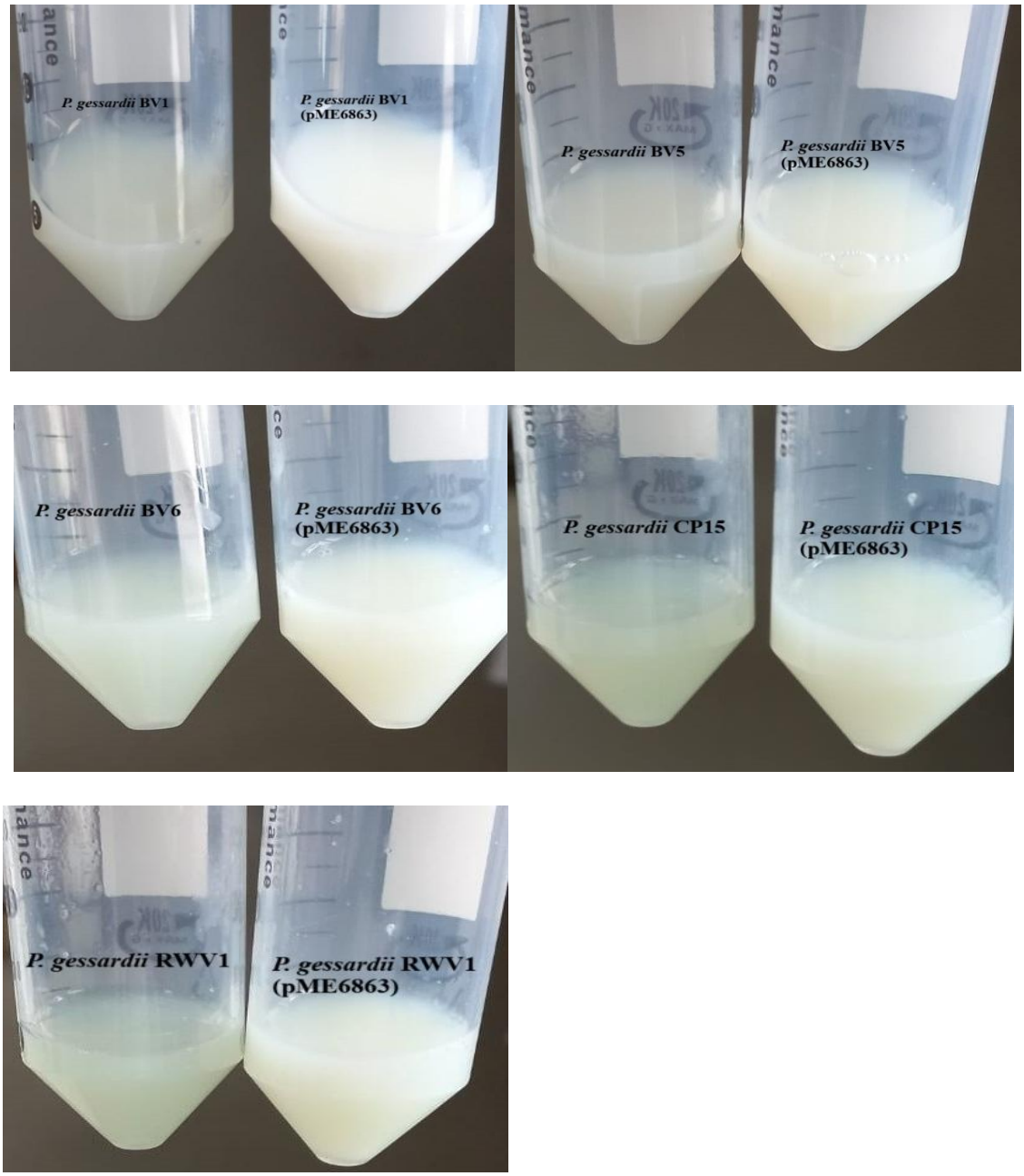

Figure 19. Spoilage activity in milk inoculated with wild-type of *P. gessardii* (left) and conjugated-type of *P. gessardii* (right).

With regard to proteolytic activity, as reported in **Table 10**, it was significantly decreased in milk samples inoculated with conjugated *P. gessardii* strains comparing with the wild type. These results suggest that the spoilage activity in *P. gessardii* is regulated by AHL-QS based system. The results here are in line with prior studies demonstrated the association of the AHL-QS system with spoilage and proteolytic activity NXR by *P. fluorescence* and *P. azotoformans* isolated from raw milk (Liu et al., 2007, Yuan et al., 2020). In addition, the presence of *luxR* solo here in the isolates of *P. gessardii* might be involved in the regulation spoilage-related genes expression by response to the AHLs being endogenously produced. However, this is still further investigation to illustrate such potential relationship.

Table 10. Proteolytic activity by wild-type and conjugated *P. gessardii* strains estimated by TNBS assay. Results are represented as OD420 adjusted for blank values. Data are shown as mean ± S.D. * indicates P-value < 0.05.

Strain	**Wild-type**	**Conjugated-type**
BV1	2.08	0.65*
BV5	1.88	0.93*
BV6	1.78	1.00*
CP15	1.91	0.86*
RWV1	1.74	0.64*

3.4 Construction *luxI* mutants of P. gessardii

3.4.1 Cloning the inner part of luxI into the pGEM vector.

Three fragments of representing the inner parts of the *rhlI*-like gene in *P. gessardii* BV6 and BV1 and *lasI*-like gene in BV6 strains were first amplified and purified (). The purified fragments from the agarose gel were then ligated into the pGEM vector and transformed into *E. coli* DH5. *E. coli* DH5 colonies that showed positive colony PCR for DNA insert transformation were grown in LB broth with ampicillin overnight at 32°C and the pGEM was purified. After that it was digested with Xbal and Xhol to purify and obtain clean DNA insert. In this case, two bands should appear, one representing the plasmid itself and the second representing the digested fragment **(Figure 21)**.

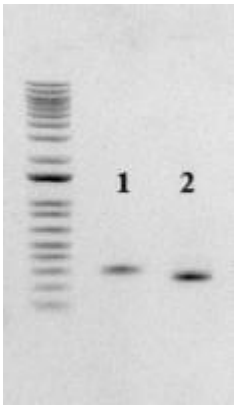

Figure 20. PCR amplification of the inner part of the *rhlI*-like (1) and *lasI*-like (2) genes in BV6

.

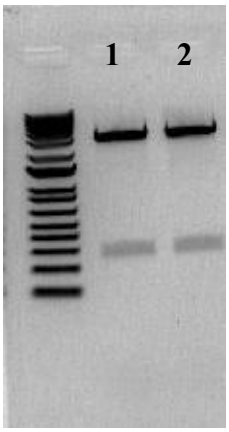

Figure 21. Digested pGEM, previously cloned with the DNA insert of the *luxI* genes, with Xhol and Xbal. Numbers 1 and 2 refer to the results from BV6 (*rhlI*) and BV6 (*lasI*). The upper band shows the pGEM plasmid while the lower band is the digested fragment.

3.4.2 Transformation of the DNA insert into the pKNOCK vector

The digested fragments from the pGEM were purified from the gel by DNA gel extraction kit (Norgen Biotek Corp, Canada) and ligated into the pKNOCK vector. After that, it was transformed into *E. coli* CC118 as host cells. Colony PCR was performed to confirm the successful transformation with the same primers reported in **Table 6** and the results are shown in (**Figure 22**).

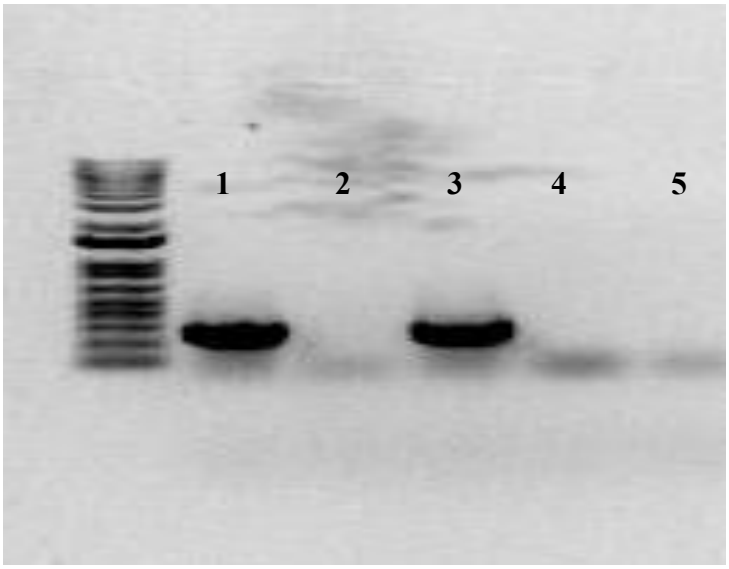

Figure 22. Colony PCR for *E. coli* CC118 random colonies transformed with the DNA insert of the *luxI* genes. Number 1, 3 and 5 refer to colonies transformed with the insert from BV6 (*rhlI*) and BV6 (*lasI*) and control, respecively.

3.4.3 Conjugation of P. gessardii *strains with* E. coli *CC118*

E. coli CC118 transformed with the DNA insert was used as donor to conjugate *P. gessardii* strains (BV6 and RWV6) allow homologues recombination to occur. The success of this process would result in insertion of the pKNOCK vector into the chromosome and disruption of the *luxI* gene as explained in **Figure 10**.**Figure *10.*** Cartoon representation of the luxI after homologous recombination. Two

external parts of the luxI are now mediated by the pKNOCK vector. PCR amplification using external forward and reverse primers for the *rhlI* and *lasI*-like genes was implemented for the wild-type and the candidate mutants. As seen in **Figure 23**, negative PCR amplification was observed in the mutant-type indicating the disruption of the both *luxI* gene, while a clear band represents the gene in the wild-type. This indicates a successful insertion of the pKNOCK and homologous recombination and disruption of the *luxI* genes. In the photo below the same results were observed for the both strain (BV6 and RWV6).

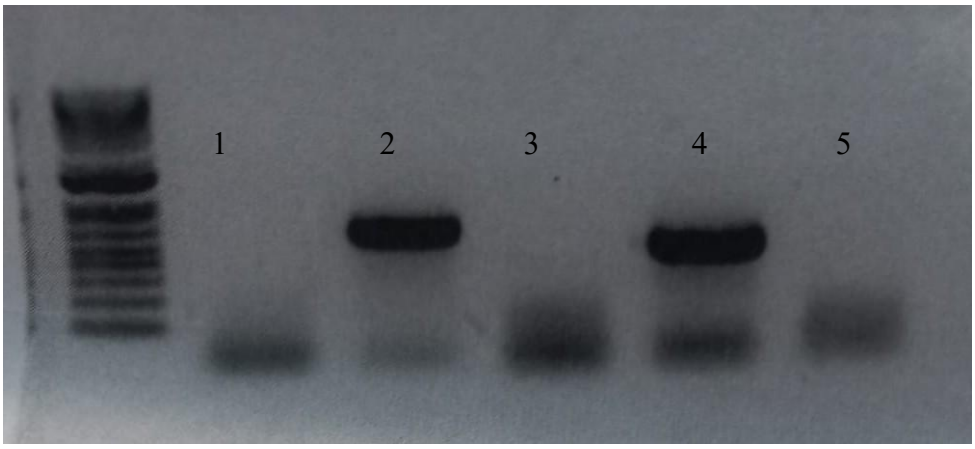

Figure 23. PCR amplification of *lasI*-like gene in candidate mutant (1) and wild-type (2) of *P. gessardii* BV6 and *rhlI*-like gene in candidate mutant (3) and wild-type (4) of *P. gessardii* BV6 using external forward and reverse primer. No 5 indicates negative control sample.

3.4.4 Regulation of proteolytic activity by rhlI-like gene.

As seen in **Figure 24**, the milk samples inoculated with *P. gessardii* BV6 and RWV6 (wt) were completely spoiled compared with samples inoculated with Δ *rhlI* BV6 and RWV6.

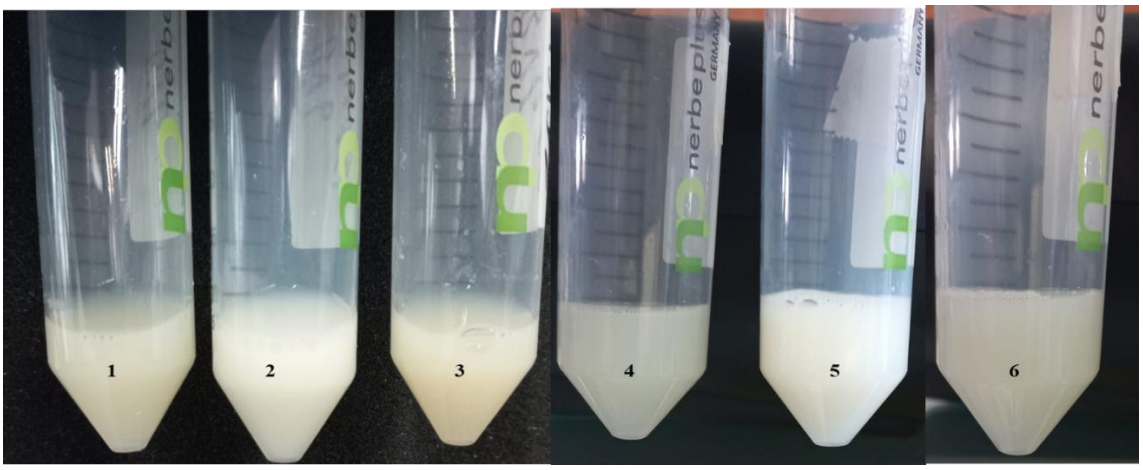

Figure 24. Milk spoilage activity after inoculation of *P. gessardii* BV6 wt, (1), *P. gessardii* BV6 Δ *rhlI* (2), *P. gessardii* BV6 Δ *lasI* (3), *P. gessardii* BV6 wt, (4), *P. gessardii* BV6 Δ *rhlI* (5) and *P. gessardii* RWV6 Δ *lasI* (*6*).

With regard to proteolytic activity, it was significantly lower by *P. gessardii* BV6 and RWV6 Δ *rhlI*- and Δ *lasI*- than the wild- type, despite there was a lesser effect on the proteolytic activity by Δ *lasI*- than Δ *rhlI*- types (**Table 11**). The results intimately indicate that QS circuits are regulated in hierarchical manner and both QS system found here are interconnected, where RhlR/RhlI-QS being the main involved in the regulation of spoilage activity by *P. gessardii*. Accordingly, the blocking of RhlR/RhlI-QS system by application of QS inhibitors will then reduce the proteolytic activity. Indeed, this hierarchy was earlier described in *P. aeruginosa* that pose the same two types of QS systems. In this species, the LasR-OdDHL (3-OXO-C12-HSL) complex activate the transcription of *rhlR*, *rhlI*, *lasI* (Lee et al., 2015).

Table 11. Proteolytic activity by wild-type and mutant *P. gessardii* strains estimated by TNBS assay. Results are represented as OD420 adjusted for blank values. Data are shown as mean ± S.D. * indicates P-value < 0.05 and statistically significant comparing with the control group.

Gene	BV6	RWV6
Wt	0.85 ± 0.03	0.94 ± 0.06
Δ *rhlI*-like	0.330 ± 0.02*	0.40 ± 0.08*
Δ *lasI*-like	0.50 ± 0.05*	0.55 ± 0.075*

3.5 Conclusion

Whole genomic sequencing revealed the diversity of the AHL-QS based system among the isolates of *P. gessardii* tested here. Two strains were found to have Rhll/RhlR and LasI/LasR-QS based systems while the rest of the strains have only RhlI/RhlR-QS system. In addition, difference types of LuxR solo were found in the mined genomes of the isolates. Heterologous expression of the AHL-degrading enzyme (lactonase) demonstrated the association of the AHLs with the proteolytic activity by the test strains. Construction of knockout mutant in the AHL synthase genes (*rhlI*- and *lasI*-like genes) showed that RhlI/RhlR- QS system is mainly the regulator QS system for proteolytic activity in *P. gessardii* BV6 and RWV6 strains.

3.6 References

Zhan, H., Li, X., Zou, X., Qu, G., Zhang, L., Li, Y., ... & Ding, T. (2025). Isolation and characterization of Pseudomonas fluorescens producing biogenic amines: AHL-mediated quorum sensing as a key regulatory mechanism. *LWT*, 117789.

Wang, D., Zhang, B., Wang, Y., Ren, L., Meng, Y., Ma, R., ... & Li, J. (2024). The effect of LuxR solo EvgA on the spoilage potential of Pseudomonas fluorescens. *Food Bioscience*, *62*, 105312.

Bai A, J., & Rai Vittal, R. (2014). Quorum sensing regulation and inhibition of exoenzyme production and biofilm formation in the food spoilage bacteria Pseudomonas psychrophila PSPF19. *Food Biotechnology*, *28*(4), 293-308.

Sambrook, J., Fritsch, E. F., & Maniatis, T. (1989). *Molecular cloning: a laboratory manual* (No. Ed. 2, pp. xxxviii+-1546).

McClean, K. H., Winson, M. K., Fish, L., Taylor, A., Chhabra, S. R., Camara, M., ... & Williams, P. (1997). Quorum sensing and Chromobacterium violaceum: exploitation of violacein production and inhibition for the detection of N-acylhomoserine lactones. *Microbiology*, *143*(12), 3703-3711.

Figurski, D. H., & Helinski, D. R. (1979). Replication of an origin-containing derivative of plasmid RK2 dependent on a plasmid function provided in trans. *Proceedings of the National Academy of Sciences*, *76*(4), 1648-1652.

Reimmann, C., Ginet, N., Michel, L., Keel, C., Michaux, P., Krishnapillai, V., ... & Haas, D. (2002). Genetically programmed autoinducer destruction reduces virulence gene expression and swarming motility in Pseudomonas aeruginosa PAO1. *Microbiology*, *148*(4), 923-932.

Better, M., Lewis, B., Corbin, D., Ditta, G., & Helinski, D. R. (1983). Structural relationships among Rhizobium meliloti symbiotic promoters. *Cell*, *35*(2), 479-485.

Robles, J. and Doers, M. (1994) pGEM®-T Vector Systems troubleshooting guide. Promega Notes 45, 19–20.

Alexeyev, M. F. (1999). The pKNOCK series of broad-host-range mobilizable suicide vectors for gene knockout and targeted DNA insertion into the chromosome of gram-negative bacteria. *Biotechniques*, *26*(5), 824-828.

Cebolla, A., Sousa, C., & Lorenzo, V. D. (2001). Rational design of a bacterial transcriptional cascade for amplifying gene expression capacity. *Nucleic acids research*, *29*(3), 759-766.

Sakaridis, I., & Lewis, M. J. (2016). Detecting a rapid method for measuring the proteolytic activity of raw and UHT milk. *SDRP Journal of Food Science & Technology*.

Tashiro, Y., Yawata, Y., Toyofuku, M., Uchiyama, H., & Nomura, N. (2013). Interspecies interaction between Pseudomonas aeruginosa and other microorganisms. *Microbes and environments*, *28*(1), 13-24.

Wittgens, A., Kovacic, F., Müller, M. M., Gerlitzki, M., Santiago-Schübel, B., Hofmann, D., ... & Rosenau, F. (2017). Novel insights into biosynthesis and uptake of rhamnolipids and their precursors. *Applied microbiology and biotechnology*, *101*(7), 2865-2878.

Bez, C., Covaceuszach, S., Bertani, I., Choudhary, K. S., & Venturi, V. (2021). LuxR solos from environmental fluorescent pseudomonads. *Msphere*, *6*(2), 10-1128.

Fernández-Piñar, R., Cámara, M., Soriano, M. I., Dubern, J. F., Heeb, S., Ramos, J. L., & Espinosa-Urgel, M. (2011). PpoR, an orphan LuxR-family protein of Pseudomonas putida KT2440, modulates competitive fitness and surface motility independently of N-acylhomoserine lactones. *Environmental Microbiology Reports*, *3*(1), 79-85.

Quintieri, L., Fanelli, F., & Caputo, L. (2019). Antibiotic resistant Pseudomonas spp. spoilers in fresh dairy products: An underestimated risk and the control strategies. *Foods*, *8*(9), 372.

Lee, J., & Zhang, L. (2015). The hierarchy quorum sensing network in Pseudomonas aeruginosa. *Protein & cell*, *6*(1), 26-41.

4 Development of *in silico* approaches for identification of QS inhibitors for the purpose of control of proteolytic activity by *P. gessardii*

4.1 Introduction

As previously discussed above, the regulation of spoilage activity is regulated by AHL-QS based system. The application of bioactive compounds that can block QS pathway is a promising strategy for food bio-preservation that also overcome the expression of virulence factors by antibiotic resistant bacteria. Several compounds were investigated as QS inhibitors against foodborne spoilage *Pseudomonas* isolates, either by acting as AHL mimics to bind with LuxR receptors or by the inhibition of AHL production by suppression of *luxI* gene. The spoilage enzymatic activity (protease, pectinase, and cellulase) was suppressed by hexanal as QS inhibitor in a *P. fluoroscens* strain isolated from lettuce (Lee et al., 2013, Zhang et al., 2018). *P. fluoescens* KM24, isolated from salmon, produced 3-oxo-C14-HSL, 3-oxo-C6-HSL, and C4-HSL, while the lipase and protease encoding genes were under-expressed due to the QS inhibitory effect of essential oil-major compounds (pinene and sabinene) on AHL production (Myszka et al., 2021). The same result of QS inhibition was observed in *P. fluoroscens* 13525 when grown with CIN, that disrupted QS mechanism by acting as a C6-HSL analogue to the LuxR receptor (Li et al., 2018). In a recent study of virtual screening of QS inhibitors, cytidine-5′-monophosphate (5′-CMP) and 5′-adenylic acid (5′-AMP) were found to block LuxR receptor in *P. fluorescens* and *S. baltica*, which lead to inhibit QS-controlled phenotypes (swimming motility, protease activity, EPS, and biofilm formation). The same results were observed when catechin was applied as QS inhibitors (Ding et al., 2019; Wang et al., 2021). However, this strategy is not yet investigated against dairy borne-

spoilage *Pseudomonas* species. In addition, as mentioned in Chapter 1, the preservative effect of probiotics by QS inhibition is also still not well investigated.

4.2 Material and methods

4.2.1 Generation of 3D LuxR models and definitions of binding pockets

To build a 3D model representative of the LuxR in *P. gessardii* isolates, the amino acid sequences were extracted from whole genomic sequencing data and uploaded on Alphafold server (https://alphafoldserver.com/). To predict the binding pocket, homologous models of LuxR bound to the ligand (AHL in this case) from *P. gessardii* were searched in the Protein Data Bank (PDB) databases. In the case of absence of such information, the amino acid sequence of LuxR proteins were blasted in UniProt (https://www.uniprot.org/) and the 3D model template with the highest structural homology was considered, in which a crystallographic ligand was already bound. Using Pymol (Version 2.3.0), both alphafold3 and template models were aligned to confirm the similarity and to ensure the coordinate consistency of the model during the docking analysis. All hydrogens were then added using Gold (Version 2022.2), and both models were saved in mol.2 format.

4.2.2 Ligands preparations

To prepare the reference ligand, the crystallographic waters were removed from the homologous 3D structure and the bound ligand was separated and saved as individual files for the docking experiments. Then, a library of bioactive compounds (**Table 12**) was prepared using DataWarrior (Version 5.0.0). The smile codes for the compounds were obtained from the PubChem database into DataWarrior to generate 3D conformers. All the ligands were then protonated at pH 7 using OpenBabel (version 3.1.1) software and saved in mol.2 format.

Table 12. Bioactive compounds virtually screened as potential QS inhibitors.

Test compound		
C4-HSL	Pentadecanoic acid	Rosmarinic acid
4-tert-butylcatechol	Guaiazulene	Luteolin
Berberine	Gallic acid	Epicatechin
Vanillic acid	p-Coumaric acid	Quinine
4-Hydroxy benzoic acid	Farnesol	Caftaric acid
Veratrol	Octadecyl acetate	Chlorogenic acid
Kojic acid	Chalcone	Kaempferol-3-glucoside
Salicylic acid	Oleic acid	Quercetin-3-glucoside
2–5 Dihydroxy benzoic acid	Octadecyl acetate	
Sabinene hydrate	t- Caffeic acid	
Cinnamic Acid	Anacardic acid	
Chamazulene	Harmine	
Tetradecanoic acid	Ferulic acid	
Nerolidol	2,4-Di-tert-butyl phenol	
Syringic acid	Citric acid	
7-hydroxycoumarin	Sinapic acid	
Saponin	Curcumin	
t-cinnamaldehyde	Kaempferol	
Procyanidin B2	Quercetin	
Tannic acid	Catechins	

4.2.3 Docking analysis

The Gold software was used to perform the docking of the ligands on the optimized 3D LuxR model of *P. gessardii*. Goldscore function was employed to indicate the binding affinity of the ligand to the protein. The higher the value is the better interaction of the ligand with the protein. This function considers 4 components in sorting the binding scores: 1) Protein-ligand hydrogen bond energy (external H-bond); 2) Protein-ligand van der Waals (vdW) energy; 3) Ligand internal vdW energy; 4) Ligand torsional strain energy (Vieira et al., 2024).

To validate the docking protocol, the reference ligand extracted from the 3D homology model was re-docked to the LuxR protein (without the bound ligand) and the result interaction was compared with the original 3D conformation bound with the ligand. This state provides insights into the reproducibility and accuracy of the docking protocol to predict the geometry and orientation of the binding pose (Vieira et al., 2022). The docking procedure was inspired by prior studies performed computational studies to validate and characterize QS inhibitors (Fernandes et al., 2024, Leitão et al., 2024, Leitão et al., 2025).

4.2.4 Bacterial strains, growth conditions and chemicals

P. gessardii strains (BV1, BV5, BV6, CP15, RWV1 and RWV6) were routinely grown in LB media at 25°C overnight. Salicylic acid (SA, ≥ 99% purity), *trans*-cinnamaldehyde (CIN, ≥ 95% purity), tannic acid (TA, ≥ 95% purity), were purchased from Sigma-Aldrich (Milan, Italy). SA, TA, and CIN were dissolved in DMSO to obtain a stock solution with concentrations of 20 mg/ml, 4 mg/ml, and 100 µl/ml, respectively.

4.2.5 Determination of minimum inhibitory concentrations (MIC)

The broth microdilution method was employed to determine the MIC of SA, TA, and CIN against *Pseudomonas* strains. Briefly, SA, TA and CIN were serially double diluted in LB broth. One hundred microliters of each concentration were added to 96-well plate and mixed with 100 µl of 1:100 diluted fresh overnight *Pseudomonas* culture in LB. Positive control wells contained DMSO, while negative control wells contained only media. The plate was then incubated at 28℃ for 24 hours. The lowest concentration that induced complete growth inhibition was defined as the MIC value. The MIC and ½ MIC values were then re-assessed for their antimicrobial effect in skim milk medium using plate counting method, compared with control cultures (without the test compound). In case there was no inhibitory effect at the concentrations tested in LB medium, the compound was tested in skim milk medium at the starting concentration.

4.2.6 *Effect of SA, TA, and CIN on the proteolytic activity by P. gessardii*

Skim milk (5%) was prepared, inoculated with fresh overnight cultures of *Pseudomonas* strains (1%), and added with SA, TA and CIN at non-inhibitory concentrations. Positive control was set as skim milk inoculated with *Pseudomonas* and DMSO only while negative control as blank samples included skim milk with SA, TA, and CIN only. All samples were incubated at 25℃ and 4℃ for 2 and 5 days, respectively. The proteolytic activity was evaluated as described in **3.2.6** section**.** The OD values obtained from the TNBS assay were normalized per cell density (OD420 / number of logs) for both positive and test samples. The assay was independently replicated three times, and the mean and standard deviation were calculated. Independent t-test using Excel software was used to test the statistical difference between the control and test group. The growth inhibitory effect of SA, TA, and CIN was evaluated by plate counting method using LB agar media.

4.2.7 Control of proteolytic activity of P. gessardii *by probiotic lactic acid bacteria*

A range of probiotic strains (*Lacticaseibacillus rhamnosus* GG, *Limosilactobacillus plantarum* LM2, *Lacticaseibacillus casei* 393, *Lactiplantibacillus plantarum* 299v, *Lacticaseibacillus paracasei* p21283, *Lactobacillus acidophilus* LA-5, *Lactobacillus acidophilus* LA-3 were tested for their potential to control proteolytic activity without antibacterial effect. The strains were grown in de Man, Rogosa, and Sharpe (M.R.S) medium at 37℃ under anaerobic conditions for 24 hours. The cultures were centrifuged at 6500 rpm for 15 minutes at 4℃ and the cell free supernatant (CFS) was filtered by 0.22 µm filter membrane to remove any cell debris. To test for presence of potential QS inhibitors in the CFS, it was added into the skim milk medium at 5% and the test strain (BV6 strain was selected due to its high protease activity) was then inoculated at 1%. The samples were incubated at 25 ℃ and 4 ℃ for 2 and 5 days, respectively. Inoculated skim milk medium with M.R.S only was served as a control. The proteolytic activity was assessed by TNBS assay as explained earlier in **4.2.6**, plate counting method was also used to confirm no antibacterial effect was observed. Independent t-test using Excel software was used to test the statistical difference between the control and test group.

4.2.8 Predictive QS inhibition mechanism of the tested probiotic strains

The strain that showed the highest inhibitory effect on the proteolytic activity was searched for its metabolites in the literature and their interaction with the LuxR was simulated using the same *in silico* approach explained above. The binding energy score was employed to estimate the binding ability of each compound. The C4-HSL was used as a reference ligand.

4.3 Results and discussion

4.3.1 Generation and validation of the 3D luxR model

Due to the lack of experimentally determined LuxR structures from *P. gessardii*, and the necessity to define binding sites for *in silico* analysis of quorum sensing inhibition. AlphaFold was employed to generate high-quality models of LuxR from *P. gessardii* using the amino acid sequences obtained from whole genome sequencing (**Appendix E**: LuxR amino acid sequences). All were built with high quality scores (higher than the score threshold 0.8) concerning the similarity with the true structure and relative prediction of the subunit positions (**Table 13**). These AlphaFold models were validated by comparing their predicted domains and overall structure to known LuxR family proteins. Results of blast searching in UniProt found out that the LuxR-homologue (HTH-type quorum-sensing regulator RhlR bound with C4-HSL, PDB code: 8B4A) shares 66% identity with LuxR proteins of all the *P. gessardii* strains. The protein family domains for the LuxR protein (autoinducer binding and DNA-binding domains coded as PF03472 and PF00196, respectively) were also present in the homologue (RhlR). In fact, annotation of the assembled genomes showed that the AHL-based QS system has a high homology to the RhlI/R system.

Table 13. Quality scores of the 3D models built by alpha server. The pTM score refers to the overall similarity of the model to the true structure. The ipTM score provide information about the reliability of the model in terms of the subunits positions within the complex.

Code	ipTM	pTM
BV1	0.82	0.85
BV5	0.83	0.86
BV6	0.82	0.85
CP15	0.81	0.85
RWV1	0.84	0.86
RWV6	0.84	0.86

The absence of *P. gessardii* LuxR templates in the PDB required adopting the binding cavity coordinates from the crystallographic structure of RhlR (PDB 8B4A) for docking simulations, which were confirmed for coordinate consistency and similar topology by structural alignment in PyMOL. Alignment of the alpha models of LuxR with the reference 3D model extracted from UniProt (RhlR) confirmed their 3D structural similarity **Figure *25***.

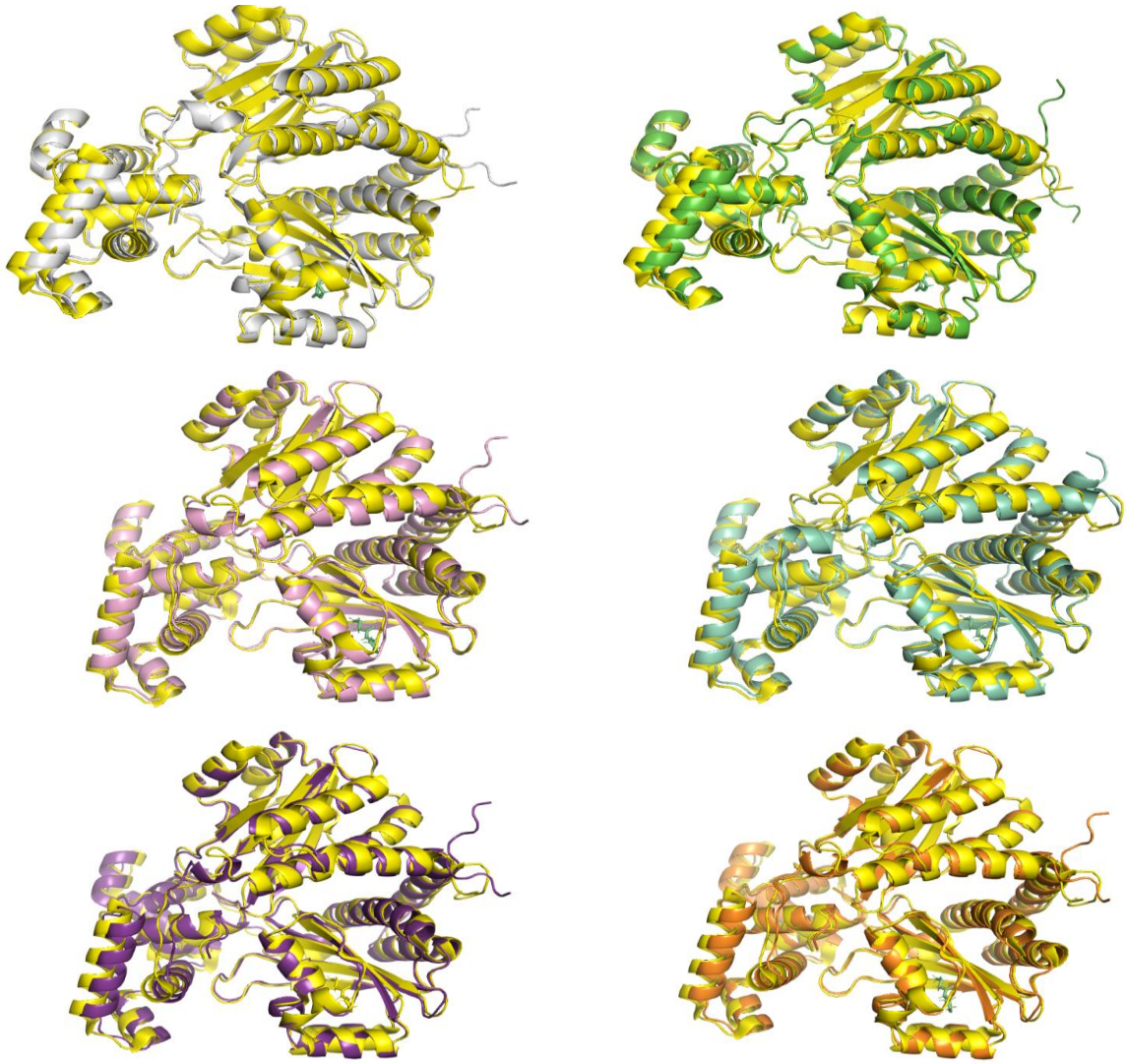

Figure 25. Images A, B, C, D, E, F, illustrates the alignment of 3D PDB reference model (8B4A) colored in yellow with alpha LuxR models of *P. gessardii* BV1, BV5, BV6, CP15, RWV1 and RWV6, respectively. Figures produced by Pymol (Version 2.3.0).

While structural homology is a practical solution in the absence of direct experimental structures, it inherently poses some limitations when inferring binding sites across related but distinct proteins: 1) Sequence divergence, even in conserved domains, can alter key side chains or local folding, impacting ligand specificity and binding affinity. 2) Homology-based binding site prediction assumes conservation of binding cavity topology, but differences in loop regions or subdomain orientation could yield inaccurate pocket geometries. 3) Allosteric effects and dynamic conformational changes unique to each protein may not be captured in static homology models. 4) The biological context, such as interaction partners and membrane environment, often differs across species, further complicating functional inference. In this study, alignment and docking validations (re-docking of native ligand to separated protein, comparison of key interacting residues) were performed to mitigate these modeling inaccuracies. The results exhibited that the ligand was re-docked to the same cavity site in the same model before it was separated (**Figure 26**), reflecting that the docking protocol can be successfully implemented for the test ligands. However, experimental validation such as mutagenesis or co-crystallization with ligands, would ideally represent a stronger, but also much more costly alternative for unambiguous binding site identification and characterization, particularly when translating findings between species like *P. gessardii* and *P. aeruginosa*.

Since *P. gessardii* BV5 and RWV1 have the same LuxR amino acid sequence and the same between *P. gessardii* BV6 and CP15 (**Appendix F**: Multile alignment of LuxR amino acid sequences**)**, only LuxR of *P. gessardii* BV1, BV5, BV6 and RWV6 were considered for docking analysis.

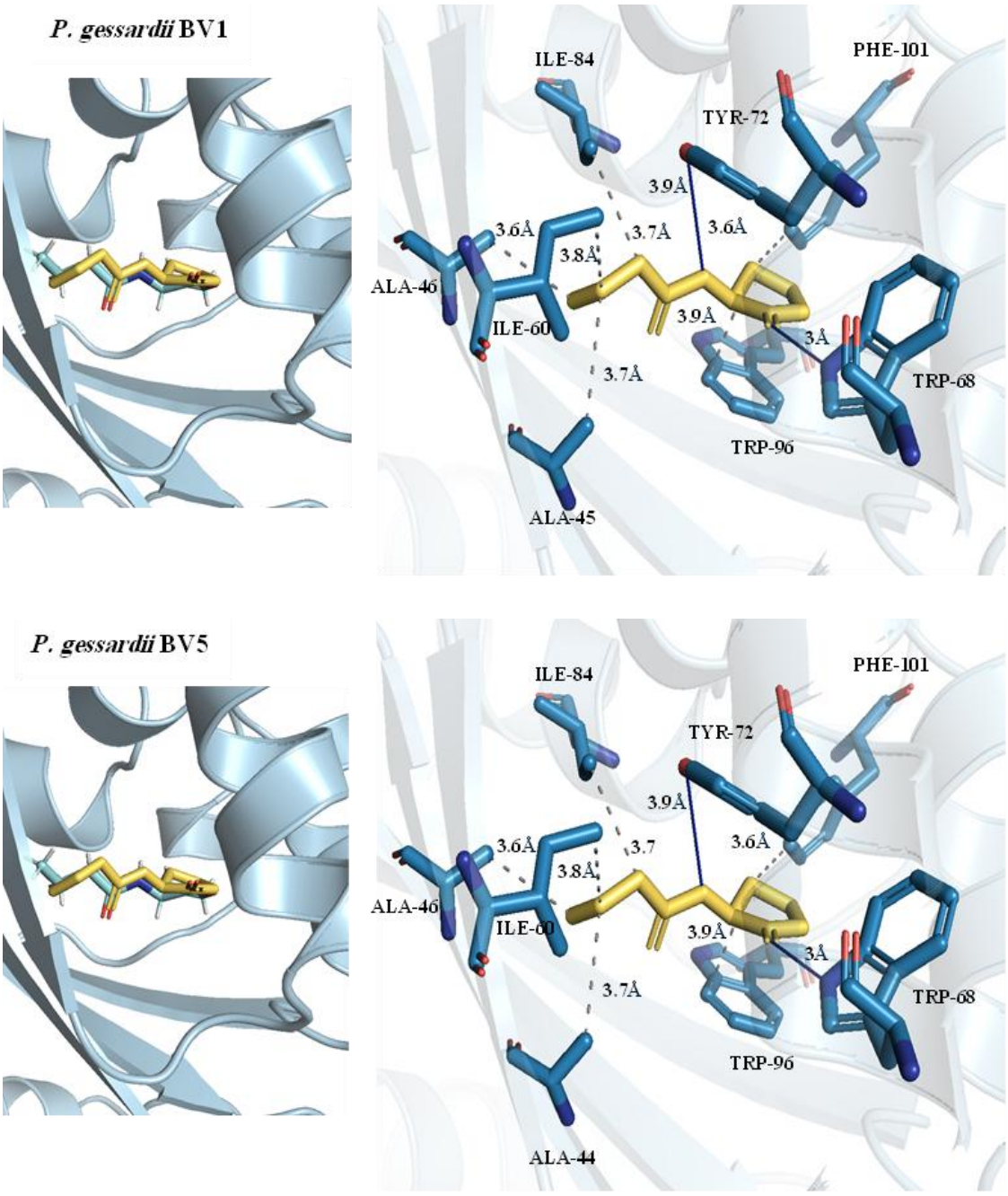

Figure 26A. Re-docking the reference ligand separated from the reference LuxR model (*P. gessardii* BV1 and BV5). The yellow ligand represents the ligand redocked while ligand in blue shows the same ligand originally bound. Figures produced by Pymol (Version 2.3.0).

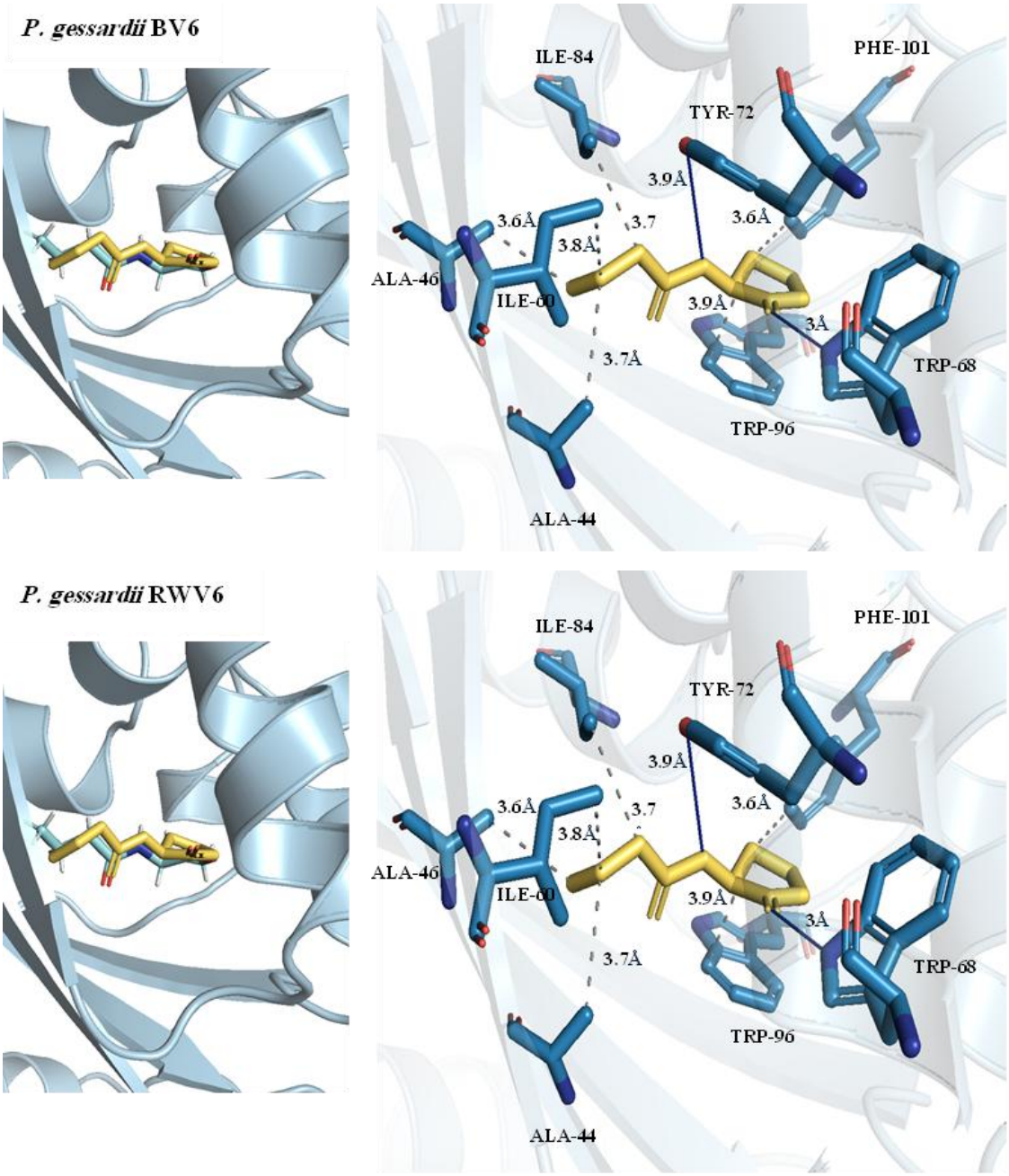

Figure 26B. Re-docking the reference ligand separated from the reference LuxR model (*P. gessardii* BV6 and RWV6). The yellow ligand represents the ligand redocked while ligand in blue shows the same ligand originally bound. Figures produced by Pymol (Version 2.3.0).

4.3.2 Interaction of the test polyphenols with the luxR

The interaction of target compounds with the LuxR, comparing with the native ligand (C4-HSL), was simulated by GOLD software that employs Goldscore function to rank the ligands according to their binding affinity. Comparing with the reference ligand, C4-HSL in this case, salicylic acid (SA) and cinnamaldehyde (CIN) scored higher, suggesting that they could disrupt QS pathway by interaction of LuxR.

Table 14. Results of molecular docking scores of the test polyphenols using GOLD software. Normalized score is calculated by dividing the fitness scores by number of non-H atoms.

Compound	M.W	No of non-H atom	Fittnnes score	Normalized score
Salicylic acid	138.00	10.00	46.66	4.66
t-cinnamaldehyde	132.16	10.00	46.13	4.61
C4-HSL	171.20	12.00	54.52	4.54
Vanillic acid	168.15	12.00	51.86	4.32
4-Hydroxy benzoic acid	138.12	10.00	43.21	4.32
Veratrol	138.17	10.00	43.13	4.31
4-tert-butylcatechol	166.22	12.00	50.23	4.19
Sabinene hydrate	154.25	11.00	45.97	4.18
Cinnamic Acid	148.16	11.00	45.06	4.10
Chamazulene	184.28	14.00	57.06	4.08
Tetradecanoic acid	228.37	16.00	65.14	4.07
Nerolidol	222.37	16.00	63.37	3.96
Syringic acid	198.17	14.00	54.77	3.91
7-hydroxycoumarin	162.14	12.00	46.88	3.91
Pentadecanoic acid	242.40	17.00	64.08	3.77
Guaiazulene	198.31	15.00	56.23	3.75
Gallic acid	170.12	12.00	44.95	3.75
p-Coumaric acid	164.16	12.00	44.15	3.68
Farnesol	222.37	16.00	58.69	3.67
Octadecyl acetate	312.54	22.00	78.52	3.57
Chalcone	208.26	16.00	56.98	3.56
Oleic acid	282.47	20.00	71.08	3.55

Table 14. *Continued*

Compound	M.W	No of non-H atom	Fittnnes score	Normalized score
Harmine	212.25	16.00	53.90	3.37
Ferulic acid	194.19	14.00	46.32	3.31
2,4-Di-*tert*-butyl phenol	206.33	15.00	48.83	3.26
Citric acid	192.12	13.00	41.11	3.16
cis−11-Eicosenamide	309.54	22.00	69.52	3.16
Sinapic acid	224.21	16.00	49.49	3.09
Curcumin	368.38	27.00	52.20	1.93
Kaempferol	286.24	21.00	39.69	1.89
Quercetin	302.24	22.00	34.92	1.59
Catechins	290.27	21.00	33.02	1.57
Rosmarinic acid	360.32	26.00	40.84	1.57
Luteolin	286.24	21.00	31.95	1.52
Epicatechin	290.27	21.00	23.60	1.12
Quinine	324.42	24.00	25.37	1.06
Caftaric acid	312.23	22.00	17.80	0.81
Chlorogenic acid	354.31	25.00	-8.78	-0.35
Kaempferol-3-glucoside	448.38	32.00	-17.29	-0.54
Quercetin-3-glucoside	464.38	33.00	-21.17	-0.64
Berberine	336.37	25.00	-23.09	-0.92
Procyanidin B2	578.52	42.00	-195.07	-4.64
Tannic acid	1701.20	122.00	-605.42	-4.96
Saponin	1223.36	85.00	-430.73	-5.07
Octadecyl acetate	312.54	22.00	77.10	3.50
t- Caffeic acid	180.16	13.00	45.03	3.46
Anacardic acid	348.53	25.00	86.08	3.44

4.3.3 Interaction of CIN and SA with luxR of P. gessardii

The interaction of CIN and SA with the LuxR, comparing with the native ligand (C4-HSL) was simulated by GOLD software that employs Goldscore function to rank the ligands according to their binding affinity. Tannic acid (TA) that did not show any binding affinity to the LuxR, due to the high size (M.W = 1701.2) that makes it challenging to fit in the binding pocket, was included as a negative control in the *in vitro* test of proteolysis inhibition. CIN and SA were predicted to bind with the LuxR with binding scores of 46.13 and 46.60, respectively, slightly lower than the scores of the reference. However, when the scores were normalized for the ligand size (score per heavy atom, they scored similarly to the reference, pointing that CIN and SA highly compete with the native ligand to bind the LuxR. The docking scores were the same for all the analyzed LuxRs.

In addition, as reported in (**Table 15**), they perform nearly with C4-HSL in terms of the ability to form hydrophobic interactions. Torsion scores for CIN and SA were lower than that of the reference ligands, implying that they demonstrate more flexible conformations for binding within the cavity site.

Table 15. Non-polar, ligand clash and torsion scores of C4-HSL, CIN and SA

Ligand name	Non-polar	Ligand. Clash	Ligand. Torsion
C4-HSL	-35.87	00.00	00.49
CIN	-38.99	00.00	00.11
SA	-31.24	00.00	00.12

In parallel with the *in vitro* analysis, both CIN and SA displayed significant control of proteolytic activity, SA being the most inhibitory while the CIN activity is temperature-dependent. Based on these results, SA can be used as a compound reference for future computational studies screening for QS inhibitors in *P. gessardii*. With regard to TA, it did not illustrate any binding affinity to the LuxR due to the high size (M.W = 1701.2) that makes it challenging to fit in the binding pocket. To understand deeper the interactions of the ligands with LuxR, Protein-Ligand Interaction Profiler (PLIP) tool was used, which illustrates the contact amino acids and the type of bond. **Table 16** reports the binding amino acids in the cavity site that were shared by both reference and test ligand to interact with by forming hydrophobic bonds. **Figure 27** and **Figure *28*** present the fitting and interactions of SA and CIN in the binding pocket of LuxR competitively with native ligand. As can be remarkably seen, the amino acids (TYR-72, TYR-68, ALA-111, PHE-101 and TRP-96) were common target residues for SA and CIN to bind with by forming hydrophobic interactions.

Table 16. Amino acid residues interact with both the reference and test ligands.

	Strain			
Ligand	**BV1**	**BV5**	**BV6**	**RWV6**
SA	PHE-101, TRP-96, TYR-72	PHE-101, TRP-68, TYR-72	PHE-101, TRP-68, TRP-96, TYR-72	PHE-101, TRP-68, TYR-72
CIN	PHE-101, TRP-68, TRP-96, TYR-72	PHE-101, TRP-68, TRP-96, TYR-72	TRP-68, TRP-96	PHE-101, TRP-68, TRP-96, TYR-72

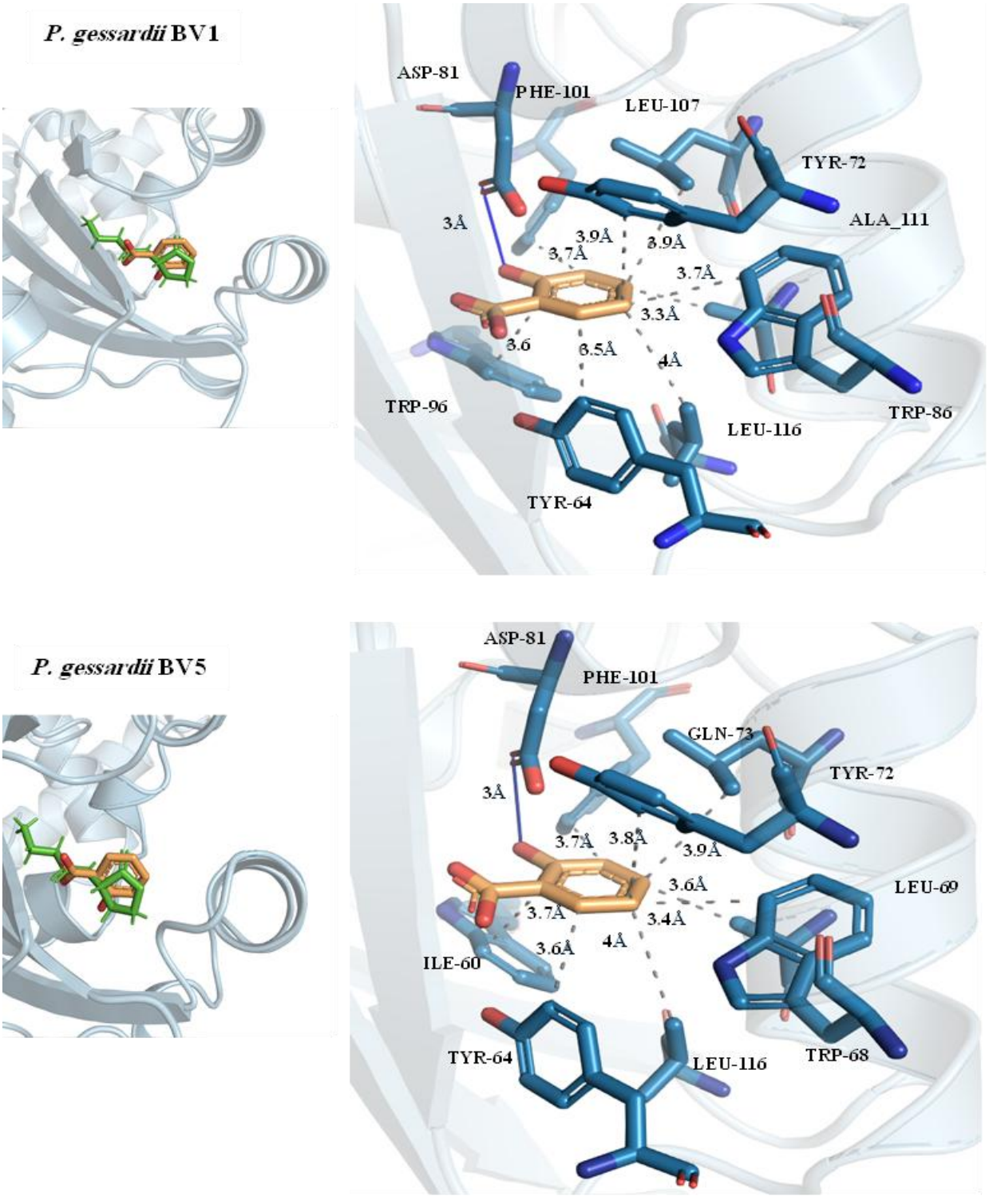

Figure 27A. Binding of C4-HSL (green ligand) and SA (orange ligand) in the cavity site of LuxR of *P. gessardii* BV1 and BV5, and the interactions of SA with the contact amino acids. Figures produced by Pymol (Version 2.3.0).

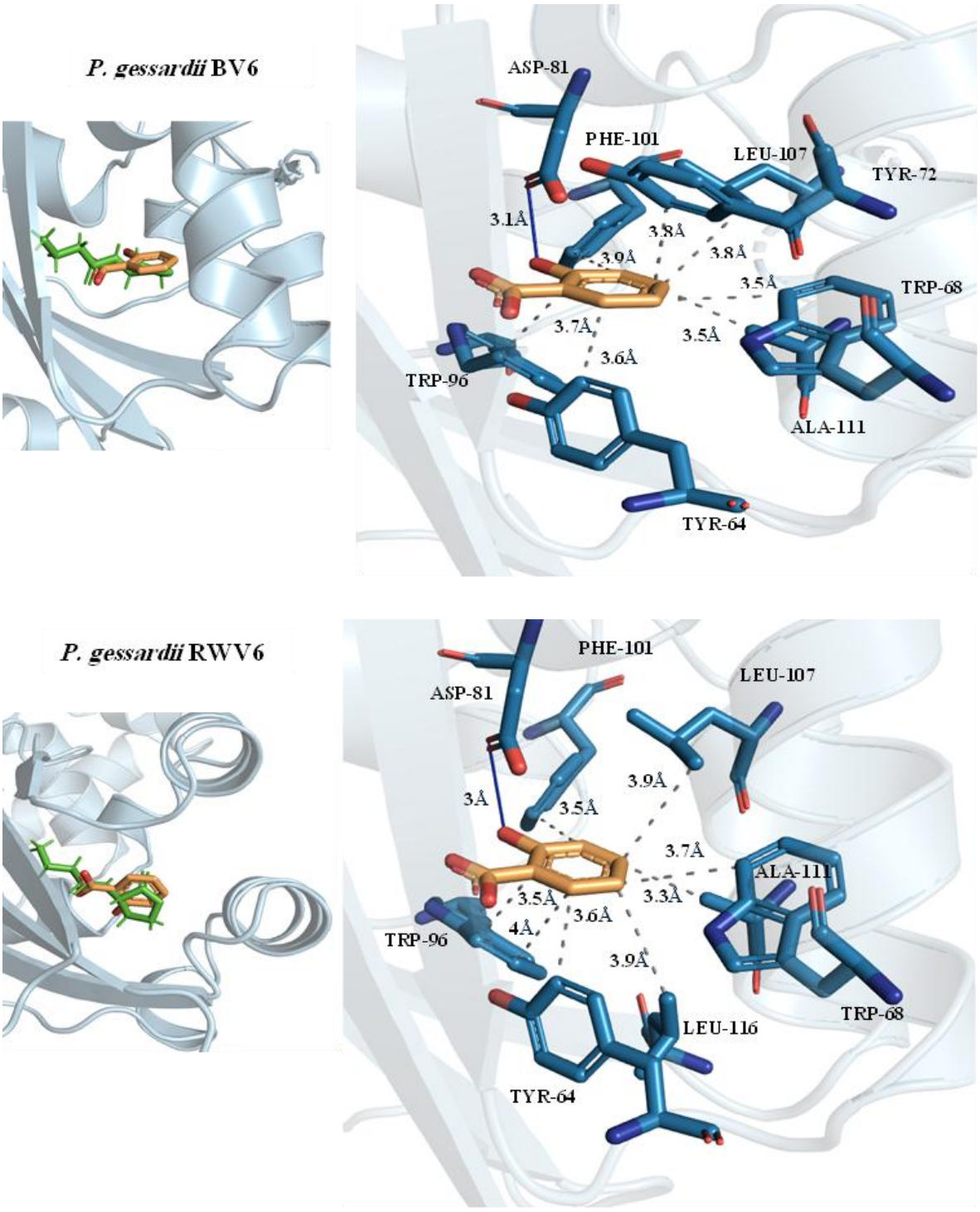

Figure 27B. Binding of C4-HSL (green ligand) and SA (orange ligand) in the cavity site of LuxR of *P. gessardii* BV6 and RWV6, and the interactions of SA with the contact amino acids. Figures produced by Pymol (Version 2.3.0).

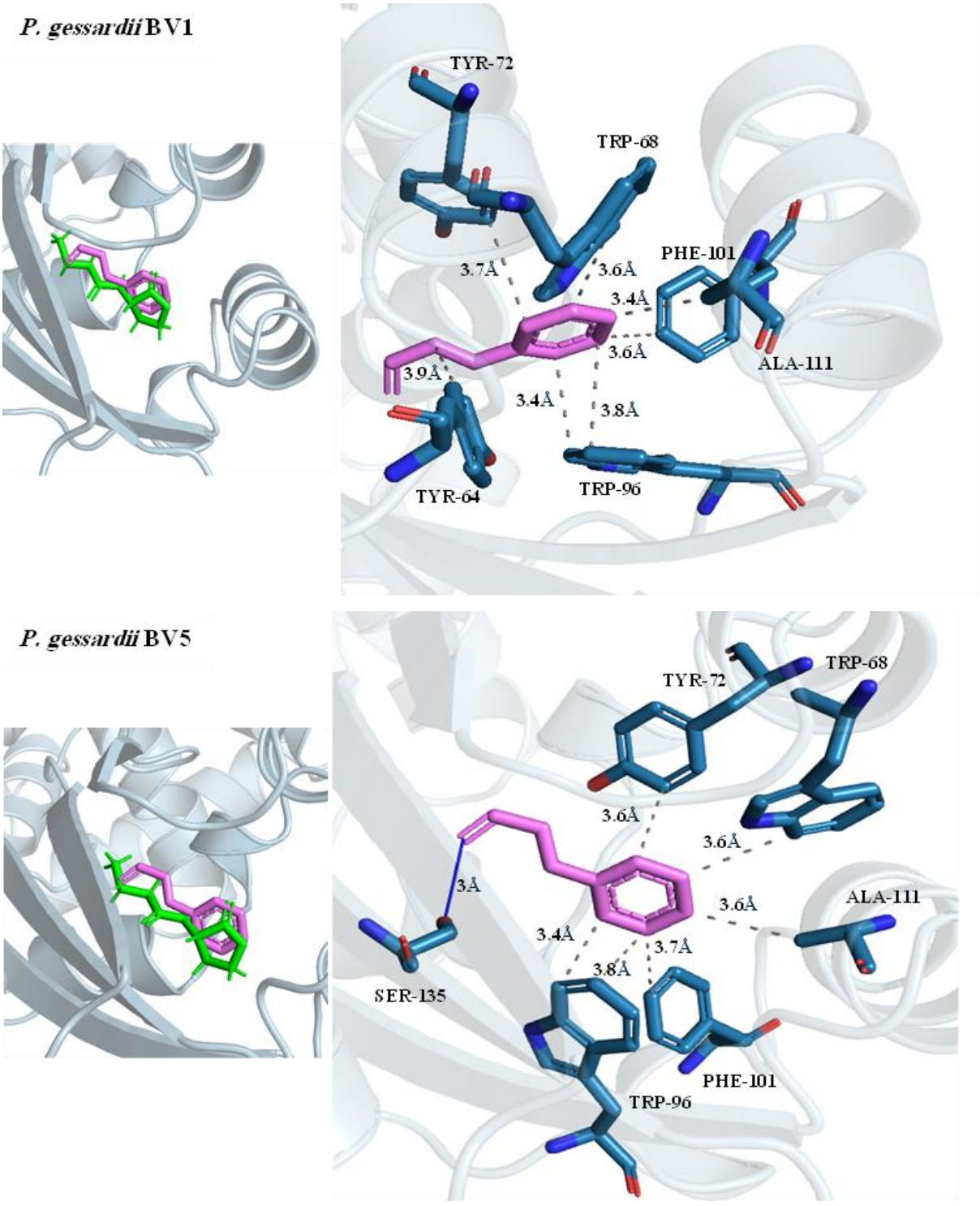

Figure 28A. Binding of C4-HSL (green ligand) and CIN (violet ligand) in the cavity site of LuxR of *P. gessardii* BV1 and BV5, and the interactions of SA with the contact amino acids. Figures created by Pymol (Version 2.3.0).

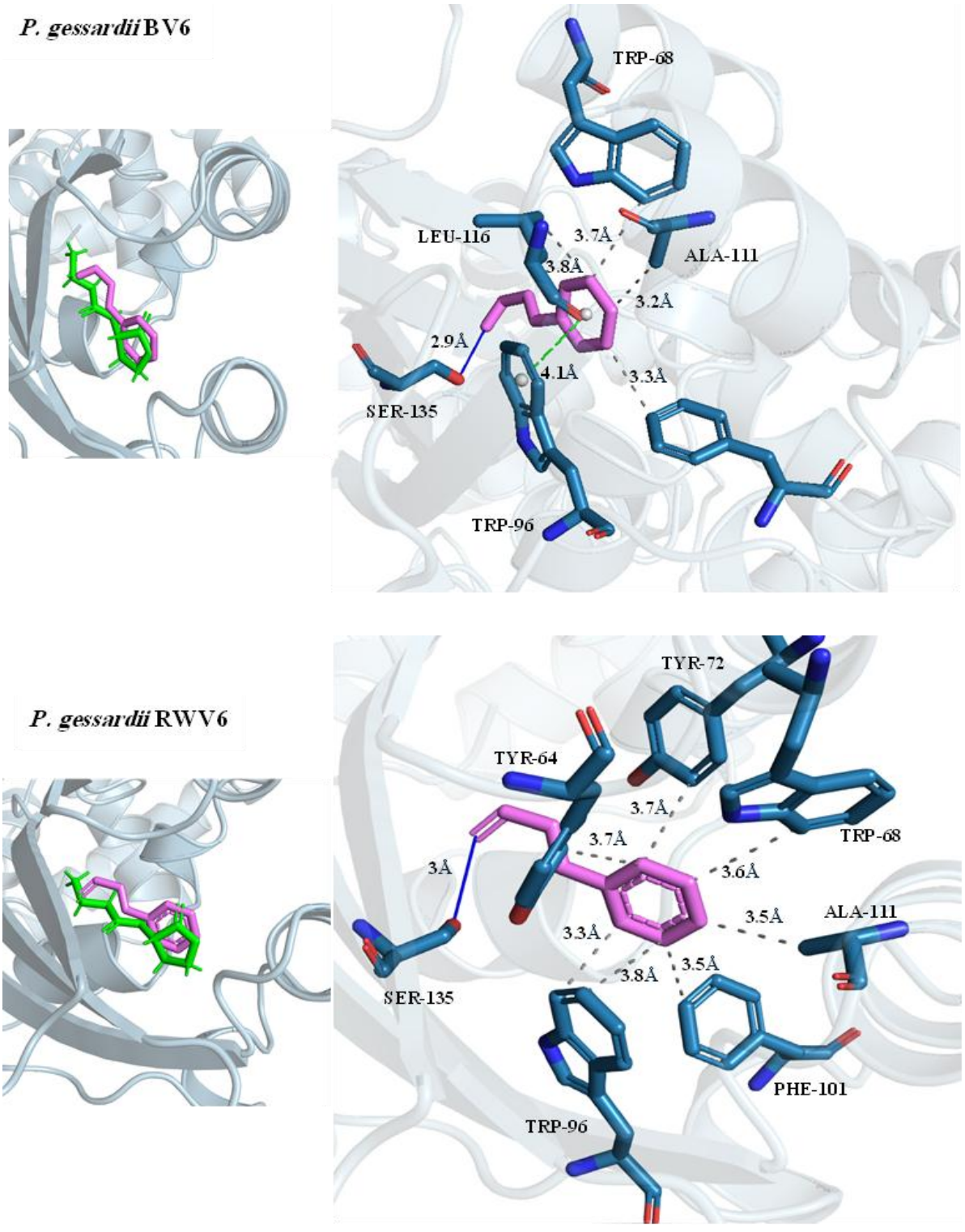

Figure 28B. Binding of C4-HSL (green ligand) and CIN (violet ligand) in the cavity site of LuxR of *P. gessardii* BV6 and RWV6, and the interactions of SA with the contact amino acids. Figures created by Pymol (Version 2.3.0).

4.3.4 Effect of SA and CIN on proteolytic activity.

SA, TA, and CIN were here tested for their effect on proteolytic activity at non-inhibitory concentrations, potentially due to their QS inhibitory effect, considering that proteolytic activity is regulated by AHL-QS system. The methodology applied here to test the anti-QS activity is based on prior studies, where spoilage Pseudomonas, having LuxR/LuxI-QS system, was grown with the test compounds (test group) and without (control group) at sub-inhibitory concentrations (Wang et al., 2021; Zhang et al., 2018; Yang et al., 2024).

In LB medium, the MIC values of TA and CIN were 0.120 mg/mL and 0.468 µl/mL, respectively. No growth inhibitory effect of SA was observed when tested at first concentration of 0.750 mg/mL. In skim milk medium, concentration of TA at MIC (0.120 mg/mL) value inhibited the growth but not at ½ MIC (0.060 mg/mL). When CIN was tested at 1 MIC and ½ MIC concentration, both values were growth inhibitory at both temperatures. Therefore, CIN was re-tested at different concentrations lower than 0.234 µl/mL. The highest subinhibitory concentration was 0.180 µl/mL at 25 °C for all the strains, while at 4 °C it was 0.150 µl/mL for P. gessardii RWV6, BV5 and CP15 and 0.130 µl/mL for *P. gessardii* RWV1, BV1 and BV6. With regard to SA, 0.750 mg/mL caused a slight growth inhibition (~1 log) and 0.550 mg/mL was the non-inhibitory concentration for all the strains at both temperatures. Results of plate counting (CFU/mL) for the effect of TA, CIN and SA at non-inhibitory concentrations on the growth of the test isolates in skim milk medium are reported in **Table 17** and **Table 18**.

Table 17. Growth of *P. gessardii* isolates after 2 days of incubation at 25°C without (C) and with (T) addition of the QS inhibitors. Data are shown as Mean ± SD.

	Number of logs (C)			Number of logs (T)					
Strain	**SA**	**CIN**	**TA**	**SA**	**P - value**	**CIN**	**P - value**	**TA**	**P - value**
BV1	8.52 ± 0.05	8.66 ± 0.12	8.48 ± 0.44	8.71± 0.16	0.60	8.80 ± 0.12	0.20	8.39 ± 0.07	0.50
BV5	8.81 ± 0.03	8.35 ± 0.16	8.60 ± 0.05	8.72 ± 0.33	0.43	8.62 ± 0.13	0.08	8.58 ± 0.07	0.70
BV6	8,70 ± 0.04	8.85 ± 0.22	8.87 ± 0.04	8.70 ± 0.18	0.80	8.75 ± 0.40	0.62	8.86 ± 0.05	0.94
RWV1	8.83 ± 0.02	8.65 ± 0.01	8.81 ± 0.06	8.64 ± 0.23	0.17	8.55 ± 0.15	0.17	8.40 ± 0.28	0.07
RWV6	8.65 ± 0.05	8.89 ± 0.06	8.62 ± 0.07	8.59 ± 0.02	0.08	8.75 ± 0.08	0.07	8.54 ± 0.09	0.31
CP15	8.90 ± 0.03	8.50 ± 0.27	8.57 ± 0.06	8.72 ± 0.08	0.02	8.69 ± 0.25	0.46	8.46 ± 0.05	0.08

Table 18. Growth of *P. gessardii* isolates after 5 days of incubation at 4°C without (C) and with (T) addition of the QS inhibitors. Data are shown as Mean ± SD.

	Number of logs (C)			Number of logs (T)					
Strain	**SA**	**CIN**	**TA**	**SA**	**P - Value**	**CIN**	**P - value**	**TA**	**P - value**
BV1	8.27 ± 0.05	8.33 ± 0.14	8.35 ± 0.04	8.10 ± 0.08	0.10	8.20 ± 0.02	0.15	8.25 ± 0.15	0.20
BV5	8.89 ± 0.04	8.82 ± 0.12	8.77 ± 0.13	8.59 ± 0.14	0.08	8.56 ± 0.13	0.08	8.48 ± 0.10	0.08
BV6	8.72 ± 0.02	8.44 ± 0.26	8.30 ± 0.10	8.63 ± 0.03	0.20	8.36 ± 0.30	0.73	8.19 ± 0.06	0.19
RWV1	8.44 ± 0.04	8.40 ± 0.10	8.52 ± 0.1	8.45 ± 0.12	0.94	8.35 ± 0.05	0.6	8.39 ± 0.13	0.50
RWV6	8.54 ± 0.07	8,49 ± 0.05	8.54 ± 0.10	8.60 ± 0.10	0.21	8.38 ± 0.17	0.35	8.60 ± 0.02	0.15
CP15	8.42 ± 0.11	8.69 ± 0.10	8.50 ± 0.08	8.31 ± 0.09	0.50	8.52 ± 0.13	0.16	8.39 ± 0.13	0.30

The ability of the tested compounds to control the proteolytic activity was dependent on the strain and incubation temperature. In **Figure 29**, the proteolytic activity normalized per cell density is reported. SA showed the most suppressive effect on the proteolytic activity, except against RWV6 strain, with higher efficacy at 25℃ than 4℃ (**Figure 29**). On the contrary, CIN demonstrated a better inhibition of proteolytic activity by *P. gessardii* BV6 (63%) and *P. gessardii* RWV6 (60%) at 4℃ (**Figure 29C and F**). These two strains showed higher proteolysis at 4℃ than BV1, BV5, RWV1 and CP15 isolates whose proteolytic activity at 4℃ was not affected at significant levels, when CIN was added. The proteolytic activity at 25℃ by the latter strains was significantly decreased, still slightly, after incubation with CIN (**Figure 29A-B, D-E**). Regarding tannic acid, it caused a modest reduction in the proteolytic activity only against BV6 strain at 25℃ (30% proteolysis inhibition) (**Figure 29C**). No anti-proteolytic activity of TA was observed at 25℃ against the rest of the trains (**Figure 29A-B, D-**F). In addition, the proteolysis at 4℃, between the control and test groups was almost equal except that there was a slight, not statistically significant, inhibition in the proteolytic activity by BV1 and BV6 strains, respectively (**Figure 29A and C**).

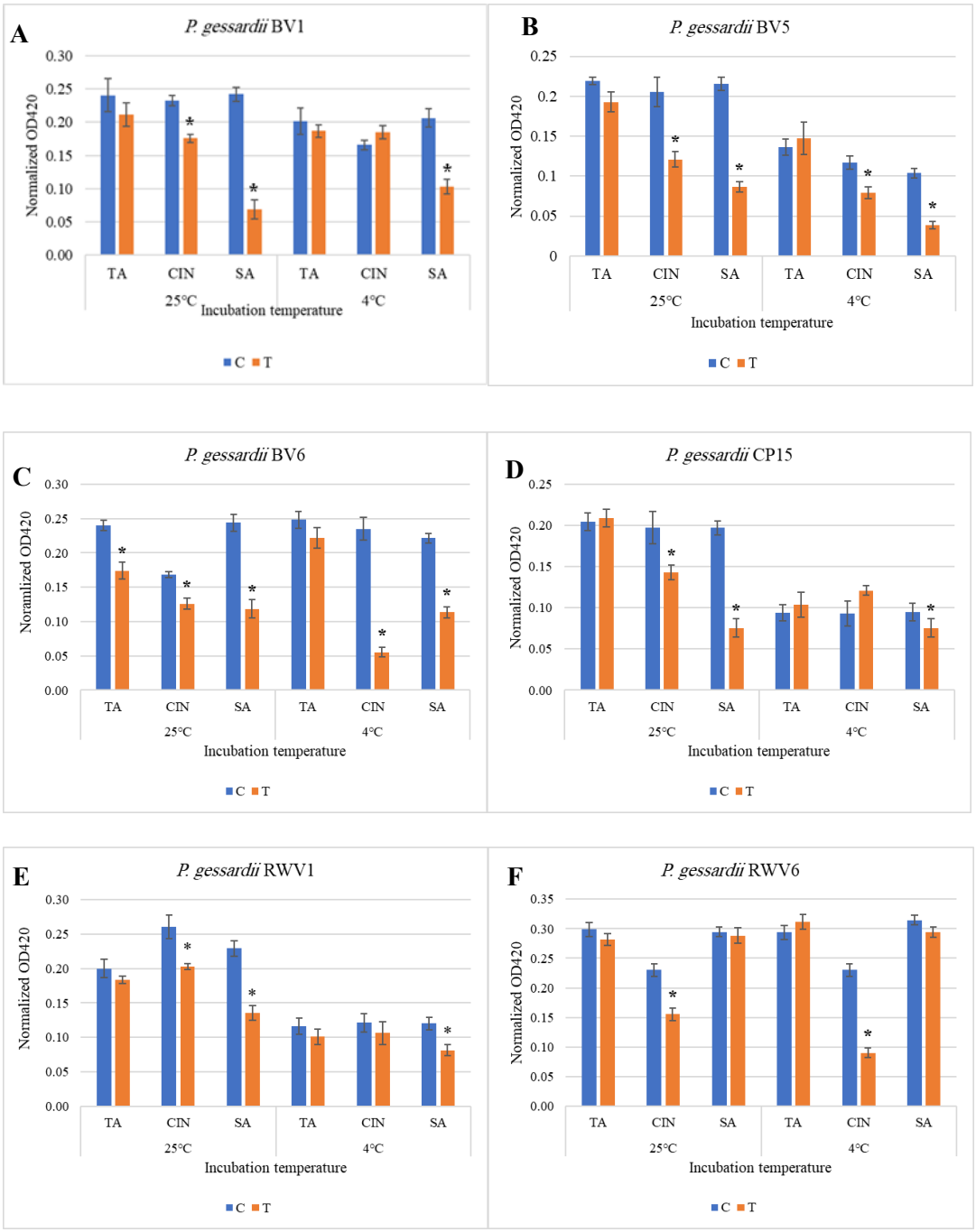

Figure 29. Impact of tannic acid (TA), cinnamaldehyde (CIN) and salicylic acid (SA) on the proteolytic activity of *P. gessardii* strains estimated by trinitrobenzenesulfonic acid (TNBS) assay and normalized per cell density. Data are presented in Mean ± SD. * indicates p-value < 0.05. Blue and orange bars represent control (test strain grown in skim milk + DMSO) and test (test strain grown in skim milk + test QS inhibitor) groups, respectively.

Polyphenols are known for their positive effects on human health (e.g., lower risk of cardiovascular diseases, gut microbiota, inflammation, and hypertension) (Fraga et al., 2019). At the same time, they also improve food quality by acting as antioxidant and antimicrobial agents against foodborne pathogenic and spoilage bacteria (Papuc et al., 2017). More specifically, a rising area of research postulates that polyphenols provide an extra role in bacterial biocontrol through QS disruption. Paving the way for future applications of polyphenols at clinical and food industry level. For instance, epigallocatechin reduced the biofilm formation by *Campylobacter jejuni* and *Salmonella typhimurium* by repression of *luxS* of gene that is responsible for the autoinducer production (AI-2). Phenolic acids such as gallic acid, caffeic acid and chlorogenic acid inhibited the biofilm formation by Staphylococcus aureus due to their interference with Agr-like QS system (Bouyahya et al., 2022). *P. aeruginosa* is the most researched Gram-negative pathogen that poses two types of AHL-QS systems (*lasR*/*lasI* and *rhlR*/*rhlI*). As recently confirmed in the review of Vadakkan et al (2024), many polyphenols (e.g., quercetin, eugenol, carvacrol, citral and chlorogenic acid) were found to curb expression of main QS-regulated genes (*lasR*, *lasI*, *rhlR*, *rhlI*) in *P. aeruginosa*. SA and CIN at sub-MIC concentrations interacted with RhlR and LasR protein in *P. aeruginosa*. Subsequently, biofilm formation and protease production were reduced by 54% and 31%, respectively, due to the QS inhibition effect of SA. While CIN induced 26% and 65% inhibition in biofilm formation and protease production, respectively (Ahmed et al., 2019). Additionally, CIN at 0.10 µl/mL also demonstrated an amelioratory effect on biofilm formation and protease production in *P. fluoroscens* 13525 by 54.48% and 58%, respectively (Li et al., 2018). In the same study, the volatile base nitrogen (TVB-N) content was significantly reduced during 15-day cold storage of fish fillets contaminated with *P. fluoroscens* 13525 and treated with CIN at sub-MIC values compared to untreated samples, referring to the preservative role of CIN in aquatic products

through QS inhibition. In a like manner, SA and CIN at sub-MIC concentrations (0.1 mg/mL) reduced biofilm formation, motility, and exopolysaccharide synthesis by *P. fluoroscens* isolates from spoiled lettuce and yellow croaker (Zhang et al., 2018; Hong et al., 2021). The mechanism of QS inhibition in these studies refers to the binding ability of CIN and SA to LuxR-homologue in *P. flouroscens* in competition with the primary ligands (C4-HSL and C6-HSL). The attenuating effects of CIN and SA on the spoilage factors, as described above, are in parallel with our results, where the proteolytic activity of the *P. gessardii* isolates was decreased after the addition of the same compounds (**Figure 29**).

4.3.5 Inhibitory effect of L. acidophilus *LA-5 on proteolysis by* P. gessardii *BV6*

Seven probiotic strains were tested for their potential ability to control proteolytic activity, without antimicrobial effect, which could putatively refer to QS disruption. Among the strains, *L. acidophilus* LA-5 has significantly inhibited the proteolytic activity in the group of milk samples added with the CFS comparing with the control group, at both incubation temperature and without antimicrobial effect **(Figure 30)**. This strongly suggests a presence of QS inhibitors in the metabolites of *L. acidophilus* LA-5. The chemical composition of this postbiotic form this strain was extensively analyzed in the studies of Moradi et al (2019) and Nasri et al (2024). The compounds in these studies were tested for their ability to interact with the LuxR protein of *P. gessardii* BV6 using the same *in silico* approach as explained in the previous sections of **4.2.1**, **4.2.2** and **4.2.3**. The compounds that potentially block the RhlR-like receptor in *P. gessardii* BV6 are reported in **Table 19.** Lactic acid, butyric acid, nonanal, capraldehyde, 3-Methyl-2-pyrazinyl methanol and ethyl lactate exhibited higher docking scores the reference ligand of C4-HSL. The rest of the compounds scored closely to C4-HSL, albeit slightly lower, this could still compete with C4-HSL to bind with the RhlR-like receptor. Collectively, *L. acidophilus* LA-5 produces a wide range of metabolites that could disrupt QS pathway.

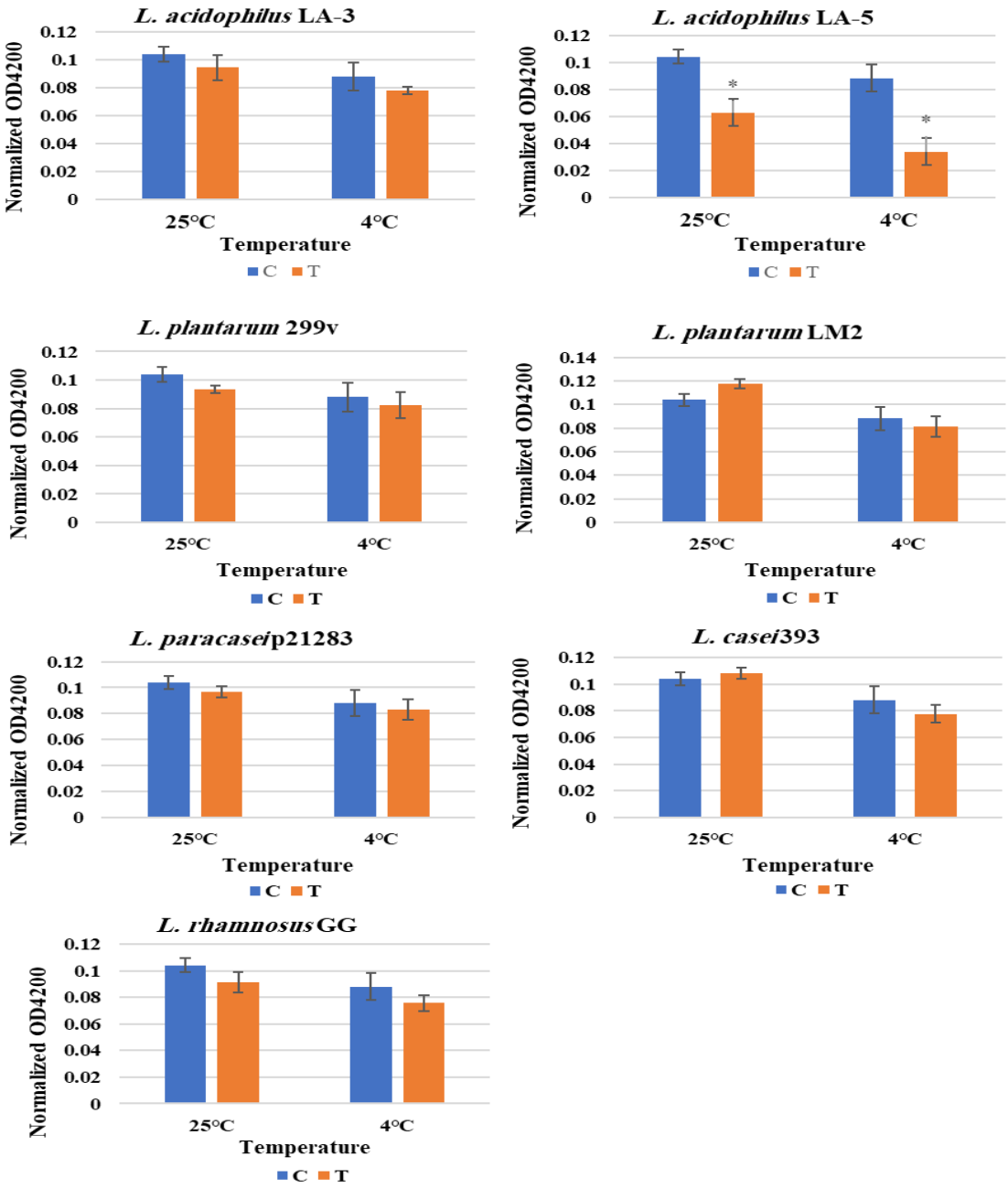

Figure 30. The result of the proteolytic activity of *P. gessardii* BV6 co-cultured with MRS broth (C) and CFS (T) evaluated by TNBS assay, the data are adjusted for the number of logs in each group to rule out antimicrobial effect of the CFS. * Indicates P-value < 0.05 and statistically significant comparing with the control group.

Table 19. Docking scores of previously identified metabolites of LA-5 simulated for their affinity to bind with the RhlR-like protein of *P. gessardii* BV6.

Name	No of non-H atom	Fittnne s score	Normalized score	Nonpolar score	Ligand. clash	Ligand. torsion
Lactic acid	6	32.65	5.44	-12.44	0.00	0.03
Acetic acid	4	21.60	5.40	-7.39	0.00	0.00
butyric acid	6	32.24	5.37	-20.45	0.00	0.02
Nonanal	10	50.35	5.04	-42.36	0.00	0.18
Capraldehyde	11	54.45	4.95	-46.24	0.00	0.13
3-Methyl-2-pyrazinyl methanol	9	43.60	4.84	-28.76	0.00	0.02
Ethyl lactate	8	38.33	4.79	-22.99	0.00	0.06
C4-HSL	12	56.63	4.72	-36.38	0.25	
Tridecyl alcohol	14	65.46	4.68	-54.46	0.00	0.78
Benzoic acid	9	41.86	4.65	-30.87	0.00	0.05
Methyl lactate	7	32.53	4.65	-17.07	0.00	0.01
malic acid	9	41.48	4.61	-15.45	0.00	0.16
1-Tetradecanol	15	67.55	4.50	-56.59	0.00	0.43
3,5-Dihydroxy-2-methyl-4H-pyran-4-one	10	44.60	4.46	-26.55	0.00	0.00
2,3-Dihydro-3,5-dihydroxy-6-methyl-4H-pyran-4-one	10	43.43	4.34	-26.36	0.00	0.00
4-Hydroxy benzoic acid	10	43.21	4.32	-30.86	0.00	0.02
Protocatechuic acid	11	46.95	4.27	-27.34	0.02	0.02
2–5 Dihydroxy benzoic acid	11	46.03	4.18	-28.22	0.00	0.54
Chamazulene	14	57.06	4.08	-61.12	0.00	0.06
Tetradecanoic acid	16	65.14	4.07	-57.51	0.00	0.66

As discussed in 1the first chapter, QS inhibition by probiotic lactic acid bacteria is primarily highlighted against foodborne pathogenic bacteria. Yet, QS inhibition against foodborne-spoilage bacteria, in particular, *Pseudomonas* species is still limited. In a recent study (Lv et al., 2021), a wide range of *lactobacillus* isolates from fermented foods were screened for their ability to reduce violacein production by CV026 biosensor strain, which is indicator of QS inhibition. One isolate of *L. plantarum* from pickle showed complete inhibition of violacein production and was included for further analysis to test its ability to control the spoilage factors of *Aeromonas sobria* isolate from spoiled turbot. The metabolites of this *lactobacillus* strain were extracted using ethyl acetate and added to the *Aeromonas sobria* culture at sub-MICs. Consequently, the protease activity, motility and biofilm formation were significantly reduced indicating an effect of QS inhibition. In a similar study (Xinran et al., 2023), the CFS from *L. crustorum* ZHG2-1, an isolate from fermented cucumber, fully degraded the AHL produced from spoilage strain of *P. fluorescence*. In addition, the ethyl acetate extract of the ZHG2-1 metabolites reduced the spoilage factors of this *Pseudomonas* strain (exopolysaccharides, proteases, lipases, biogenic amines). However, neither the mechanism of QS inhibition and probiotic properties of the isolated strain of *Lactobacillus* are investigated in these two studies.

4.4 Conclusion

Using *in silico* approaches, 50 compounds were tested for their ability to bind with the RhlR-like receptor and compared with the reference ligand (C4-HSL). Salicylic acid and cinnamaldehyde were found to score higher the C4-HSL in terms of the binding ability. In-vitro analysis showed these compounds significantly inhibited the proteolytic activity as sub-MICs. In addition, postbiotic compounds from *L. acidophilus* LA-5 were also predicted to bind with the RhlR-like receptor, which subsequently reduced proteolysis at non-growth inhibitory concentrations.

4.5 References

Lee, D. H., Kim, J. B., Kim, M., Roh, E., Jung, K., Choi, M., ... & Heu, S. (2013). Microbiota on spoiled vegetables and their characterization. Journal of food protection, 76(8), 1350-1358.

Zhang, Y., Kong, J., Huang, F., Xie, Y., Guo, Y., Cheng, Y., ... & Yao, W. (2018). Hexanal as a QS inhibitor of extracellular enzyme activity of *Erwinia carotovora* and *Pseudomonas fluorescens* and its application in vegetables. Food chemistry, 255, 1-7.

Myszka, K., Tomaś, N., Wolko, Ł., Szwengiel, A., Grygier, A., Nuc, K., & Majcher, M. (2021). In situ approaches show the limitation of the spoilage potential of *Juniperus phoenicea* L. essential oil against cold-tolerant *Pseudomonas fluorescens* KM24. Applied Microbiology and Biotechnology, 105(10), 4255-4268.

Li, T., Wang, D., Liu, N., Ma, Y., Ding, T., Mei, Y., & Li, J. (2018). Inhibition of quorum sensing-controlled virulence factors and biofilm formation in *Pseudomonas fluorescens* by cinnamaldehyde. International journal of food microbiology, 269, 98-106.

Ding, T., Li, T., & Li, J. (2019). Virtual screening for quorum-sensing inhibitors of Pseudomonas fluorescens P07 from a food-derived compound database. *Journal of Applied Microbiology*, *127*(3), 763-777.

Wang, Y., Wang, Y., Chen, J., Koseki, S., Yang, Q., Yu, H., & Fu, L. (2021). Screening and preservation application of quorum sensing inhibitors of Pseudomonas fluorescens and Shewanella baltica in seafood products. *Lwt*, *149*, 111749.

Fraga, C. G., Croft, K. D., Kennedy, D. O., & Tomás-Barberán, F. A. (2019). The effects of polyphenols and other bioactives on human health. Food & function, 10(2), 514-528.

Papuc, C., Goran, G. V., Predescu, C. N., Nicorescu, V., & Stefan, G. (2017). Plant polyphenols as antioxidant and antibacterial agents for shelf-life extension of meat and meat products: Classification, structures, sources, and action mechanisms. Comprehensive Reviews in Food Science and Food Safety, 16(6), 1243-1268.

Bouyahya, A., Chamkhi, I., Balahbib, A., Rebezov, M., Shariati, M. A., Wilairatana, P., ... & El Omari, N. (2022). Mechanisms, anti-quorum-sensing actions, and clinical trials of medicinal plant bioactive compounds against bacteria: a comprehensive review. Molecules, 27(5), 1484.

Vadakkan, K., Sathishkumar, K., Mapranathukaran, V. O., Ngangbam, A. K., Nongmaithem, B. D., Hemapriya, J., & Nair, J. B. (2024). Critical review on plant-derived quorum sensing signaling inhibitors in pseudomonas aeruginosa. Bioorganic Chemistry, 107649.

Ahmed, S. A., Rudden, M., Smyth, T. J., Dooley, J. S., Marchant, R., & Banat, I. M. (2019). Natural quorum sensing inhibitors effectively downregulate gene expression of Pseudomonas aeruginosa virulence factors. Applied microbiology and biotechnology, 103, 3521-3535.

Li, T., Wang, D., Liu, N., Ma, Y., Ding, T., Mei, Y., & Li, J. (2018). Inhibition of quorum sensing-controlled virulence factors and biofilm formation in *Pseudomonas fluorescens* by cinnamaldehyde. International journal of food microbiology, 269, 98-106.

Hong, X., Wang, Y., Chen, S., & Zhu, J. (2021). Efficacy of ten structurally related essential oil components on anti-biofilm and anti-quorum sensing against fish spoilers Pseudomonas and Aeromonas. Journal of Aquatic Food Product Technology, 30(4), 462-473.

Moradi, M., Mardani, K., & Tajik, H. (2019). Characterization and application of postbiotics of Lactobacillus spp. on Listeria monocytogenes in vitro and in food models. *Lwt*, *111*, 457-464.

Nasri, F., Alizadeh, A., İncili, G. K., Hayaloğlu, A. A., & Moradi, M. (2024). Investigating Chemical Composition and Functionality of Lactobacillus acidophilus LA-5 Postbiotics Prepared in Classic and Cheese Whey Media. *Probiotics and Antimicrobial Proteins*, 1-15.

Lv, X., Cui, T., Du, H., Sun, M., Bai, F., Li, J., & Zhang, D. (2021). Lactobacillus plantarum CY 1-1: A novel quorum quenching bacteria and anti-biofilm agent against Aeromonas sobria. *LWT*, *137*, 110439.

Xinran, L., Xin, W., Yangrui, W., Fengling, B., Fangchao, C., Xiqian, T., ... & Xiaohua, G. (2023). Quorum Quenching Effects of Lactobacillus crustorum ZHG2-1 on Pseudomonas fluorescens. *Journal of Chinese Institute of Food Science & Technology/Zhongguo Shipin Xuebao*, *23*(11).

5 Conclusions and future works

P. gessardii is highly concerned as proteolytic species being present in raw milk. It plays a role in the spoilage activity of milk/dairy products in dual routes through protease production. First, by affect the quality of raw milk itself during cold storage. Second, these enzymes are thermostable that stay active even after thermal processing and during the storage of the dairy product. Biosensor assays employing CV026 (cross-feeding and TLC-overlay) found for the first time the production of C4-HSL as a main short-chain AHL product while production of long AHLs is still scarce. This was confirmed by UPLC-MS analysis. Whole genomic sequencing revealed that the type of AHL-quorum sensing based system is strain-dependent. RhlR/I - like and LasR/I – like quorum sensing systems were present in BV6 and RWV6 strains while RhlR/I – like QS system was only found in the rest of the strains. In addition, two types of LuxR solo were detected without presence of its cognate AHL synthase in the operon cluster. The first is found in all genomes and annotated as DNA-binding CsgD family transcriptional regulator. The second is annotated as quorum-sensing system regulator BjaR1 found in BV5 and CP15 strains. Heterologous expression of the AHL-degrading enzyme in the *P. gessardii* strains demonstrated the role of the AHLs in the proteolytic activity. *P. gessardii* BV6 and RWV6 have *rhlI*-like and *lasI*-like genes. The mutant-type in these genes showed *rhlI*-like gene is primarily involved in the regulation of proteolytic activity. Virtual screening of 50 polyphenolic compounds reported that salicylic acid and cinnamaldehyde are strong competitors with the native ligand (C4-HSL) to bind with the LuxR protein. In vitro assays reported that these two molecules significantly inhibited the proteolytic activity in milk model at 4 °C and 25 °C. Postbiotic compounds from *L. acidophilus* LA-5 significantly decreased the proteolytic activity by *P. gessardii* BV6 at 4 °C and 25 °C. The mechanism behind that is the

interaction of the metabolites with the LuxR protein as suggested by *in silico* analysis. Collectively, polyphenols and postbiotic metabolites are potential quorum sensing inhibitors to control of proteolytic activity by *P. gessardii* in raw milk and dairy products.

Despite the results of this study demonstrate the potential control of proteolytic activity by QS inhibition, there are still some limitations and future research to be addressed. First, *P. gessardii* is one of the variant species of *Pseudomonas* present in raw milk contains and the control of proteolytic activity by QS inhibition still need further investigation. For instance, *P. azotoformans*, *P. psychrophila*, *P. lactis* and *P. fluoroscens* are species that found to possess an AHL-based QS system associated with spoilage activity (Quintieri et al., 2021). Despite SA and CIN are not yet investigated for their ability to block QS pathway and proteolysis inhibition, it will be intriguing to for future studies to investigate the result of QS inhibition in these species, which will provide robust evidence for control of spoilage activity. Second, the LuxR solo was detected in the current of *P. gessardii* isolates. Additionally, it is also present in a wide range of non-AHL producing *Pseudomonas* species (Bez et al., 2021). Yet, its role in the regulation of spoilage virulence factors expression is not currently illustrated and therefore, future research should focus on identification of other proteolytic *Pseudomonas* species for the purpose of testing the association of LuxR solo and spoilage activity. If it turns out that this gene plays a role in protease production, for example, this will significantly enrich the field of QS role in food quality and help develop and identify QS inhibitors for this type of gene. Third, full transcriptomic response to QS inhibition in *P. gessardii* is warranted to obtain a wider information about the involvement of QS in other spoilage and metabolic pathway. Last but not least, the application of QS inhibition in this study was studies at lab scale. While the outcomes here are promising, control of proteolytic activity by QS inhibition should be still tested at industrial scale.

6 Appendices

6.1 Appendix A: Skim milk assay for *P. gessardii* isolates

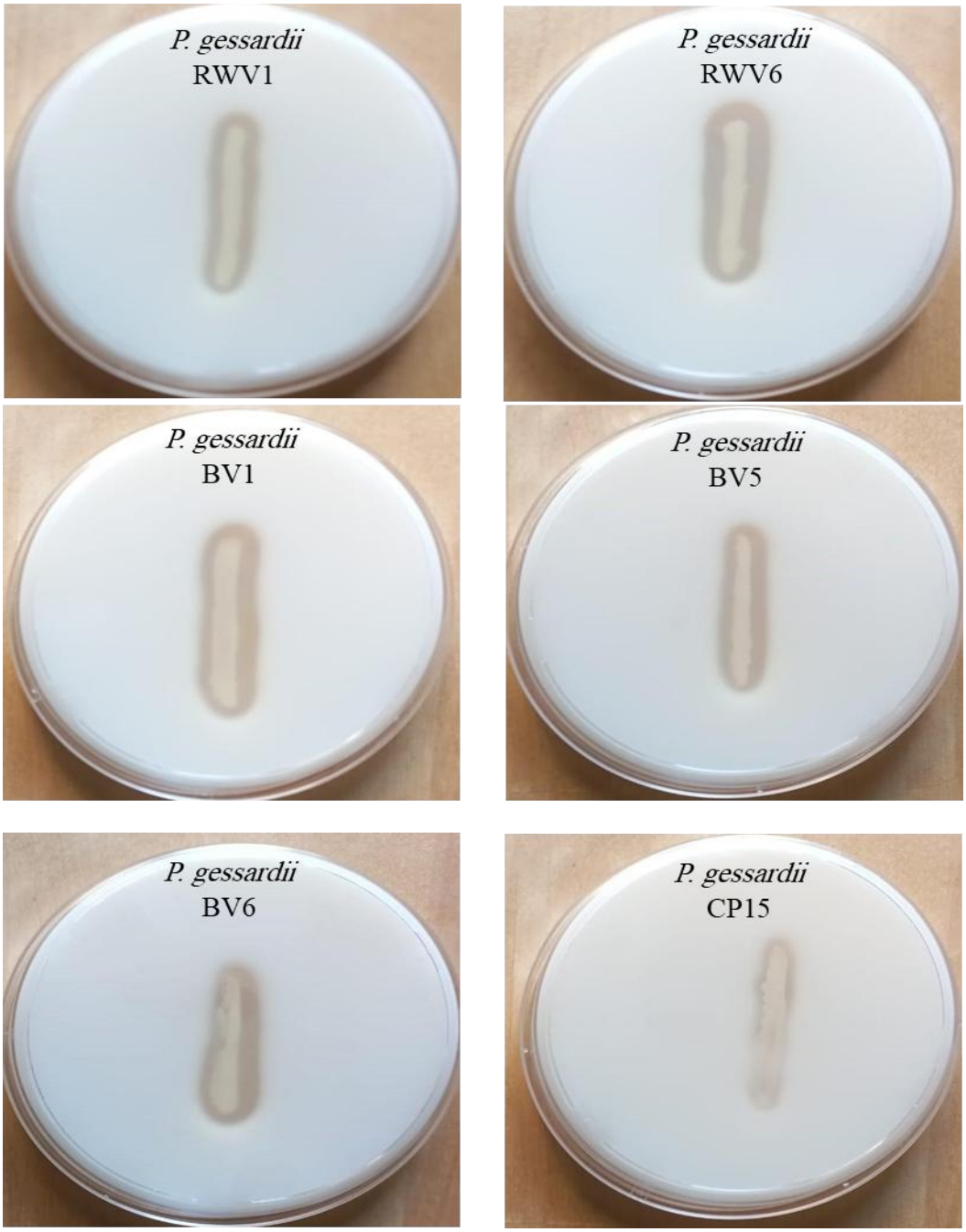

Figure S1. Proteolytic activity of *Pseudomonas* isolates on skim milk agar after 2-3 days of incubation at 4°C

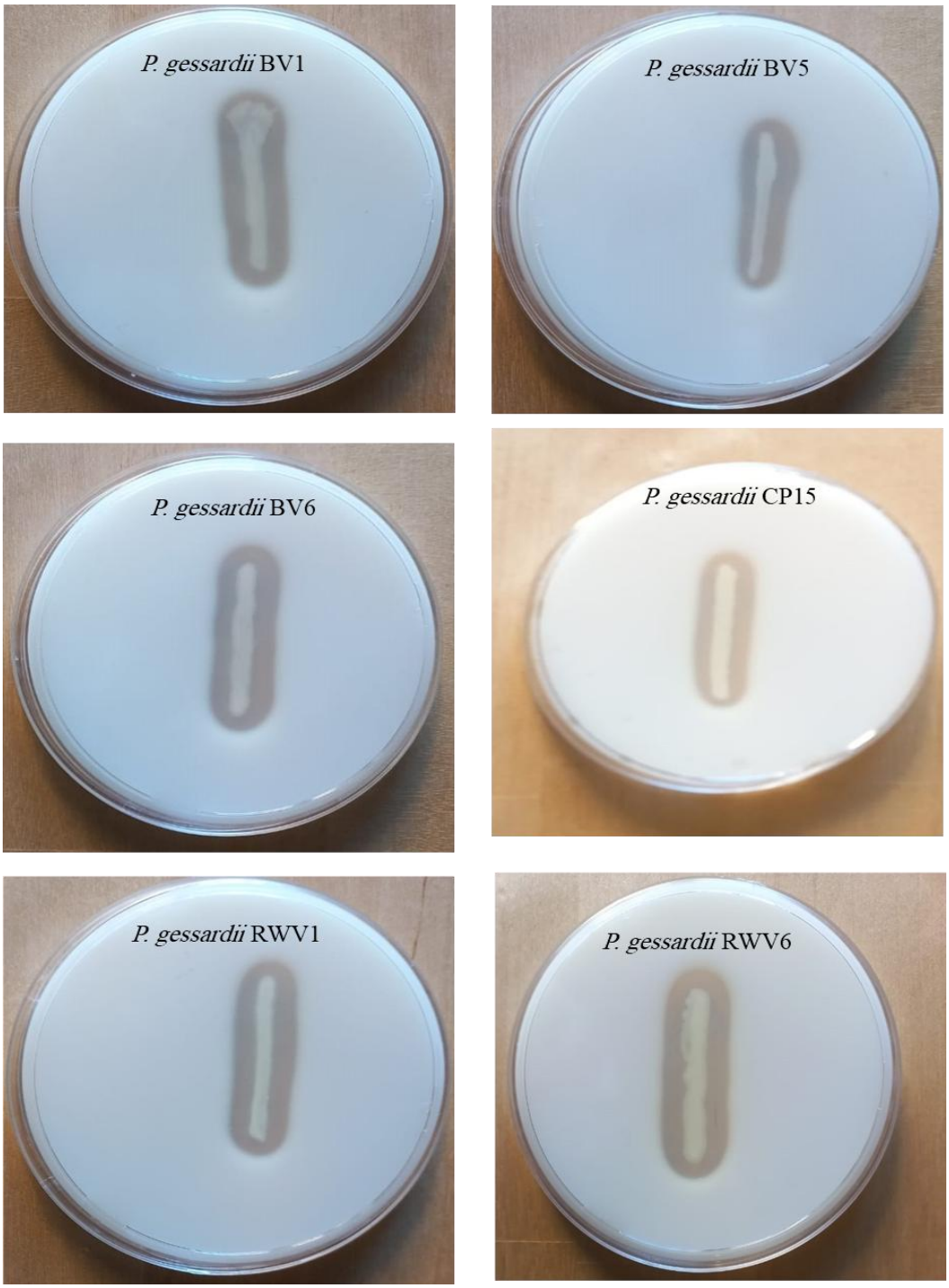

Figure S2. Proteolytic activity of *Pseudomonas* isolates on skim milk agar after 2-3 days of incubation at 25℃

6.2 Appendix B: Growth curves of *P. gessardii* strains

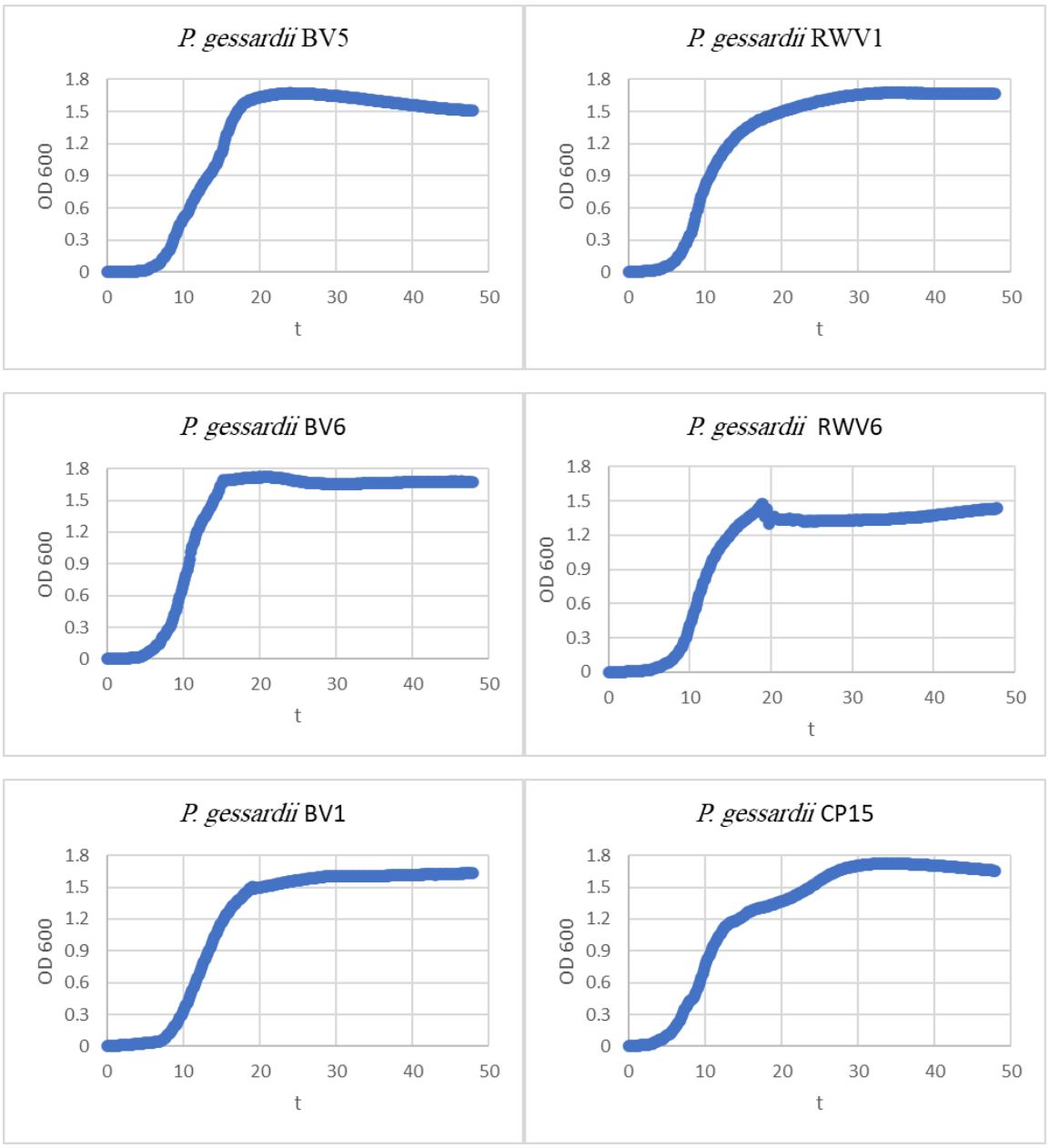

Figure S3. Growth curves of the Pseudomonas strains grown in LB at 25 °C for 48 hours. The x-axis represents the incubation time in hours (t) and the y-axis represents the absorbance value (OD 600) that was taken each 10 minutes during the incubation. Samples containing media only were set as blank.

6.3 Appendix C: Multiple alignment of *rhlI* and *lasI* genes

```
BV1_I1          ATGATCAGCATCATCACCCGCCATCACCATGAACTGTCTGCAGCCCTTGAGGACGACCTG
RWV1_I1         ATGATCAGCATCATCACCCGCCATCACCATGAACTGTCTGCAGCCCTTGAGGACGACCTG
BV5_I1          ATGATCAGCATCATCACCCGCCATCACCATGAACTGTCTGCAGCCCTTGAGGACGACCTG
CP15_I1         ATGATCAGCATCATCACCCGCCATCACCATGAACTGTCTGCAGCCCTTGAGGACGACCTG
                ************************************************************

BV1_I1          GGCCGCTATCGACACGAAGTGTTCATCGAGCAACTGGGTTGGCAACTGGACTCCACCCAC
RWV1_I1         GGCCGCTATCGACACGAAGTGTTCATCGAGCAACTGGGTTGGCAGCTGGACTCCACCCAC
BV5_I1          GGCCGCTATCGACACGAAGTGTTCATCGAGCAACTGGGTTGGCAGCTGGACTCCACCCAC
CP15_I1         GGCCGCTATCGACACGAAGTGTTCATCGAGCAACTGGGTTGGCAGCTGGACTCCACCCAC
                ******************************************* ***************

BV1_I1          GCCCGGCCCCAACGTGAATTCGATCAGTTCGACCAGGCCGACACGCGCCATATCCTCGCT
RWV1_I1         GCCCGGCCCCAACGTGAATTCGATCAGTTCGACCAGGCCGACACGCGCCATATCCTCGCC
BV5_I1          GCCCGGCCCAAACGTGAATTCGATCAGTTCGACCAGGCCGACACGCGCCATATCCTCGCC
CP15_I1         GCCCGGCCCAAACGTGAATTCGATCAGTTCGACCAGGCCGACACGCGCCATATCCTCGCC
                ********* ************************************************

BV1_I1          CTGGACACAAAAGGCCAGGTCTGCGGTTGCGCACGGCTGTTGCCAACCACCCAACCTTAT
RWV1_I1         CTGGACACAAAAGGCCAGGTCTGCGGTTGCGCACGGCTGTTGCCGACCACCCAACCTTAT
BV5_I1          CTGGACACAAAAGGCCAGGTCTGCGGTTGCGCACGGCTGTTACCGACCACCCAACCTTAT
CP15_I1         CTGGACACAAAAGGCCAGGTCTGCGGTTGCGCACGGCTGTTACCGACCACCCAACCTTAT
                ************************************** ** ***************

BV1_I1          CTGCTGTCGGAAGTCTTCGGGTTTCTGTGCGACCAGCCAAGCCCGCGCAGCCGTGACACC
RWV1_I1         CTGCTGTCGGAAGTCTTCGGGTTTCTGTGCGACCAGCCAAGCCCGCGCAGCCGTGACACC
BV5_I1          CTACTGTCGGAAGTCTTCGGGTTTCTGTGCGACCAGCCAAGCCCGCGCAGCCGTGACACC
CP15_I1         CTACTGTCGGAAGTCTTCGGGTTTCTGTGCGACCAGCCAAGCCCGCGCAGCCGTGACACC
                ** ********************************************************

BV1_I1          TGGGAAGTGTCGCGCTTTGCCGCCCGCGCCCTGGAGAAAGGCACCTTACCGATGCGCGTC
RWV1_I1         TGGGAAGTGTCGCGCTTTGCCGCCCGCGCCCTGGAGAAAGGCACCTTACCGATGCGCGTC
BV5_I1          TGGGAAGTGTCGCGCTTTGCCGCCCGCGCCCTGGAGAAAGGTACCTTACCGATGCGCGTC
CP15_I1         TGGGAAGTGTCGCGCTTTGCCGCCCGCGCCCTGGAGAAAGGTACCTTACCGATGCGCGTC
                ************************************** ******************

BV1_I1          TGGTGGAACAGCCTGCACCATGCCTGGAGCCACGGCGCCAATCAGGTGGTGGCAGTGACC
RWV1_I1         TGGTGGAACAGCCTGCACCATGCCTGGAGCCACGGCGCCAATCAGGTGGTGGCAGTGACC
BV5_I1          TGGTGGAGCAGCCTGCACCATGCCTGGAGCCACGGCGCCAATCAGGTGGTGGCAGTGACC
CP15_I1         TGGTGGAGCAGCCTGCACCATGCCTGGAGCCACGGCGCCAATCAGGTGGTGGCAGTGACC
                ******* ****************************************************

BV1_I1          ACTCCAGCGCTGGAGCGTTATTTCCTGAAAAATGGCGTGCAATTGAGTCGCCTCGGCGCC
RWV1_I1         ACTCCAGCGCTGGAGCGTTATTTCCTGAAAAATGGCGTGCAATTGAGTCGCCTCGGCGCC
BV5_I1          ACTCCAGCGCTGGAGCGTTATTTTCTGAAAAATGGCGTGCAATTGAGTCGCCTCGGCGCC
CP15_I1         ACTCCAGCGCTGGAGCGTTATTTTCTGAAAAATGGCGTGCAATTGAGTCGCCTCGGCGCC
                ********************** ***********************************

BV1_I1          CCGCAACGCGTGAACAACGACCATGTGGTAGCACTGAGTTTTCCGGCCTGGCAGAAAAAC
RWV1_I1         CCGCAACGCGTGAACAACGACCATGTGGTAGCACTGAGTTTTCCGGCCTGGCAGAAAAAC
BV5_I1          CCGCAACGCGTGAACAACGACCATGTGGTAGCACTGAGTTTTCCGGCCTGGCAGAAAAAC
CP15_I1         CCGCAACGCGTGAACAACGACCATGTGGTAGCACTGAGTTTTCCGGCCTGGCAGAAAAAC
```

Figure S4. Multiple alignment of *rhlI*-like genes between BV1, BV5, CP15 and RWV1 strains.

```
BV6_luxI1       ATGATCAGCATCATCACCCGCCATCACCATGAACTGTCTGCAGCCCTTGAGGACAACCTG
RWV6_luxI1      ATGATCAGCATCATCACCCGCCATCACCATGAACTGTCTGCAGCCCTTGAGGACGACCTG
                ************************************************** *****

BV6_luxI1       GGTCGCTACCGGCACGAAGTGTTCATCCAGCAACTGGGCTGGCAACTGGACTCCACCTAC
RWV6_luxI1      GGTCGCTACCGGCACGAAGTGTTCATCCAGCAACTGGGCTGGCAACTGGACTCCACCTAC
                ************************************************************

BV6_luxI1       GCCCTGCCCCAACGCGAATTCGACCAGTTCGACCAGGCCGACACGCGCCACATCCTCGCC
RWV6_luxI1      GCCCTGCCCCAACGCGAATTCGACCAGTTCGACCAGGCCGACACGCGCCACATCCTCGCC
                ************************************************************

BV6_luxI1       CTGGACCCAAAAGGCCAGGTCTGCGGTTGCGCGCGGCTGCTGCCAACCACACAACCTTAT
RWV6_luxI1      CTGGACCCAAAAGGCCAGGTCTGCGGTTGCGCGCGGCTGTTGCCAACCACACAACCTTAT
                ************************************ ********************

BV6_luxI1       CTGCTGTCGGAAGTCTTCGGCTTTCTGTGCGACCAGCCGAGCCCACGCAGCAGTGACACC
RWV6_luxI1      CTGCTGTCGGAAGTCTTCGGCTTTCTGTGCGACCAGCCGAGCCCACGCAGCAGTGACACC
                ************************************************************

BV6_luxI1       TGGGAAGTGTCGCGCTTTGCCGCCCGCGCCCTGGAAAAAGGCCGCCTGCCGATGCGCGTC
RWV6_luxI1      TGGGAAGTGTCGCGCTTTGCCGCCCGCGCCCTGGAAAAAGGCCGCCTGCCGATGCGCGTC
                ************************************************************

BV6_luxI1       TGGTGGAACAGCCTGCACCATGCCTGGAGCCAAGGCGCCAACCGGGTGGTGGCGGTGACC
RWV6_luxI1      TGGTGGAACAGCCTGCACCATGCCTGGAGCCAAGGCGCCAACCGGGTGGTGGCGGTGACC
                ************************************************************

BV6_luxI1       ACGCCGGCGCTGGAGCGCTACTTCCTGAAAAATGGCGTGCAGCTGAGTCGCCTCGGCTCC
RWV6_luxI1      ACGCCGGCGCTGGAGCGTTACTTCCTGAAAAATGGCGTGCAGCTGAGTCGCCTCGGCTCC
                ***************** ****************************************

BV6_luxI1       CCGCAACGGGTGAACAAAGACCATGTGGTAGCGCTGAGTTTTCCTGCCTGGCAGAAAAAC
RWV6_luxI1      CCGCAACGGGTGAACAAAGACCATGTGGTAGCGCTGAGTTTTCCTGCCTGGCAGAAAAAC
                ************************************************************

BV6_luxI1       GGCCGACTCGCGTTACAGGCGCAGTCGGCCGTTGCCTAG
RWV6_luxI1      GGCCGACTCGCGTTACAGGCGCAGTCGGCCGTTGCCTAG
                ***************************************
```

Figure S5. Multiple alignment of *rhlI*-like gene between BV6 and RWV6. Yellow and blue highlight represent the forward and reverse primers previously used in the PCR amplification.

```
BV6_LuxI2       GTGCATTTCACAATCGGTCGGCGGGATGAAATAGATAGTGAACAACTGTGCGCCATGCAT
RWV6_LuxI2      GTGCATTTCACAATCGGTCGGCGGGATGAAATAGATAGTGAGCAACTGTGCGCCATGCAT
                **************************************** ******************

BV6_LuxI2       AGGCTGCGCGCAGATGTTTTTAAAAAGCGTAAGGGCTGGGATGTTGCAATCATTGCCGAT
RWV6_LuxI2      AGGCTGCGCGCAGATGTTTTTAAAAAGCGTAAGGGCTGGGATGTTGCAATCATTGCCGAT
                ************************************************************

BV6_LuxI2       ATGGAAATTGATGGTTATGACGCACTGGAGCCTCTCTACATGCTGATCAAGGATGGCGGA
RWV6_LuxI2      ATGGAAATTGATGGTTATGACGCACTGGAGCCTCTCTACATGCTGATCAAGGATGGCGGA
                ************************************************************

BV6_LuxI2       GACAGTGAGATCAAAGGGTGCTGGCGTTTATTACCTACTACAGGCCCCTACATGCTCAGG
RWV6_LuxI2      GACAGTGAGATCAAAGGGTGCTGGCGTTTATTACCTACTACAGGCCCCTACATGCTCAGG
                ************************************************************

BV6_LuxI2       GATACTTTCTCCGAATTGCTTGAAGGGCGACCAGCGCCTGTTTCTTCCCAGGTATGGGAA
RWV6_LuxI2      GATACTTTCTCCGAGTTGCTTGAAGGGCGACCAGCGCCTGTTTCTTCCCAGGTATGGGAA
                ************** ********************************************

BV6_LuxI2       CTCAGTCGATTTGCCGTAACCCCTCGATATCCCGGTAACAAGGGGTTTTCCGACTTTACC
RWV6_LuxI2      CTCAGTCGATTTGCCGTAACCCCTCGATATCCCGGTAACAAGGGGTTTTCCGACTTTACC
                ************************************************************

BV6_LuxI2       CTGGAGGCCGTAAAGGCCATCGTTGCCTATGGTGTCGAGCAACATATCCAGGGTTATGTG
RWV6_LuxI2      CTGGAGGCCGTAAAGGCCATCGTTGCCTATGGTGTCGAGCAACATATCCAGGGTTATGTG
                ************************************************************

BV6_LuxI2       ACGGTTACAACGGTAGCGGTAGAACGAATGCTGATCAGGGCTGGCCTGGTGATCACCCGG
RWV6_LuxI2      ACGGTTACAACGGTAGCGGTAGAGCGAATGTTGATCAGGGCTGGCCTGGTGATCACCCGG
                ********************** ****** ****************************

BV6_LuxI2       CTTGGGCCGGTACGTGTCATTGGCCAGGAAAAGGCCATTGCCCTGGAAATAGATCTGGGT
RWV6_LuxI2      CTTGGGCCGGTACGTGTCATTGGCCAGGAAAAGGCCATTGCCCTGGAAATAGATCTGGGT
                ************************************************************

BV6_LuxI2       GCGGTGACTCAACGCGCGCTGTTTGGCGTATCCAGAAGTTGTTGTGGCGCTACGTTGCAG
RWV6_LuxI2      GCGGTGACTCAACGTGCGCTGTTTGGCGTATCCAGAAGTTGTTGTGGCGCTACGTTGCAG
                ************** ********************************************

BV6_LuxI2       TAG
RWV6_LuxI2      TAG
                ***
```

Figure S6. Multiple alignment of *lasI-like* genes between BV6 and RWV6 strains. Yellow and blue highlight represent the forward and reverse primers previously used in the PCR amplification.

6.4 Appendix D: Multiple alignment of *rhlR* and *lasR* genes

```
RhlR_BV1        ATGGAGAAGGAAAACGACCTCATCCGCTGGTGGAATCGCTTGCGGATAGAGATGCTCAAG
RhlR_BV5        ATGGAGAAGGAAAACGACCTCATCCGCTGGTGGAATCGCTTGCGGATAGAGATGCTCAAG
RhlR_CP15       ATGGAGAAGGAAAACGACCTCATCCGCTGGTGGAATCGCTTGCGGATAGAGATGCTCAAG
RhlR_RWV1       ATGGAGAAGGAAAACGACCTCATCCGCTGGTGGAATCGCTTGCGGATAGAGATGCTCAAG
                ************************************************************
RhlR_BV1        CAACAGGGAGGAGCACAAGTGTTCGCGCTGCTGGAGCGGGAAGTGTTGCAATTGGGGTTC
RhlR_BV5        CAACAGGGAGGAGCACAAGTGTTCGCGCTGCTGGAGCGGGAAGTGTTGCAATTGGGGTTC
RhlR_CP15       CAACAGGGAGGAGCACAAGTGTTCGCGCTGCTGGAGCGGGAAGTGTTGCAATTGGGGTTC
RhlR_RWV1       CAACAGGGAGGAGCACAAGTGTTCGCGCTGCTGGAGCGGGAAGTGTTGCAATTGGGGTTC
                ************************************************************
RhlR_BV1        GAGTATTACGCCTATGCCGTACGCCACCTGACCCCTTTTACCCGACCAAAAACCGAGATT
RhlR_BV5        GAGTATTACGCCTATGCCGTACGCCACCTGACCCCTTTTACCCGACCAAAAACCGAGATT
RhlR_CP15       GAGTATTACGCCTATGCCGTACGCCACCTGACCCCTTTTACCCGACCAAAAACCGAGATT
RhlR_RWV1       GAGTATTACGCCTATGCCGTACGCCACCTGACCCCTTTTACCCGACCAAAAACCGAGATT
                ************************************************************
rhlR_BV1        CACGGCTCTTACCCCGAAAGGTGGCTGGAACATTACCAGGAGCAAAACTACGCGGCTGTC
RhlR_BV5        CACGGCTCTTACCCCGAAAGGTGGCTGGAACATTACCAGGAGCAAAACTACGCGGCTGTC
RhlR_CP15       CACGGCTCTTACCCCGAAAGGTGGCTGGAACATTACCAGGAGCAAAACTACGCGGCTGTC
RhlR_RWV1       CACGGCTCTTACCCCGAAAGGTGGCTGGAACATTACCAGGAGCAAAACTACGCGGCTGTC
                ************************************************************
RhlR_BV1        GATCCGTCGATCCTCAGTGGCTTGCGTTCCACCGAGATGGTGCTGTGGAACGACGCACTG
RhlR_BV5        GATCCGTCGATCCTCAGTGGCTTGCGTTCCACCGAGATGGTGCTGTGGAACGACGCACTG
RhlR_CP15       GATCCGTCGATCCTCAGTGGCTTGCGTTCCACCGAGATGGTGCTGTGGAACGACGCACTG
RhlR_RWV1       GATCCGTCGATCCTCAGTGGCTTGCGTTCCACCGAGATGGTGCTGTGGAACGACGCACTG
                ************************************************************
RhlR_BV1        TTTGAAAACAGCCGCAAGCTATGGCTGGAAGCTCGGGACTGGGGTCTGTGCATCGGCGCC
RhlR_BV5        TTTGAAAACAGCCGCAAGCTATGGCTGGAAGCTCGGGACTGGGGTCTGTGCATCGGCGCC
RhlR_CP15       TTTGAAAACAGCCGCAAGCTATGGCTGGAAGCTCGGGACTGGGGTCTGTGCATCGGCGCC
RhlR_RWV1       TTTGAAAGCAGTCGCAAGCTATGGCTGGAAGCTCGGGATTGGGGTCTGTGCATCGGCGCC
                ******* *** ************************* ***********************
RhlR_BV1        ACGCTGCCGATTCGCAGCCACGATCATTCGCTGCGGGTACTGTCCGTGGCCCGGCGCCAG
RhlR_BV5        ACGCTGCCGATTCGCAGCCACGATCATTCGCTGCGGGTACTGTCCGTGGCCCGGCGCCAG
RhlR_CP15       ACGCTGCCGATTCGCAGCCACGATCATTCGCTGCGGGTACTGTCCGTGGCCCGGCGCCAG
RhlR_RWV1       ACGCTGCCGATTCGCAGCCACGATCATTCGCTGCGGGTACTGTCCGTGGCCCGGCGCCAG
                ************************************************************
RhlR_BV1        GATCCTATTTCGCGGGCTGAAAGCGACGAAATTCAATTGCGCCTGCGCTGCATCCTCGAA
RhlR_BV5        GATCCTATTTCGCGGGCTGAAAGCGACGAAATTCAATTGCGCCTGCGCTGCATCCTCGAA
RhlR_CP15       GATCCTATTTCGCGGGCTGAAAGCGACGAAATTCAATTGCGCCTGCGCTGCATCCTCGAA
RhlR_RWV1       GATCCTATTTCGCGGGCTGAAAGCGACGAAATTCAATTGCGCCTGCGCTGCATCCTCGAA
                ************************************************************
RhlR_BV1        CAGGTGACGCTGCGCCTGACAGATCTGGGCCATAACGAACGCGCCCACCCGTCGGTCTGC
RhlR_BV5        CAGGTGACGCTGCGCCTGACAGATCTGGGCCATAACGAACGCGCCCACCCGTCGGTCTGC
RhlR_CP15       CAGGTGACGCTGCGCCTGACAGATCTGGGCCATAACGAACGCGCCCACCCGTCGGTCTGC
RhlR_RWV1       CAGGTGACGCTGCGCCTGACAGATCTGGGCCATAGCGAACGCGCCCACCCGTCGGTCTGC
                ********************************** ************************
RhlR_BV1        CTCAGCCTGCGTGAGCGGGAAATTTTGCAGTGGACCGCCGACGGCAAGAGTTCAGGCGAG
RhlR_BV5        CTCAGCCTGCGTGAGCGGGAAATTTTGCAGTGGACCGCCGACGGCAAGAGTTCAGGCGAG
RhlR_CP15       CTCAGCCTGCGTGAGCGGGAAATTTTGCAGTGGACCGCCGACGGCAAGAGTTCAGGCGAG
RhlR_RWV1       CTCAGCCTGCGTGAGCGGGAAATTTTGCAGTGGACCGCCGACGGCAAGAGTTCAGGCGAG
                ************************************************************
RhlR_BV1        ATCGCGCTGATCCTGACCATCTCCATCAACACGGTGAACTTTCACCTCAAGACCATCCAG
RhlR_BV5        ATCGCGCTGATCCTGACCATCTCCATCAACACGGTGAACTTTCACCTCAAGACCATCCAG
RhlR_CP15       ATCGCGCTGATCCTGACCATCTCCATCAACACGGTGAACTTTCACCTCAAGACCATCCAG
RhlR_RWV1       ATCGCGCTGATCCTGACCATCTCCATCAACACGGTGAACTTTCACCTCAAGGCCATCCAG
                ************************************************ ********
RhlR_BV1        AAGAAATTCGGCGCAGCCAACAAGACACTGGCGGCTGCCTATGCCGCCGCACTGGGCCTG
RhlR_BV5        AAGAAATTCGGCGCAGCCAACAAGACACTGGCGGCTGCCTATGCCGCCGCACTGGGCCTG
RhlR_CP15       AAGAAATTCGGCGCAGCCAACAAGACACTGGCGGCTGCCTATGCCGCCGCACTGGGCCTG
RhlR_RWV1       AAGAAATTCGGCGCAGCCAACAAGACACTGGCGGCTGCCTATGCCGCCGCACTGGGCCTG
                ************************************************************
```

Figure S7. Multiple alignment of *rhlR*-like genes between BV1, BV5, CP15 and RWV1 strains.

```
RhlR_BV6        ATGGAGAAGGAGAACGACCTCATCCGCTGGTGGAATCGCTTGCGGATAGAGATGCTCACG
RhlR_RWV6       ATGGAGAAGGAGAACGACCTCATCCGCTGGTGGAATCGCTTGCGGATAGAGATGCTCACG
                ************************************************************
RhlR_BV6        CAACAGGAAGGGGCACAAGTGTTCGCACTGCTGGAGCGGGAAGTGTTGCAACTGGGGTTC
RhlR_RWV6       CAACAGGAAGGGGCACAAGTGTTCGCACTGCTGGAGCGGGAAGTGTTGCAATTGGGGTTC
                ************************************************** ********
RhlR_BV6        GAGTACTACGCCTATGGCGTACGCCACCTGACCCCGTTTACCCGCCCTAAAACCAAGATT
RhlR_RWV6       GAGTACTACGCCTATGGCGTACGCCACCTGACCCCGTTTACCCGCCCTAAAACCAAGATT
                ************************************************************
RhlR_BV6        TACGGCTCCTACCCCGAAACATGGCTGGAGCATTACAAGGAGCAAAACTACGCGGCGGTC
RhlR_RWV6       TACGGCTCCTACCCCGAAACATGGCTGGAGCATTACAAGGAGCAAAACTACGCGGCGGTC
                ************************************************************
RhlR_BV6        GATCCGTCGATTCTCAGTGGCTTGCGTTCCACCGAGATGGTGCTGTGGAACGACGCACTG
RhlR_RWV6       GATCCGTCGATTCTCAGTGGCTTGCGTTCCACCGAGATGGTGCTGTGGAACGACGCACTG
                ************************************************************
RhlR_BV6        TTTGATAACAGCCGCAAGCTATGGCTGGAAGCCCGGGATTGGGGCTTGTGCATCGGCGCC
RhlR_RWV6       TTTGATAACAGCCGCAAGCTATGGCTGGAAGCCCGGGATTGGGGCTTATGCATCGGCGCC
                ********************************************** ************
RhlR_BV6        ACACTGCCGATTCGCAGCCACGATCATTCGCTGCGGGTACTGTCGGTGGCCCGGCGCCAG
RhlR_RWV6       ACACTGCCGATTCGCAGCCACGATCATTCGCTGCGGGTACTGTCGGTGGCCCGGCGCCAG
                ************************************************************
RhlR_BV6        GACCAGATTTCCCAGGCCGAAAGCGACGAGATTCAATTGCGCCTGCGCTGCATCCTCGAA
RhlR_RWV6       GACCAGATTTCCCAGGCCGAAAGCGACGAGATTCAATTGCGCCTGCGCTGCATCCTCGAA
                ************************************************************
RhlR_BV6        CAGGTGACACAGCGCCTGACAGACCTTGGCCATAGCGAACGCTGCCATCAGTCGGTATGC
RhlR_RWV6       CAGGTGACACAGCGCCTGACAGACCTTGGCCATAGTGAACGCTGCCATCAGTCGGTCTGC
                ********************************** ******************** ***
RhlR_BV6        CTCAGCCAGCGGGAGCGGGAGATTTTGCAGTGGACCGCCGATGGCAAGAGTTCAGGCGAG
RhlR_RWV6       CTCAGCCAGCGGGAGCGGGAGATTTTGCAGTGGACCGCCGATGGCAAGAGTTCAGGCGAG
                ************************************************************
RhlR_BV6        ATCGCGCTGATCCTGACCATCTCCATCAACACGGTGAATTTTCACCTCAAGGCCATCCAG
RhlR_RWV6       ATCGCGCTGATCCTGACCATCTCCATCAACACGGTGAATTTTCACCTCAAGGCCATCCAG
                ************************************************************
RhlR_BV6        AAGAAATTCGGGGCGGCCAACAAGACACTGGCGGCAGCGTATGCCGCCGCACTGGGCCTG
RhlR_RWV6       AAGAAATTCGGGGCGGCCAACAAGACACTGGCGGCTGCCTATGCCGCCGCACTGGGCCTG
                ********************************** ** ********************
RhlR_BV6         ATCTAG
RhlR_RWV6        ATCTAG
                 ******
```

Figure S8. Multiple alignment of *rhlR*-like genes between BV6 and RWV6 strains.

```
lasR-BV6        ATGGATTTTATTGATGAACTTGTGCGGTTGAATGGGTTGGAAACCCAGGAGCAATGGTTT
lasR-RWV6       ATGGATTTTATTGATGAACTTGTGCGGTTGAATGGGTTGGAAACCCAGGAGCAATGGTTT
                ************************************************************
lasR-BV6        TCAGCTATCGAAAAAATCAACGACAAGTATGGGTTTACCAAAGTCCTGATCGGGTTGTTG
lasR-RWV6       TCAGCTATCGAAAAAATCAACGACAAGTATGGGTTTACCAAAGTCCTGATCGGGTTGTTG
                ************************************************************
lasR-BV6        CCCAAGTATGATGCCGATTTGAGTGCTGCGATGATTGTCAGTAACTATCCGATGGCCTGG
lasR-RWV6       CCCAAGTATGATGCCGATTTGAGTGCTGCGATGATTGTCAGTAACTATCCGATGGCCTGG
                ************************************************************
lasR-BV6        CGAAGTCGCTATGACCAATTGCGTTATGCAACTATTGATCCTGTGGTTGTTTATTCGTTT
lasR-RWV6       CGAAGTCGCTATGACCAATTGCGTTATGCAACTATTGATCCTGTGGTTGTTTATTCGTTT
                ************************************************************
lasR-BV6        AAAAATGTCAGGCCCGTTGTCTGGGATGAGTCATTGTATTGCACGCCCCGCCAACGAGAG
lasR-RWV6       AAAAATGTCAGGCCCGTTGTCTGGGATGAGTCATTGTATTGCACGCCCCGCCAACGAGAG
                ************************************************************
lasR-BV6        TTTCGCGAAGAGGCCAACGCTTATGGACTTTCCAGGGGGATCACTTTTCCCCTGCATGGA
lasR-RWV6       TTTCGCGAAGAGGCCAACGCTTATGGACTTTCCAGGGGGATCACTTTTCCCCTGCATGGA
                ************************************************************
lasR-BV6        CCTCAGGGACAGTTCGGTACTTTCAGTCTGGCGGTAGACGCTCAAGACATTGCTGGAACG
lasR-RWV6       CCTCAGGGACAGTTCGGTACTTTCAGTCTGGCGGTAGACGCTCAAGACATTGCTGGAACG
                ************************************************************
lasR-BV6        ACACGTCATATCAATGCCATGATTCCAAAATTATCCATTCTTAAAGATGTCATTCTGCAA
lasR-RWV6       ACACGTCATATCAATGCCATGATTCCAAAATTATCCATTCTTAAAGATGTCATTCTGCAA
                ************************************************************
lasR-BV6        AGCGCTTTGGACGGTGCGGGCAAGTTGACTGGAGCAAGGGTGATTTCCCTGACGACTCGT
lasR-RWV6       AGCGCTTTGGACGGTGCGGGCAAGTTGACTGGAGCAAGGGTGATTTCCCTGACGACTCGT
                ************************************************************
lasR-BV6        GAGAAAGAGATTCTCAAGTGGTGCGCCGTCGGGAAAAGCTCCTGGGATATTTCCAGGATC
lasR-RWV6       GAGAAAGAGATTCTCAAGTGGTGCGCCGTCGGGAAAAGCTCCTGGGATATTTCCAGGATC
                ************************************************************
lasR-BV6        TGTGGCTGTTCGGAAGCCAATATCAATTATCACTTTGCGAGTATCAACACCAAGTTTGGC
lasR-RWV6       TGTGGCTGTTCGGAAGCCAATATCAATTATCACTTTGCGAGTATCAACACCAAGTTTGGC
                ************************************************************
lasR-BV6        GTTGCGTCCCGTCGGGCTGCCGCAGTGAAAGCTGTTTCGCTCGGGCTGATCAGCCTCTAG
lasR-RWV6       GTTGCGTCCCGTCGGGCTGCCGCAGTGAAAGCTGTTTCGCTCGGGCTGATCAGCCTCTAG
                ************************************************************
```

Figure S9. Multiple alignment of *lasR*-like genes between BV6 and RWV6 strains.

6.5 Appendix D Multiple alignment of *luxR* solo genes

```
CsgD-BV5      ATGGTCAACTGGCGAAACACACGATTACCCAAACTTGAAGGTGAAGATGAGGTAACGACG
CsgD-CP15     ATGGTCAACTGGCGAAACACACGATTACCCAAACTTGAAGGTGAAGATGAGGTAACGACG
CsgD-RWV1     ATGGTCAACTGGCGAAACACACGATTACCCAAACTTGAAGGTGAAGATGAGGTAACGACG
CsgD-BV1      ATGGTCAACTGGCGAAACACACGATTACCCAAACTTGAAGGTGAAGATGAGGTAACGACG
              ************************************************************
CsgD-BV5      ATGTTTGAAGCCGCTCTGAACATTACCTATGAGCTAGGTTTTGAATATTGCGGTTTTATC
CsgD-CP15     ATGTTTGAAGCCGCTCTGAACATTACCTATGAGCTAGGTTTTGAATATTGCGGTTTTATC
CsgD-RWV1     ATGTTTGAAGCCGCTCTGAACATTACCTATGAGCTAGGTTTTGAATATTGCGGTTTTATC
CsgD-BV1      ATGTTTGAAGCCGCTCTGAACATTACCTATGAGCTAGGTTTTGAATATTGCGGTTTTATC
              ************************************************************
CsgD-BV5      ATGGGCTCCAATGCTCTCTACCGCCCTAACAGAAGTATCCATCTCAACAACTATCCGGAT
CsgD-CP15     ATGGGCTCCAATGCTCTCTACCGCCCTAACAGAAGTATCCATCTCAACAACTATCCGGAT
CsgD-RWV1     ATGGGCTCCAATGCTCTCTACCGCCCTAACAGAAGTATCCATCTCAACAACTATCCGGAT
CsgD-BV1      ATGGGCTCCAATGCTCTCTACCGCCCTAACAGAAGTATCCATCTCAACAACTATCCGGAT
              ************************************************************
CsgD-BV5      GAATGGAACAAAATCTACAAAACAGAAAACTACTTTGAAATCGACCCTTTGGTTGTTCAC
CsgD-CP15     GAATGGAACAAAATCTACAAAACAGAAAACTACTTTGAAATCGACCCTTTGGTTGTTCAC
CsgD-RWV1     GAATGGAACAAAATCTACAAAACAGAAAACTACTTTGAAATCGACCCTTTGGTTGTTCAC
CsgD-BV1      GAATGGAACAAAATCTACAAAATAGAAAACTACTTTGAAATCGACCCTTTGGTTGTTCAC
              ********************** ***********************************
CsgD-BV5      TGTAAGCGCGATGTGCTGCCGCTTGTATGGGAAGAGAAAACCTTTTCCGCAGTACCTGAC
CsgD-CP15     TGTAAGCGCGATGTGCTGCCGCTTGTATGGGAAGAGAAAACCTTTTCCGCAGTACCTGAC
CsgD-RWV1     TGTAAGCGCGATGTGCTGCCGCTTGTATGGGAAGAGAAAACCTTTTCCGCAGTACCTGAC
CsgD-BV1      TGTAAGCGCGATGTGCTGCCGCTTGTATGGGAAGAGAAAACCTTTTCCGCAGTACCTGAC
              ************************************************************
CsgD-BV5      ATGTGGGCTCACGTACAAGCCCAAGGCCTGAATTTCGGCTGGGCCCAGTCGGTGCACGAT
CsgD-CP15     ATGTGGGCTCACGTACAAGCCCAAGGCCTGAATTTCGGCTGGGCCCAGTCGGTGCACGAT
CsgD-RWV1     ATGTGGGCTCACGTACAAGCCCAAGGCCTGAATTTCGGCTGGGCCCAGTCGGTGCACGAT
CsgD-BV1      ATGTGGGCTCACGTACAAGCCCAAGGCCTGAATTTCGGCTGGGCCCAGTCGGTGCACGAT
              ************************************************************
CsgD-BV5      TTCCGGGGCTTCTTCAGTATGATCAACCTGGGACGACGCAAGGGGCCGGTGCAGGCCCAT
CsgD-CP15     TTCCGGGGCTTCTTCAGTATGATCAACCTGGGACGACGCAAGGGGCCGGTGCAGGCCCAT
CsgD-RWV1     TTCCGGGGCTTCTTCAGTATGATCAACCTGGGACGACGCAAGGGGCCGGTGCAGGCCCAT
CsgD-BV1      TTCCGGGGCTTCTTCAGTATGATCAACCTGGGACGACGCAAGGGGCCGGTGCAGGCCCAT
              ************************************************************
CsgD-BV5      GAGCTCTATGAAAAAGCGGGCCAGGTTCTGTGGATATGCCATGCCTTGCATGCCGTGGCG
CsgD-CP15     GAGCTCTATGAAAAAGCGGGCCAGGTTCTGTGGATATGCCATGCCTTGCATGCCGTGGCG
CsgD-RWV1     GAGCTCTATGAAAAAGCGGGCCAGGTTCTGTGGATATGCCATGCCTTGCATGCCGTGGCG
CsgD-BV1      GAGCTCTATGAAAAAGCGGGCCAGGTTCTGTGGATATGCCATGCCTTGCATGCCGTGGCG
              ************************************************************
CsgD-BV5      GCGCAAACCTACAGCCTGGGGCCGACTTTCCAGTGCCCCACCAAACTCACCAGCCGCGAG
CsgD-CP15     GCGCAAACCTACAGCCTGGGGCCGACTTTCCAGTGCCCCACCAAACTCACCAGCCGCGAG
CsgD-RWV1     GCGCAAACCTACAGCCTGGGGCCGACTTTCCAGTGCCCCACCAAACTCACCAGCCGCGAG
CsgD-BV1      GCGCAAACCTACAGCCTGGGGCCGACTTTCCAGTGCCCCACCAAACTCACCAGCCGCGAG
              ************************************************************
CsgD-BV5      ACAGAGATCCTGCAATGGTCGGCACTGGGCAAAACTGCGGCTGATATCGCCACAATTCTC
CsgD-CP15     ACAGAGATCCTGCAATGGTCGGCACTGGGCAAAACTGCGGCTGATATCGCCACAATTCTC
CsgD-RWV1     ACAGAGATCCTGCAATGGTCGGCACTGGGCAAAACTGCGGCTGATATCGCCACAATTCTC
CsgD-BV1      ACAGAGATCCTGCAATGGTCGGCACTGGGCAAAACTGCGGCTGATATCGCCACAATTCTC
              ************************************************************
CsgD-BV5      TGCCTATCGGAACGTACCGTCGGTTTTCACATCAGCAGTGCGATGAGGAAGCTGGGGGTC
CsgD-CP15     TGCCTATCGGAACGTACCGTCGGTTTTCACATCAGCAGTGCGATGAGGAAGCTGGGGGTC
CsgD-RWV1     TGCCTATCGGAACGTACCGTCGGTTTTCACATCAGCAGTGCGATGAGGAAGCTAGGGGTC
CsgD-BV1      TGCCTATCGGAACGTACCGTCGGTTTTCACATCAGCAGTGCGATGAGGAAGCTGGGGGTC
              ************************************************** ******
CsgD-BV5      AGCAATAAAATCGCCGCCGTGATCAGCGCCGTGAGAAACGGTCTTTTTTAA
CsgD-CP15     AGCAATAAAATCGCCGCCGTGATCAGCGCCGTGAGAAACGGTCTTTTTTAA
CsgD-RWV1     AGCAATAAAATCGCCGCCGTGATCAGCGCCGTGAGAAACGGTCTTTTTTAA
CsgD-BV1      AGCAATAAAATCGCCGCCGTAATCAGCGCCGTGAGAAACGGTCTTTTTTAA
              ******************* ******************************
```

Figure S10. Multiple alignment of *csgD*-like gene between BV1, BV5, CP15 and RWV1 strains.

```
CsgD-BV6        ATGGTCAACTGGCGCAACACACGTCTACCCAAACTAGAAGGTGAGGATGAGGTGACGACT
CsgD-RWV6       ATGGTCAACTGGCGCAACACACGTCTACCCAAACTAGAAGGTGAGGATGAGGTGACGACT
                ************************************************************
CsgD-BV6        ATGTTCGAGGCTGCTCTGAACATTACCTATGAGCTGGGCTTTGAATATTGCGGTTTTATG
CsgD-RWV6       ATGTTCGAGGCTGCTCTGAACATTACCTATGAGCTGGGCTTTGAATATTGCGGTTTTATG
                ************************************************************
CsgD-BV6        ATGGGCTCCAATGCGGTTTATCAGCCATTCAAGAACATCCACCTCAATAATTATCCAAGT
CsgD-RWV6       ATGGGCTCCAATGCGGTTTATCAGCCATTCAAGAACATCCACCTCAATAATTATCCAAGT
                ************************************************************
CsgD-BV6        GAATGGAACACTCTCTACAAAACAGAACATTACTTCGATATGGACCCGCTGGTCAGCCAC
CsgD-RWV6       GAATGGAACACTCTCTACAAAACAGAACATTACTTCGATATGGACCCGCTGGTCAGCCAC
                ************************************************************
CsgD-BV6        TGCAAACGCGATGTACTGCCCATCGTCTGGGAAGAAAAAACCTACTCTGCAGTGCCGGAC
CsgD-RWV6       TGCAAACGCGATGTATTGCCCATCGTCTGGGAAGAAAAAACCTACTCTGCAGTGCCGGAC
                *************** ********************************************
CsgD-BV6        ATGTGGGTTCACTTGCAAGCCCAGGGTCTCAATTTTGGCTGGGCGCAGTCGGTGCATGAC
CsgD-RWV6       ATGTGGGTTCACTTGCAAGCCCAGGGTCTCAATTTTGGCTGGGCGCAGTCGGTGCATGAC
                ************************************************************
CsgD-BV6        TTCCGTGGCTTTTTCAGCATGATCAACCTGGGACGACGCCAGGAACCGGTGCAAGCCCAG
CsgD-RWV6       TTCCGTGGCTTTTTCAGCATGATCAACCTGGGACGACGCCAGGAACCGGTGCAAGCCCAG
                ************************************************************
CsgD-BV6        GAACTGTATGAGAAAGCCGGCCAGGTCTTGTGGATCTGCCATGCCTTGCATACCGTCGCG
CsgD-RWV6       GAACTGTATGAGAAAGCCGGCCAGGTCTTGTGGATCTGCCATGCCTTGCATACCGTCGCG
                ************************************************************
CsgD-BV6        GCCCAGGCCTATGCCAAGGAGCCGGCCTGCCAGTGCCCCACCAAGCTCACCAGTCGCGAG
CsgD-RWV6       GCCCAGGCCTATGCCAAGGAGCCGGCCTGCCAGTGCCCCACCAAGCTCACCAGTCGCGAG
                ************************************************************
CsgD-BV6        ACCGAAATCCTGCAATGGTCGGCACTGGGCAAGACAGCTGCCGATATCGCGACAATTCTC
CsgD-RWV6       ACCGAAATCCTGCAATGGTCGGCACTGGGCAAGACAGCTGCCGATATCGCGACAATTCTC
                ************************************************************
CsgD-BV6        TGCCTGTCCGAGCGCACTGTCGGTTTTCATATCAGCAGTGCGATGCGCAAGCTGGGGGTG
CsgD-RWV6       TGCCTGTCCGAGCGCACTGTCGGTTTTCATATCAGCAGTGCGATGCGCAAGCTGGGGGTG
                ************************************************************
CsgD-BV6        AGCAATAAGATTGCCGCGGTGATCACGGCAGTCAAACACGGCCTTTTTTGA
CsgD-RWV6       AGCAATAAGATTGCCGCGGTGATCACGGCAGTCAAACACGGCCTTTTTTGA
                **************************************************
```

Figure S11. Multiple alignment of *csgD*-like gene between BV6 and RWV6 strains.

```
BjaR1-BV5       GTGATCCCCGGTGTGGCCGAGGCAGCCTTGCGAATCGTCCTGGAGATAGAGCGCGCCTCG
BjaR1-CP15      GTGATCCCCGGTGTGGCCGAGGCAGCCTTGCGAATCGTCCTGGAGATAGAGCGCGCCTCG
                ************************************************************
BjaR1-BV5       ACGCTCTCGTTGATTCAGAAGGTCGTTCGTTCCTTTACCAAGCGTTTTGGCTACGACCGT
BjaR1-CP15      ACGCTCTCGTTGATTCAGAAGGTCGTTCGTTCCTTTACCAAGCGTTTTGGCTACGACCGT
                ************************************************************
BjaR1-BV5       TTCGTCCTTTTTTCTGCCTCATCGGCACGGGACGACGTGGTCGAGCGCATTTATTGGGTC
BjaR1-CP15      TTCGTCCTTTTTTCTGCCTCATCGGCACGGGACGACGTGGTCGAGCGCATTTATTGGGTC
                ************************************************************
BjaR1-BV5       GAAGGAAATTGGTTGGGCGACGGCCAGGCGGTCGATGCCGAAACCTACGTTCGGCGTTGC
BjaR1-CP15      GAAGGAAATTGGTTGGGCGACGGCCAGGCGGTCGATGCCGAAACCTACGTTCGGCGTTGC
                ************************************************************
BjaR1-BV5       CCGGTCACCCGTCACATTCTGGAGGCCCGCGAACCCTTCTTTTGGACGAAAACCCAATGT
BjaR1-CP15      CCGGTCACCCGTCACATTCTGGAGGCCCGCGAACCCTTCTTTTGGACGAAAACCCAATGT
                ************************************************************
BjaR1-BV5       GAAAGCGGGGGCAGTTATCGTGTGGTCCGCCGTCCGGTCGGTGACGGCCCGCACGGTTTG
BjaR1-CP15      GAAAGCGGGGGCAGTTATCGTGTGGTCCGCCGTCCGGTCGGTGACGGCCCGCACGGTTTG
                ************************************************************
BjaR1-BV5       CAGGTACCCGTTTTTGGTCCCTTGGGCCTTGAGGGCGCCATGAGCCTGGGCGGGGAGCAG
BjaR1-CP15      CAGGTACCCGTTTTTGGTCCCTTGGGCCTTGAGGGCGCCATGAGCCTGGGCGGGGAGCAG
                ************************************************************
BjaR1-BV5       GTCGATAGCAGCCCCGACGTTCGCCTGGTGTTGGGGATCGTGGCCACAGCGGCTTTTTTT
BjaR1-CP15      GTCGATAGCAGCCCCGACGTTCGCCTGGTGTTGGGGATCGTGGCCACAGCGGCTTTTTTT
                ************************************************************
BjaR1-BV5       TCCGCTCGCCGATTGCTGGAAGCACCAAGCATTGACGTGGTCAGGCAGCTCTCAGGTCGC
BjaR1-CP15      TCCGCTCGCCGATTGCTGGAAGCACCAAGCATTGACGTGGTCAGGCAGCTCTCAGGTCGC
                ************************************************************
BjaR1-BV5       GAGCGCGAGGTGTTGACCTGGACGGCTGCGGGGCGACGTCAGGCCGATATCGCCGCAGCG
BjaR1-CP15      GAGCGCGAGGTGTTGACCTGGACGGCTGCGGGGCGACGTCAGGCCGATATCGCCGCAGCG
                ************************************************************
BjaR1-BV5       CTCGGGTTGTCGGAGCGAACCGTGGAAAACCATCTACGCGCGGCGCGGCGCCGTCTCGGG
BjaR1-CP15      CTCGGGTTGTCGGAGCGAACCGTGGAAAACCATCTACGCGCGGCGCGGCGCCGTCTCGGG
                ************************************************************
BjaR1-BV5       GTGGCAACTACAGCACAAGCCATCAAGATCGCCATTCGGAATGGTGACCTTGGCGACTGA
BjaR1-CP15      GTGGCAACTACAGCACAAGCCATCAAGATCGCCATTCGGAATGGTGACCTTGGCGACTGA
                ************************************************************
```

Figure S12. Multiple alignment of *bjaR1*-like gene between CP15 and BV5 strains.

6.6 Appendix E: LuxR amino acid sequences

Strain code	Amino acid sequence
BV1	MEKENDLIRWWNRLRIEMLKQQGGAQVFALLEREVLQLGFEY YAYAVRHLTPFTRPKTEIHGSYPERWLEHYQEQNYAAVDPSILS GLRSTEMVLWNDALFENSRKLWLEARDWGLCIGATLPIRSHD HSLRVLSVARRQDPISRAESDEIQLRLRCILEQVTLRLTDLGHNE RAHPSVCLSLREREILQWTADGKSSGEIALILTISINTVNFHLKA IQKKFGAANKTLAAAYAAALGLI
BV5	MEKENDLIRWWNRLRIEMLKQQGGAQVFALLEREVLQLGFEY YAYAVRHLTPFTRPKTEIHGSYPERWLEHYQEQNYAAVDPSILS GLRSTEMVLWNDALFENSRKLWLEARDWGLCIGATLPIRSHD HSLRVLSVARRQDPISRAESDEIQLRLRCILEQVTLRLTDLGHNE RAHPSVCLSLREREILQWTADGKSSGEIALILTISINTVNFHLKTI QKKFGAANKTLAAAYAAALGLI
CP15	MEKENDLIRWWNRLRIEMLTQQEGAQVFALLEREVLQLGFEY YAYGVRHLTPFTRPKTKIYGSYPETWLEHYKEQNYAAVDPSILS GLRSTEMVLWNDALFDNSRKLWLEARDWGLCIGATLPIRSHD HSLRVLSVARRQDQISQAESDEIQLRLRCILEQVTQRLTDLGHS ERCHQSVCLSQREREILQWTADGKSSGEIALILTISINTVNFHLK AIQKKFGAANKTLAAAYAAALGLI
BV6	MEKENDLIRWWNRLRIEMLTQQEGAQVFALLEREVLQLGFEY YAYGVRHLTPFTRPKTKIYGSYPETWLEHYKEQNYAAVDPSILS GLRSTEMVLWNDALFDNSRKLWLEARDWGLCIGATLPIRSHD HSLRVLSVARRQDQISQAESDEIQLRLRCILEQVTQRLTDLGHS ERCHQSVCLSQREREILQWTADGKSSGEIALILTISINTVNFHLK AIQKKFGAANKTLAAAYAAALGLI
RWV1	MEKENDLIRWWNRLRIEMLKQQGGAQVFALLEREVLQLGFEY YAYAVRHLTPFTRPKTEIHGSYPERWLEHYQEQNYAAVDPSILS GLRSTEMVLWNDALFENSRKLWLEARDWGLCIGATLPIRSHD HSLRVLSVARRQDPISRAESDEIQLRLRCILEQVTLRLTDLGHNE RAHPSVCLSLREREILQWTADGKSSGEIALILTISINTVNFHLKTI QKKFGAANKTLAAAYAAALGLI
RWV6	MEKENDLIRWWNRLRIEMLKQQGGAQVFALLEREVLQLGFEY YAYAVRHLTPFTRPKTEIHGSYPERWLEHYQEQNYAAVDPSILS GLRSTEMVLWNDALFESSRKLWLEARDWGLCIGATLPIRSHD HSLRVLSVARRQDPISRAESDEIQLRLRCILEQVTLRLTDLGHSE RAHPSVCLSLREREILQWTADGKSSGEIALILTISINTVNFHLKA IQKKFGAANKTLAAAYAAALGLI

6.7 Appendix F: Multile alignment of LuxR amino acid sequences

```
BV5             MEKENDLIRWWNRLRIEMLKQQGGAQVFALLEREVLQLGFEYYAYAVRHLTPFTRPKTEI
RWV1            MEKENDLIRWWNRLRIEMLKQQGGAQVFALLEREVLQLGFEYYAYAVRHLTPFTRPKTEI
                ************************************************************

BV5             HGSYPERWLEHYQEQNYAAVDPSILSGLRSTEMVLWNDALFENSRKLWLEARDWGLCIGA
RWV1            HGSYPERWLEHYQEQNYAAVDPSILSGLRSTEMVLWNDALFENSRKLWLEARDWGLCIGA
                ************************************************************

BV5             TLPIRSHDHSLRVLSVARRQDPISRAESDEIQLRLRCILEQVTLRLTDLGHNERAHPSVC
RWV1            TLPIRSHDHSLRVLSVARRQDPISRAESDEIQLRLRCILEQVTLRLTDLGHNERAHPSVC
                ************************************************************

BV5             LSLREREILQWTADGKSSGEIALILTISINTVNFHLKTIQKKFGAANKTLAAAYAAALGL
RWV1            LSLREREILQWTADGKSSGEIALILTISINTVNFHLKTIQKKFGAANKTLAAAYAAALGL
                ************************************************************

BV5             I
RWV1            I
                *


CP15             MEKENDLIRWWNRLRIEMLTQQEGAQVFALLEREVLQLGFEYYAYGVRHLTPFTRPKTKI
BV6              MEKENDLIRWWNRLRIEMLTQQEGAQVFALLEREVLQLGFEYYAYGVRHLTPFTRPKTKI
                 ************************************************************

CP15             YGSYPETWLEHYKEQNYAAVDPSILSGLRSTEMVLWNDALFDNSRKLWLEARDWGLCIGA
BV6              YGSYPETWLEHYKEQNYAAVDPSILSGLRSTEMVLWNDALFDNSRKLWLEARDWGLCIGA
                 ************************************************************

CP15             TLPIRSHDHSLRVLSVARRQDQISQAESDEIQLRLRCILEQVTQRLTDLGHSERCHQSVC
BV6              TLPIRSHDHSLRVLSVARRQDQISQAESDEIQLRLRCILEQVTQRLTDLGHSERCHQSVC
                 ************************************************************

CP15             LSQREREILQWTADGKSSGEIALILTISINTVNFHLKAIQKKFGAANKTLAAAYAAALGL
BV6              LSQREREILQWTADGKSSGEIALILTISINTVNFHLKAIQKKFGAANKTLAAAYAAALGL
                 ************************************************************

CP15             I
BV6              I
                 *
```

Figure S12. Multiple alignment of LuxR proteins of the *P. gessardii* isolates using CLUSTLW method.

7 Publications

1. **Salman, M. K**., Abuqwider, J., & Mauriello, G. (2023). Anti-quorum sensing activity of probiotics: the mechanism and role in food and gut health. Microorganisms, 11(3), 793.

2. **Salman, M. K**., & Mauriello, G. 2023. Special issue “Probiotics and their metabolism”. Microorganisms, 11(3), 687.

3. The following manuscript is under review stage where a minor revision was required: **Salman, M. K**., Giordano, I., Tommonaro, G., Cutignano, A., Sousa, S. F., Borges, A., Mauriello, G., & Abbamondi, G. R. (year). Characterization of AHL-Mediated Quorum Sensing in Pseudomonas gessardii from Raw Milk and Insights into Control of Proteolytic Activity. Int. J. Food Microbiol.